

Functional analysis of crosstalk in DNA mismatch repair

Inauguraldissertation

Zur Erlangung des Grades
Doktor der Naturwissenschaften

Dr. rer. nat

des Fachbereiches Biologie und Chemie
der Justus-Liebig-Universität Giessen

vorgelegt von

Dipl.-Biol. Roger J. Heinze

geboren am 5. 11. 1980 in Zwickau

Giessen, 2010

The present study has been carried out at the Institute of Biochemistry, Justus-Liebig University Giessen, between October 2006 and July 2010, under supervision of Prof. Dr. Peter Friedhoff. This work was supported by the DFG funded IRTG (International Research Training Group) „*Enzymes and Multienzyme complexes acting on nucleic acids*“ and by the EU-Project „mismatch2model“.

Dean:

Prof. Dr. Volkmar Wolters

Institut für Ökologie, FB 08
Justus-Liebig-Universität Gießen
Heinrich-Buff-Ring 26
35392 Gießen

Advisor:

Prof. Dr. Peter Friedhoff

Institut für Biochemie, FB 08
Justus-Liebig Universität
Heinrich-Buff-Ring 58
35392 Giessen

Co-advisor:

Prof. Dr. Gabriele Klug

Institut für Mikro- und Molekularbiologie
Justus-Liebig Universität
Heinrich-Buff-Ring 26-32, L 234
35392 Giessen

Erklärung

„Ich erkläre: Ich habe die vorgelegte Dissertation selbständig und ohne unerlaubte fremde Hilfe und nur mit den Hilfen angefertigt, die ich in der Dissertation angegeben habe. Alle Textstellen, die wörtlich oder sinngemäß aus veröffentlichten Schriften entnommen sind, und alle Angaben, die auf mündlichen Auskünften beruhen, sind als solche kenntlich gemacht. Bei den von mir durchgeführten und in der Dissertation erwähnten Untersuchungen habe ich die Grundsätze guter wissenschaftlicher Praxis, wie sie in der „Satzung der Justus-Liebig-Universität Gießen zur Sicherung guter wissenschaftlicher Praxis“ niedergelegt sind, eingehalten.“

Giessen, den 9. August 2010

(Roger Heinze)

Danksagung

Herrn Prof. Dr. Alfred Pingoud danke ich für die Möglichkeit meinen Dokortitel in seinem Institut zu erlangen, die vielen hilfreichen Ratschläge und Diskussionen in den Seminaren, die aufheiternden Kommentare sowie die konstruktive Kritik zu meiner Arbeit.

Herrn Prof. Dr. Peter Friedhoff danke ich für die Aufnahme in seine Arbeitsgruppe und das IRTG, die anhaltend gute Betreuung und Unterstützung mit den vielen guten Ideen und hilfreichen Kommentaren zur richtigen Zeit, seine unendliche Geduld, die stetige Motivation sowie das Vertrauen in mich und meine Arbeit.

Frau Prof. Dr. Gabriele Klug danke ich für die Übernahme des Zweitgutachtens sowie die gute Zusammenarbeit und Ko-Betreuung im Rahmen des IRTGs

Ein großer Dank geht an Ina Dern, die mich am Anfang meiner Arbeit eingewiesen und begleitet hat.

Ein riesengroßer Dank geht an das Sekretariat mit Anja, Ina und Karina, die mir bei den vielen bürokratischen und organisatorischen Problemen geholfen und mich immer an die wichtigen Termine erinnert haben.

Ich danke der MMR-Gruppe: Andi, Ines, Karo, Laura, Micha, Michele und besonders Caro für das gute Teamwork beim Versuch die Rätsel zu lösen, welche uns das MMR-System aufgibt. Danke Caro, dass du so gut mit mir ausgekommen bist und für die lustigen Tage.

Ich danke allen Mitgliedern des Instituts für Biochemie und des IRTG's für die gute Zusammenarbeit und Atmosphäre, das regelmäßige Versorgen mit neuen wissenschaftlichen Erkenntnissen in den Seminaren und Diskussionsrunden sowie für die interessanten Konferenzen und Auslandsaufenthalte. Ein besonderer Dank geht an Ines Fonfara für die seelische und moralische Unterstützung in Moskau.

Ein besonderer Dank geht an Sveta und die Arbeitsgruppe von Prof. Dr. Tatjana Oretskaya für die freundliche Aufnahme, das gute Teamwork und die Unterstützung während meiner Aufenthalte in Moskau

Allen meinen Freunden und Weggefährten, die mit mir die vielen Jahre in Giessen verbracht haben, danke ich für die abwechslungsreiche und unvergesslich schöne Zeit. Ganz besonders danke ich Dennis, Evangelos, Oli und Tom für die vielen wissenschaftlichen Diskussionen bei Bier und Musik. Ich bin froh euch alle zu kennen.

Mein größter Dank geht an meine Eltern, Jürgen und Sylvia Heinze, für ihre grenzenlose Unterstützung, ihr Vertrauen in mich und meine Arbeit, ihre vielen hilfreichen Ratschläge zum Leben und ihre Liebe. Ich danke euch von ganzem Herzen für alles, was ihr für mich getan habt. Ohne euch wäre dies alles nicht möglich gewesen.

Publication

Heinze R. J., Giron-Monzon L., Solovyova A., Elliot S. L., Geisler S., Cupples C. G., Connolly B. A. and Friedhoff P.:

Physical and functional interactions between Escherichia coli MutL and the Vsr repair endonuclease.

Nucleic Acids Research, 2009 Jul;37(13):4453-63. Epub 2009 May 27

Winkler I., Marx A. D., Lariviere D., **Heinze R. J.**, Cristovao M., Reumer A., Curth U., Sixma T. K. and Friedhoff P.:

Chemical trapping of the dynamic MutS-MutL complex formed in DNA mismatch repair in Escherichia coli.

The Journal of Biological Chemistry, 2011 May 13;286(19):17326-37. Epub 2011 Mar 15

Workshops and conferences

November 2009 Amsterdam, Niederlande: EU-Projekt „mismatch2model (mm2m)“ Meeting

Presentation: “With or without U: Crosstalk between MMR and BER in E. coli”

Oktober 2009 Gießen, Deutschland: GGL Konferenz

Presentation: “With or without U: Crosstalk between MMR and BER in E. coli”

September 2009 Posen, Polen: IRTG-Workshop “Bioinformatik”

Juni 2009 Whistler, Kanada: ASM Konferenz "DNA repair and mutagenesis"

Poster: "Physical and functional interaction between E. coli MutL and the Vsr endonuclease"

Mai 2009 Paris, Frankreich: mismatch2model (mm2m) Meeting

Presentation: "Generation of circular DNA substrates containing mismatches and modifications to study DNA mismatch repair in vitro"

März 2009 Schloss Rauischholzhausen, Deutschland: IRTG- / MC RTN "DNA Enzyme" Workshop „Pathway to a European Career"

Oktober 2008 Gießen, Deutschland: GGL Konferenz

Poster: "Activation of MutH and UvrD by MutL during MMR"

März 2008 Schloss Rauischholzhausen, Deutschland: IRTG workshop

Poster: "Trapping transient MutL-MutH complexes"

Februar 2008 Moskau, Russland: IRTG Offspring-Meeting

Presentation: "Creation of long circular DNA containing mismatches or modifications"

Juni 2007 Suzdal, Russland: IRTG-Workshop

Presentation: "Dangerous liaison: Trapping transient MutL-MutH complexes – Functional and structural characterization"

Oktober 2006 Gießen, Deutschland: IRTG Kick-Off-Meeting

Summary

Beside the repair of numerous different DNA lesions (mismatches, IDL's) that appear during replication or recombination, the DNA mismatch repair (MMR) system also recognizes and eliminates mismatches caused by spontaneous or actively induced deamination that are mainly repaired by the very-short patch repair (VSPR) or base-excision repair (BER) (1-4). Consequently, precise but almost unknown mechanisms guarantee the complex and coordinated crosstalk between these repair pathways that can either compete or cooperate for process of T:G and U:G mismatches *in vivo* (5,6). Considering the role of MMR in several processes of DNA metabolism (1), it is of interest to understand how the crosstalk in DNA mismatch repair is regulated in order to assure that DNA is repaired correctly and unfavoured or simultaneous repair processes resulting in additional DNA lesions are avoided. Although under investigation since over 25 years, discovering and monitoring how MMR proteins hand off damages or mismatches to suitable downstream repair factors and therefore interact with components involved in other DNA repair pathways remains still a significant challenge.

General aim of this study was to investigate whether and how VSPR and BER have an influence on the mechanism of MMR thereby regulating the crosstalk in DNA mismatch repair. For that reason, it was investigated in detail how these in principle competing systems affect the functions of MutS and MutL as the transient *damage sensor and signalling complex* which plays the major role in damage signalling and recruitment of downstream repair factors (7,8). To this end, generation of suitable circular DNA substrates as well as development of specific DNA repair assays was required for complete reconstitution of initial steps in MMR, VSPR and BER *in vitro* and for subsequent investigations in mutual influences by these pathways during repair of a common target.

In consideration of the fact that specific mismatch recognition and binding by MutS denotes the first step in MMR, established FRET assays (*Fluorescence*

Resonance Energy Transfer) were performed to analyze whether and how processing of T:G and U:G mismatches by Vsr or UDG affects further mismatch recognition by the damage sensor MutS. This assay allows detection of specific mismatch-provoked DNA bending by MutS during formation of the *initial recognition complex* (IRC) which is essential for initial steps in DNA mismatch repair (9).

The results achieved in this work reveal in which way MMR, VSPR and BER affect each other during the crosstalk to assure that the DNA substrate is repaired efficiently. It turned out that Vsr (VSPR) belongs to the group of effector proteins such as MutH and UvrD (both MMR) that are recruited and activated in a mismatch- and ATP-dependent manner by the *damage sensor and signalling complex* (MutSL) (cooperation). However, these effector proteins in principle compete for recruitment and activation by the transient MutSL complex and consequently for initiation of repair (competition). The obtained results explain the observations made *in vivo* and the functional connection between MMR and VSPR suggests that MutS, MutL and Vsr build up a repair system (*enhanced VSPR*) that guarantees fast and efficient restoration of the DNA methylation pattern in *E. coli* when Vsr is limiting. Finally, the developed DNA repair assays permit to investigate whether enhanced VSPR is a general pathway also used in other organisms. Generation of suitable circular DNA substrates might also allow studying the crosstalk of MMR with further competing DNA repair systems.

Due to the fact that binding of the same T:G mismatch by MutS and Vsr simultaneously is mutual exclusive, the achieved results support the model in which MutS leaves the mismatch in form of a *sliding clamp* and a transient mobile MutSL complex recruits and activates downstream repair factors in order to initiate repair. This model is also supported by the fact that activation of MutH by MutSL is efficient when the DNA damage is only a few base pairs away from the next strand discrimination signal.

In contrast to VSPR, the BER system in principle prevents misengaged procession of DNA by the MMR machinery via quickly conversion of a U:G mismatch into a non-mismatch due to release of uracil. Although the appearing AP-site denotes an important DNA lesion that is structurally similar to an IDL,

surprisingly this damage is not recognized by MutS. Consequently, formation of the transient MutSL complex and subsequent activation of effector proteins resulting in eventually misengaged procession of DNA will be avoided. The possibility to convert a mismatch into a non-mismatch by UDG might be used for further functional studies of the *multiple loading* model which is used to explain how initiation and completion of MMR is achieved (7).

To answer the question whether MutS indeed leaves a mismatch after recognition in form of the proposed *sliding clamp*, it was attempted to couple MutS covalently to the DNA while binding to a T:G mismatch, thereby trapping the transient MutS-DNA complex for further functional and structural studies. Using the single-cysteine variants of MutS N468C and N497C as well as a modified DNA substrate it was possible to trap two transient MutS-DNA complexes via thiol-specific site-directed crosslinking and therefore to put a leash on MutS. Both complexes were successfully purified and represent the optimal starting point for further functional (ATPase activity, DNA bending, initiation of MMR) and structural studies (crystallization of the *sliding clamp*) in steps after mismatch recognition by MutS.

Zusammenfassung

Das DNA *mismatch repair* (MMR) System erkennt und beseitigt neben einer Vielzahl unterschiedlicher Replikationsfehler (*mismatches*, IDL's) auch diejenigen Basenfehlpaarungen (*mismatches*), die nach spontaner oder aktiv induzierter Deaminierung entstehen und bevorzugt durch das *very-short patch repair* (VSPR) oder *base-excision repair* (BER) System repariert werden (1-4). Aus diesem Grund gewährleisten nicht im Detail verstandene Mechanismen ein komplexes und koordiniertes Zusammenspiel (*crosstalk*) dieser Reparatursysteme, welche bei der Prozessierung von T:G bzw. U:G Basenfehlpaarungen *in vivo* sowohl konkurrieren als auch kooperieren können (5,6). Da das MMR-System eine wichtige Rolle bei zahlreichen Prozessen im DNA Metabolismus spielt, ist es von Interesse zu verstehen, wie dieser *crosstalk* reguliert wird und so gewährleistet werden kann, dass die DNA effizient repariert wird. Obwohl seit 25 Jahren erforscht, ist es weiterhin eine Herausforderung, zu untersuchen, wie das MMR-System einen DNA-Schaden an geeignete Effektor-Proteine übergibt und dabei mit Komponenten potentiell konkurrierender Reparatursysteme funktionell interagiert.

In der vorliegenden Arbeit wurde daher *in vitro* untersucht, ob und wie VSPR bzw. BER auf bedeutende Aspekte im Mechanismus des MMR-Systems Einfluß nehmen und so den *crosstalk* regulieren. So wurde besonders analysiert, welche Auswirkungen die Anwesenheit eines konkurrierenden Systems auf die Funktionen des transient gebildeten *damage sensor and signalling complex* (MutSL-Komplex) hat (7,8). Zu diesem Zweck wurden spezielle zirkuläre DNA-Substrate hergestellt, sowie spezifische Reparatur-Assays entwickelt, die es erlaubten die initialen Schritte von MMR, VSPR und BER vollständig *in vitro* zu rekonstruieren. Dadurch war es möglich, die wechselseitigen Einflüsse zweier um die Beseitigung einer T:G bzw. U:G Basenfehlpaarung konkurrierender Systeme in Konkurrenzexperimenten zu analysieren.

Da die spezifische Erkennung und Bindung eines Schadens durch MutS den ersten Schritt bei MMR darstellt, wurde mit Hilfe eines etablierten FRET-Assays (*Flourescence Resonance Energy Transfer*) untersucht, ob und wie die Prozessierung einer T:G bzw. U:G Basenfehlpaarung durch VSPR bzw. BER die *mismatch*-Erkennung beeinflusst. Dieser Assay gestattet es, das *mismatch*-abhängige Biegen (*bending*) der DNA durch MutS und somit die Bildung des für die Reparatur essentiellen *initial recognition complex* (IRC) zu detektieren (9).

In dieser Arbeit konnte erfolgreich gezeigt werden, auf welche unterschiedliche Art und Weise MMR, VSPR und BER sich gegenseitig beeinflussen und so im *crosstalk* miteinander eine effiziente Reparatur der DNA gewährleisten. So stellte sich heraus, dass Vsr (VSPR), wie MutH und UvrD (MMR), zur Gruppe der Effektor-Proteine gehört, die durch den *damage sensor and signalling complex* (MutSL-Komplex) in einer *mismatch*- und ATP-abhängigen Reaktion aktiviert bzw. stimuliert werden (Kooperation). Dabei konkurrieren diese Effektor-Proteine um die Rekrutierung und Aktivierung durch den transient gebildeten MutSL-Komplex und somit um die Initiierung der Reparatur (Kompetition). Die erzielten Ergebnisse erklären die *in vivo* beobachtete funktionelle Beziehung zwischen MMR und VSPR und lassen vermuten, dass MutS, MutL und Vsr in *E. coli* ein eigenständiges Reparatur-System (*enhanced VSPR*) bilden, welches eine schnelle und effiziente Wiederherstellung des DNA-Methylierungsmusters gewährleistet, auch wenn Vsr limitiert ist. Mit Hilfe der hier entwickelten Reparatur-Assays ist es möglich *in vitro* zu untersuchen, ob *enhanced VSPR* ein generelles Reparatursystem darstellt, welches auch in anderen Organismen existiert. Die angewendete Methode zur Herstellung geeigneter zirkulärer DNA-Substrate gestattet es, den *crosstalk* des MMR-Systems mit weiteren, potentiell konkurrierenden Reparatursystemen funktionell zu analysieren.

Da ausgeschlossen werden kann, dass MutS und Vsr gleichzeitig an ein T:G *mismatch* binden, unterstützen die hier erzielten Ergebnisse das Modell, bei dem MutS den zuvor erkannten Schaden in Form einer *sliding clamp* verlässt und anschließend ein transient mobiler MutSL-Komplex je nach Bedarf die anwesenden Effektor-Proteine rekrutiert und so die Reparatur einleitet (7). Dieses Modell wird

zusätzlich dadurch unterstützt, dass MutH durch MutSL effizient aktiviert wird, wenn der erkannte DNA-Schaden nur vier Basenpaare vom nächsten Strang-Diskriminierungssignal entfernt ist.

Im Gegensatz zu VSPR verhindert das BER-System im Prinzip ein unerwünschtes Prozessieren der DNA durch das MMR-System, indem UDG (BER) eine U:G Basenfehlpaarung sehr schnell durch Entfernen des Uracils „entschärft“. Obwohl die dabei entstehende AP-site einen bedeutenden DNA-Schaden darstellt und einer Insertion bzw. Deletion (IDL) strukturell ähnelt, ist MutS entgegen den Erwartungen nicht mehr in der Lage diesen Schaden zu erkennen. Dadurch kann die Bildung des *damage sensor and signalling complex* (MutSL-Komplex), sowie die anschließende Rekrutierung und Aktivierung von Effektor-Proteinen nicht erfolgen und ein unerwünschtes Prozessieren der DNA wird verhindert. Die Möglichkeit mit Hilfe von UDG einen zuvor erkannten Schaden für MutS unkenntlich zu machen, kann in Zukunft zur funktionellen Untersuchung des *multiple loading* Models genutzt werden, welches beschreibt, wie das koordinierte Einleiten und Beenden von MMR gewährleistet wird (7).

Um untersuchen zu können, ob MutS wie vermutet einen Schaden nach dessen Erkennen in Form einer *sliding clamp* wieder verlässt, wurden erste Versuche unternommen MutS während der Bindung einer T:G Basenfehlpaarung kovalent an die DNA zu koppeln und so den transienten MutS-DNA Komplex für weitere funktionelle und strukturelle Studien einzufangen. Unter Verwendung der *single-cysteine* Varianten MutS N468C und N497C sowie einem mit einer Thiol-gruppe modifiziertem DNA-Substrat war es möglich zwei transiente MutS-DNA Komplexe mittels thiol-spezifischem *site-directed crosslinking* einzufangen und den mismatch sensor sozusagen an die „Leine“ zu nehmen. Diese Komplexe konnten erfolgreich aufgereinigt werden und bilden somit den optimalen Startpunkt für weitere funktionelle (z.B. ATPase Aktivität, DNA Biegung, Initiierung der DNA Reparatur) und strukturelle Studien (z.B. Kristallisation von MutS als *sliding clamp*), welche dabei helfen können, die einzelnen Schritte nach der mismatch-Erkennung genauer zu untersuchen und aufzuklären.

Abbreviations

α	alpha
ADP	adenosine diphosphate
ADPnP	adenosine 5'-(β - γ -imido) triphosphate
AP	apurinic/apyrimidinic (abasic)
ATP	adenosine triphosphate
a.u.	arbitrary unit
β	beta
BER	base-excision repair
bp	base pair
BSA	bovine serum albumin
γ	gamma
ca	circa
ccc	covalent closed circular
Δ	delta
Da	dalton
Dam	DNA adenosine methyltransferase
Dcm	DNA cytosine methyltransferase
DMSO	dimethylsulfoxide
DNA	deoxyribonucleic acid
dNTP	deoxyribonucleic triphosphate
ds	double-strand
DTT	1,4-dithiothreitol
<i>E. coli</i>	<i>Escherichia coli</i>
EDTA	ethylene diamine tetra acetate
e.g.	<i>Exempli gratia</i> (for example)
EtBr	ethidium bromide
FRET	Förster Resonance Energy Transfer
g	gram
HPLC	high performance liquid chromatography
i. e.	<i>It est</i> (such as)
IPTG	isopropyl- β -D-1-thiogalactopyranoside
k	kilo

λ	lambda (wavelength)
l	liter
LB	Luria-Bertani
lin	linear
μ	micro
m	milli
M	molar
min	minute
MMR	DNA mismatch repair
MW	molecular weight
n	nano
n.d.	not determined
nt	nucleotide
Nt.	nicking top
Nb.	nicking bottom
oc	open circular
OD	optical density
o/n	overnight
PAGE	polyacrylamide gel-electrophoresis
PCR	polymerase chain reaction
PMSF	phenylmethane sulphonyl fluoride
Pol	polymerase
r	Anisotropy
Rpm	rotations per minute
RT	room temperature
sc	supercoiled (also used for single-cysteine variants)
SDS	sodium dodecyl sulfate
sec	second
ss	single-strand
SSB	single-strand binding protein
t	time
TEMED	N,N,N',N'-tetramethylethylenediamine
TPE	Tris-phosphate-EDTA
Tris	Tris-(hydroxymethyl)-aminomethane
u	unit
UDG	uracil DNA glycosylase
UV	ultraviolet
v	volume
vs.	versus
VSPR	very-short patch repair

Table of contents

Summary	6
Zusammenfassung	4
Abbreviations	7
Table of contents	9
1 Introduction	11
<i>1.1 DNA mismatch repair - MMR</i>	14
1.1.1 MutS – the mismatch sensor.....	19
1.1.2 MutL – the molecular matchmaker	22
1.1.3 MutH – the strand discrimination endonuclease	25
1.1.4 UvrD – the strand excision helicase	26
<i>1.2 Very-short patch repair - VSPR</i>	28
1.2.1 Vsr – the mismatch recognizing endonuclease	29
1.2.2 Crosstalk between MMR and VSPR	30
<i>1.3 Base-excision repair - BER</i>	33
1.3.1 UDG – the sensor of uracil	34
1.3.2 Crosstalk between MMR and BER	36
<i>1.4 Fluorescence - FRET</i>	37
<i>1.5 Aim</i>	40
2 Materials and Methods	44
<i>2.1 Materials</i>	44
2.1.1 Reagents	44
2.1.2 Buffers	45
2.1.3 Enzymes and Proteins.....	47
2.1.4 Oligonucleotides	47
2.1.5 Plasmids.....	50
2.1.6 Strains	51
2.1.7 Protein / DNA marker	51

2.2	<i>Methods</i>	52
2.2.1	Protein expression and purification	52
2.2.2	DNA expression and purification	53
2.2.3	Site-directed mutagenesis of MutL	53
2.2.4	Generation of modified circular DNA substrates	54
2.2.5	Complementation mutator assay	56
2.2.6	Mismatch-provoked MutH endonuclease assay	56
2.2.7	Mismatch-provoked UvrD unwinding assay	57
2.2.8	Vsr endonuclease assay	57
2.2.9	Base-excision repair assay	58
2.2.10	MutS binding and DNA bending assay (FRET).....	58
2.2.11	Site-directed crosslinking of MutS to DNA	59
2.2.12	Purification of trapped MutS-DNA complexes	61
3	Results	62
3.1	<i>Generation of circular DNA repair substrates</i>	62
3.2	<i>Monitoring methyl-directed mismatch repair (MMR) in vitro</i>	66
3.2.1	Mismatch-provoked strand discrimination by MutH	67
3.2.2	Mismatch-provoked strand excision by UvrD	68
3.2.3	Reconstitution of UvrD/RecJ-independent MMR <i>in vitro</i>	72
3.3	<i>Crosstalk between MMR and VSPR in E. coli</i>	74
3.3.1	Initiation of very-short patch repair (VSPR) <i>in vitro</i>	75
3.3.2	Vsr inhibits activation of MutH by MutS and MutL.....	77
3.3.3	Vsr endonuclease activity is stimulated by MutS and MutL.....	79
3.3.4	Reconstitution of enhanced VSPR <i>in vitro</i>	82
3.3.5	Intermediate of VSPR triggers initiation of MMR.....	85
3.4	<i>Crosstalk between MMR and BER in E. coli</i>	90
3.4.1	Initiation of base-excision repair (BER) <i>in vitro</i>	91
3.4.2	Intermediate of BER inhibits initiation of MMR	92
3.4.3	AP-sites avoid formation of the IRC	95
3.5	<i>Trapping of transient MutS-DNA complexes</i>	102
4	Discussion	111
5	References	128

1 Introduction

Maintaining of genome stability and DNA integrity denotes a fulltime challenge for all organisms. Permanent attack by endogenous metabolic products and exogenous environmental factors results in modification of the chemical DNA structure which may alter the encoded message (10). DNA damages or mismatches arise thousands of times per day due to oxidation, deamination, methylation and alkylation of bases, X-rays, replication errors or UV light. To guarantee the stability and integrity of the genome, several important DNA repair pathways have evolved that recognize and remove different types of lesions (11,12). A failure of these repair processes with critical importance for life results in cell-cycle arrest, cell death or causes diseases such as cancer (Figure 1-1) (13).

As the consequence of evolution some of these DNA repair systems have overlapping specificities, giving rise to the need to coordinate their activities in a well-nuanced relationship (crosstalk). The repair of DNA mismatches caused by misincorporation or chemical modification of bases falls into this category (Figure 1-2) (6). Unlike replication errors that mainly occur in the nascent DNA strand, chemical modifications can affect bases in both strands. Especially repair of U:G and T:G mismatches caused by spontaneous or induced deamination of cytosine and 5-methylcytosine (5meC) appears to be a straightforward task for the repair machinery (14). Uracil represents a distinctive foreign base in DNA and 5-methylcytosine is used by many organisms ranging from bacteria to mammals as a physical or epigenetic tag that allows them to distinguish between DNA from different sources lacking this modification. A wide variety of biological phenomena including restriction-modification, gene silencing, epigenetic inheritance and stimulation of an immune response use C5-methylation of DNA (15-17).

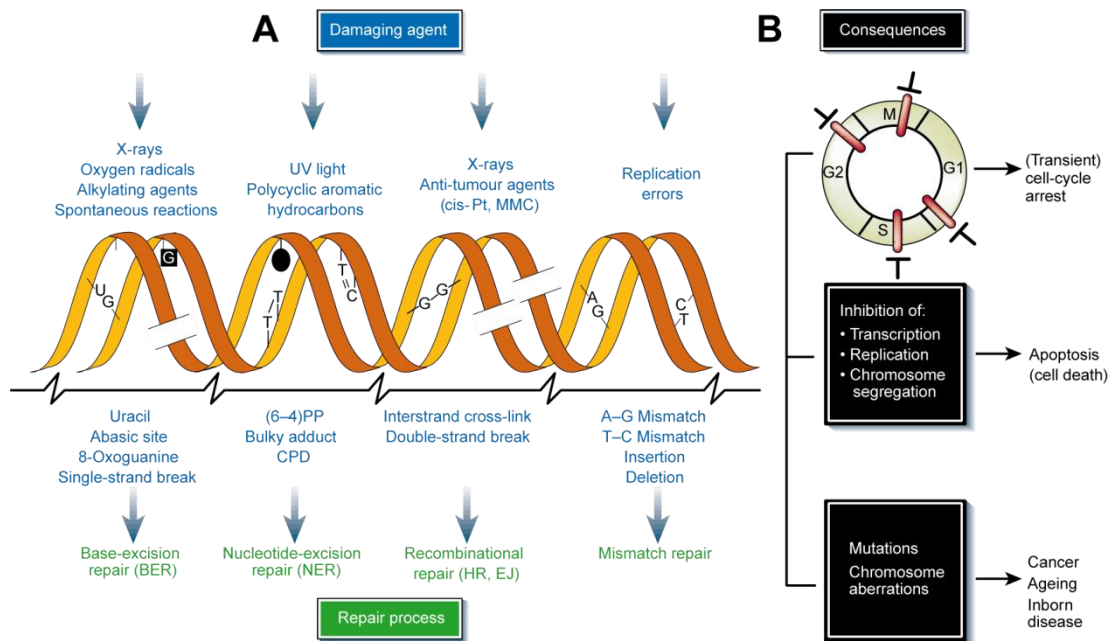


Figure 1-1: DNA damage, repair mechanisms and consequences

A: Endogenous and exogenous DNA damaging agents (top); examples of induced DNA lesions (middle); and relevant DNA repair mechanisms responsible for repair of the lesions (bottom). **B:** Effects of DNA damage on cell-cycle progression (top) and DNA metabolism (middle). Long-term consequences of DNA injury (bottom) include permanent changes in the DNA sequence (point mutations or chromosome aberrations) and their biological effects. Abbreviations: cis-Pt and MMC, cisplatin and mitomycin C, respectively (both DNA-crosslinking agents); (6-4)PP and CPD, 6-4 photoproduct and cyclobutane pyrimidine dimer, respectively (both induced by UV light); BER, base-excision repair; NER, nucleotide-excision repair; HR, homologous recombination; EJ, end joining (11).

The highly conserved DNA mismatch repair (MMR) system which is in the focus of this study, recognizes and removes various DNA mismatches as well as small insertion and deletion loops (IDL's) that arise during replication or recombination (1,2). Although in principle a target for MMR, repair of U:G and T:G mismatches caused by deamination require repair systems capable of excising the irregular and potentially mutagenic base, irrespective of the DNA strand it is located in and therefore repair by MMR seems of little use here. Even if such mismatches arise during replication, repair directed to the newly synthesized strand would generate mutations whenever the lesion occurred in the parental DNA strand (Figure 1-2). On the other hand, MMR in non-replicating DNA would fix mutations because of the inability of this system to identify the mutagenic base (6). In general these

lesions are removed by specialized systems such as the base-excision repair (BER) system which is the primary DNA repair pathway that corrects DNA lesions caused by oxidation, alkylation and deamination of bases or the very-short patch repair (VSPR) system found in many bacteria (3,4). Notably, beside repair of mismatches induced by deamination, also other lesions require a coordinated crosstalk in DNA mismatch repair. Oxidation of G results in an 8-oxoG:A mismatch after replication that is either recognized by MMR or MutY/OGG (8-oxoguanine DNA-glycosylase) which belongs to one of various BER systems (18). Furthermore, methylation of G produces a O⁶-methylguanine:C lesion that is also targeted by MMR or MGMT (O⁶-Methylguanine-DNA methyltransferase) (19).

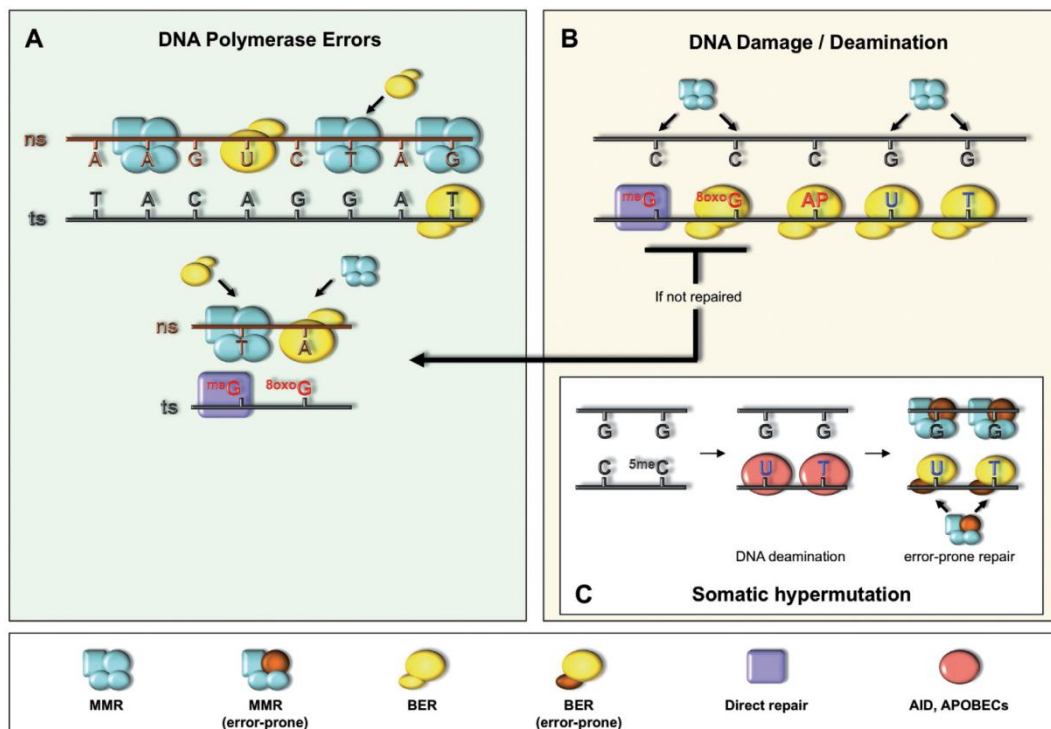


Figure 1-2: Repair of single base mismatches arising under various circumstances

The panels schematically illustrate the involvement of different pathways contributing to the repair of mismatches emerging from DNA polymerase errors (A), by DNA damage (B) or induced during somatic hypermutation (C) (6).

In consideration of fact that deamination or oxidation events trigger in principle initiation of various DNA repair systems simultaneously, crosstalk between these systems in order to assure that DNA is repaired efficiently and correctly is obvious. So far, the mechanisms that regulate the complex and coordinated crosstalk between MMR, VSPR and BER during repair of a common target are not well understood and therefore in the focus of this study. Discovering and monitoring how MMR proteins hand off damages or mismatches to suitable downstream repair factors and therefore interact with components involved in other DNA repair pathways remains a significant challenge.

1.1 DNA mismatch repair - MMR

Misincorporation of bases that escape proofreading during DNA replication results in the formation of mismatches and insertion or deletion loops (IDLs). The DNA mismatch repair (MMR) system plays a central role in maintaining genome stability and DNA integrity by correcting DNA replication errors, thereby decreasing the mutation rate by a factor of 100-1000 (20,21). The link between human cancer and defects in MMR led to an extensive research on this DNA repair system. Mutations in mismatch repair genes correlate with cancer predisposition syndromes such as hereditary nonpolyposis colon cancer (HNPCC) and familial colorectal cancer (22,23). In addition, inactivation of mismatch repair genes by promoter methylation was observed in some sporadic tumors (24). Especially useful for cancer research is the renowned instability of long repetitive DNA sequences, i.e. microsatellites. These are replicated inaccurately owing to frequent strand slippage and inefficient proofreading, leaving MMR as the major guardian against microsatellite deterioration. For this reason, microsatellite mutability is now an established biomarker for loss of MMR activity in tumor cells (25). MMR is also involved in the response of cells to DNA damaging agents, such as oxidating and methylating agents, X-rays, UV light and DNA intercalators (6). Moreover, MMR proteins link DNA damage recognition to cell-cycle checkpoint activation and survival (Figure 1-1). Intermediates of this process induce DNA damage signalling

and trigger apoptosis (1). Loss of their function results in decreased apoptosis, increased cell survival, and resistance to chemotherapy (25). Likewise, defects in the mismatch repair system of prokaryotes cause an increased mutation rate that could lead to a rise in survival under stress conditions. This has implications in evolution and emergence of drug resistant strains of pathogenic microbes (25). MMR proteins are also involved in preventing recombination between similar but non-identical DNA sequences, meiotic chromosome pairing and segregation, immunoglobulin class switching and somatic hypermutation (1,26,27).

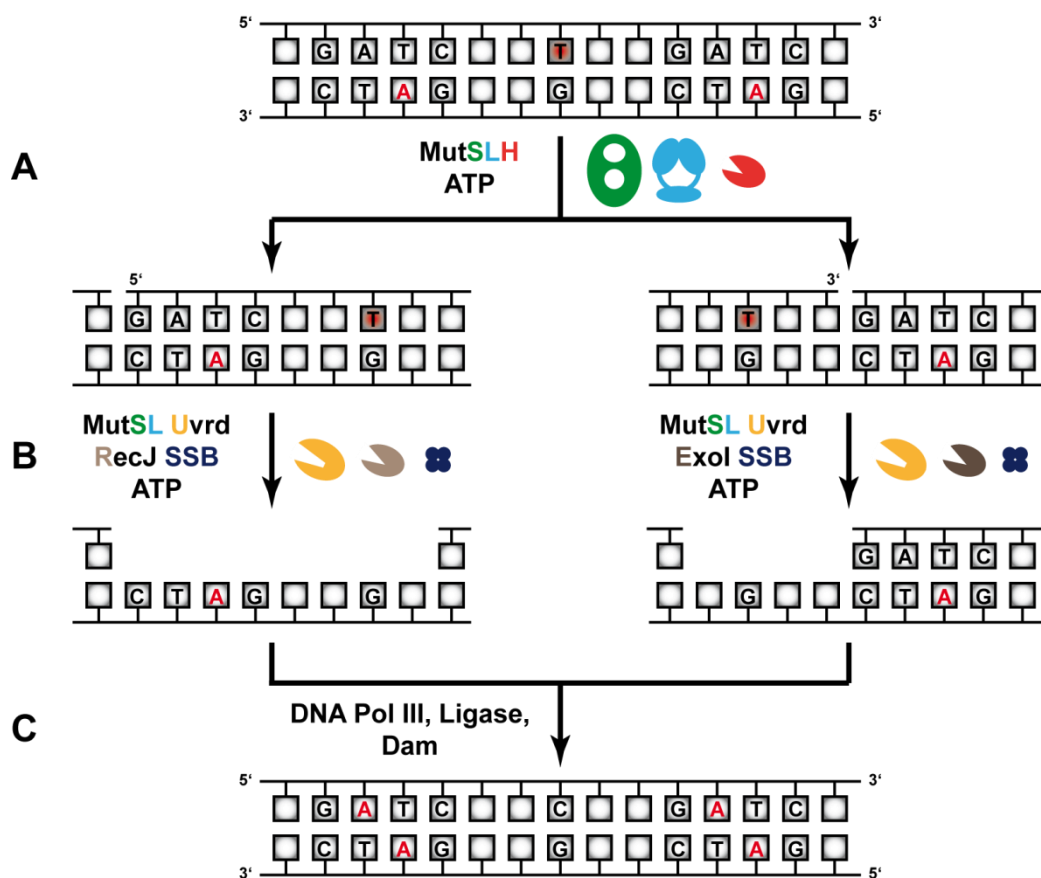


Figure 1-3: Overview of methyl-directed mismatch repair in *E. coli*

A: Mismatch recognition and strand discrimination: Mismatched T (red square) is recognized by MutS (green) resulting in recruitment of MutL (blue) and subsequent activation of MutH (red). Strand discrimination by MutH occurs up to 1000 bp away either upstream (left) or downstream of the mismatch (right). **B:** Mismatch-provoked strand unwinding and degradation: DNA unwinding by UvrD towards the mismatch and single-strand degradation by orientation-dependent exonucleases generates a single-strand gap, protected by SSB. **C:** DNA re-synthesis: Restoration of C:G basepair and methylation pattern (red letters) by DNA polIII and the Dam methyltransferase, respectively. Finally, the nick is sealed by a ligase.

The *E. coli* methyl-directed mismatch repair system is the best characterized MMR pathway and has been reconstituted completely *in vitro*, reviewed in (2,25). Three proteins, MutS, MutL and MutH, are important to perform mismatch recognition and strand discrimination which is required for accurate initiation of DNA mismatch repair. MutS and MutL are evolutionarily conserved and homologues have been found among all kingdoms of life (20,28). This suggests that the basic mechanisms of mismatch repair are similar in all organisms. MMR is initiated after mismatch or IDL recognition and binding by MutS, which plays a role as a damage and mismatch sensor (Figure 1-3) (29,30). Mismatch-provoked induced conformational changes in MutS result in recruitment of MutL, the next key protein in MMR (7). MutL is a so called molecular matchmaker and has the capability to activate or stimulate downstream effector molecules in an ATP-hydrolysis dependent manner (31,32). Activation of the latent MutH endonuclease by MutL is required for strand discrimination in *E. coli* during MMR. MutH nicks the erroneous and transiently unmethylated daughter strand at a hemi-methylated GATC-site (Figure 1-3A).

Considering that strand incision by MutH can occur up to 1000 base pairs away and either downstream or upstream of a mismatch, several models exist how mismatch recognition is coupled to strand discrimination by MutSL (Figure 1-4) (33,34). In the most prominent model, the transient *damage sensor and signalling complex* (MutSL) is mobile and dissociates from the mismatch after recognition due to formation of a *sliding clamp* by MutS which is triggered by binding, but not hydrolysis of ATP (*Sliding clamp* model) (7,35). In the second model, mismatch binding by MutS induces polymerization of MutL on the DNA towards a hemi-methylated GATC-site (Polymerization model) (36). In the last model, MutS is stationary and stays at the mismatch together with MutL. MutH is activated at the target site via looping of the DNA in an ATP-dependent manner (*Looping* model) (37).

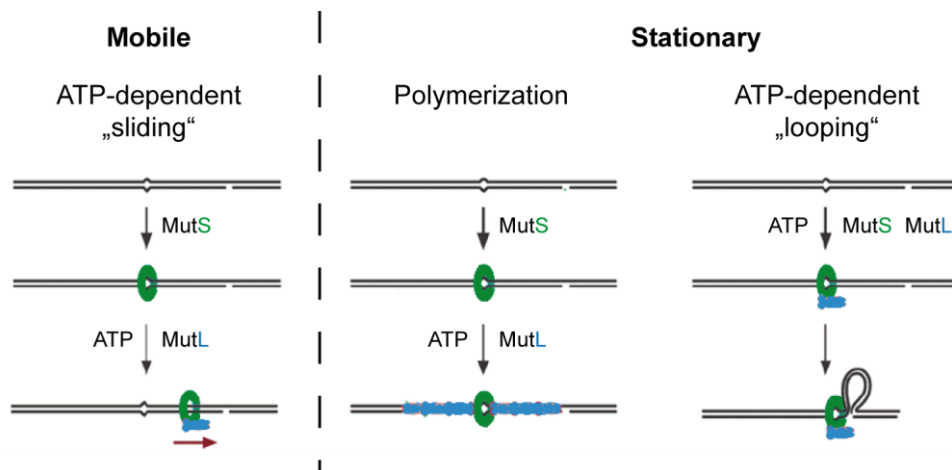


Figure 1-4: Models for coupling of mismatch recognition and strand discrimination
(Modified after Iyer, Pluciennik et al. 2006)

Finally, the generated nick by MutH serves as an entry point for further repair. In *E. coli*, mismatch-provoked activation of the UvrD helicase by MutSL promotes DNA unwinding starting from the nick towards a mismatch and therefore allows excision of the erroneous DNA strand (38,39). The appearing single-strand is degraded by several exonucleases and depending on the orientation, ExoI is necessary for DNA degradation when strand discrimination occurred downstream whereas RecJ is required when the nick was introduced upstream of the mismatch (33,40). During MMR, the parental DNA strand is protected by the single-strand binding protein SSB to avoid degradation (Figure 1-3B) (41,42). Re-synthesis of DNA and nick sealing which is achieved by polymerase III and ligase, respectively, complete the repair process. In an additional step the hemi-methylated GATC-site is fully methylated by the DNA adenosine methyltransferase (Dam) to restore the methylation pattern after replication (Figure 1-3C) (43).

The eukaryotic MMR system shares main features of the *E. coli* MMR system and has been also reconstituted *in vitro* (Table 1-1) (2,44). MutS homologues MSH2-MSH6 (MutS α) and MSH2-MSH3 (MutS β) recognize different types of mismatches and initiate repair (45-47). Another MutS homologue, MSH4-MSH5, is involved in meiotic recombination (48,49). Homologues of MutL, MLH1-PMS2 (MutL α), MLH1-MLH2 (MutL β) and MLH1-MLH3 (MutL γ), take also part in the

repair of different types of damages and mismatches (50-52). Considering that no MutH homologue has been detected in eukaryotic and most of bacterial genomes so far, the question how strand discrimination occurs in these systems is still unclear. Discontinuities, gaps or nicks that arise in the DNA during replication have been suggested as the discrimination signal in the organisms that lack MutH homologues (2). The lack of a functional MMR system results in various forms of genomic instability like elevated frequencies of point and DNA slippage mutations, chromosomal rearrangements, gene amplification and radio-resistant DNA synthesis (53-55). In mammals, the mutator phenotype conferred by loss of MMR activity contributes to the initiation and promotion of multi-stage carcinogenesis (24,56). The main form of cancer that results from the loss of MMR functionality is the hereditary nonpolyposis colon cancer (21).

Table 1-1: Comparison of *E. coli* and eukaryotic MMR components

<i>E. coli</i>	Homologue	Function
MutS	MutS α (MSH2/MSH6) MutS β (MSH2/MSH3) MSH4/MSH5	Recognition of mismatches Recognition of IDL's Meiotic recombination
MutL	MutL α (MLH1/PMS2) MutL β (MLH1/PMS1) MutL γ (MLH1/MLH3)	Molecular matchmaker with intrinsic endonuclease unknown Repair of IDL's, Meiotic recombination
MutH	-	Strand discrimination
UvrD	-	Strand excision
ExoI, VII, X, RecJ	EXO1	Strand degradation
Polymerase III	DNA-Polymerase δ	Strand synthesis
SSB	RPA	Involved in strand excision and synthesis
DNA-ligase	DNA-ligase	Nick sealing
Dam	-	Methylation of GATC-sites

1.1.1 MutS – the mismatch sensor

Efficient initiation of MMR requires the discrimination between intact and damaged DNA by the repair machinery. The key component in this process is MutS which has the capability for mismatch recognition and damage signalling (57). Insights into mismatch recognition come from co-crystal structures of both *E. coli* and *Taq* MutS bound to heteroduplex DNA, respectively (58-60). The prokaryotic MutS protein consists of two identical, “comma” shaped subunits forming a symmetric homo-dimer which is similar to the Greek letter θ , with two adjacent channels (Figure 1-5) (59,61). Co-crystal structures also revealed that heteroduplex DNA is threaded through the larger of the both channels, but the functional significance of the empty channel is still unknown. However, size and charge of the smaller channel suggest that it might also be able to accommodate a DNA segment (62).

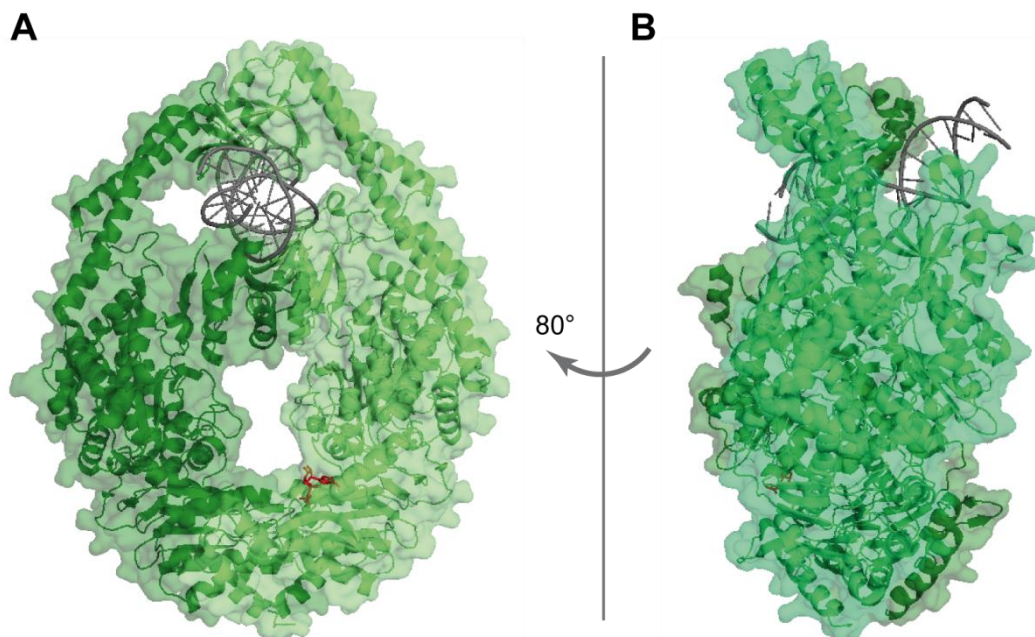


Figure 1-5: Crystal structure of the MutS-DNA complex

A: *E. coli* MutS homo-dimer in complex with DNA front view (pdb code: 1e3m). DNA (grey) is threaded through the upper, larger channel. Mismatch binding monomer contains the ADP (red) and is coloured in light green. **B:** Side view by rotation of 80°. DNA is kinked with an angle of ~60°, thereby forming the *initial recognition complex* (IRC) (59).

Each monomer subunit consists of at least five distinct domains important for MutS structure and function. Mismatch recognition is achieved by the N-terminal located *mismatch-recognition* domain (residues 2-115). The *clamp* domain (residues 444-503) is supposed to be required for *sliding clamp* formation after binding of ATP. Moreover, the *mismatch-recognition* domain possesses no overall positive charge, suggesting that the *clamp* domain is also involved in DNA scanning. The C-terminus contains the *ATPase* domain (residues 568-765), including the Walker ATP-binding motif and the primary MutS dimerization interface of the *helix-turn-helix* domain (*HTH*, residues 766-800). Since the truncated form of MutS was used for crystallization, the structure of the C-terminal 53 amino acids (CTD, residues 800-853) remains to be determined. Moreover, no structural data is available of MutS binding to homoduplex DNA (scanning) or forming a *sliding clamp* in the presence of ATP (63).

MutS is proposed to scan DNA in search for a mismatch, thereby testing the flexibility of the DNA (57,64). The energetic difference between a normal and a mismatched base pair is thought to be around 2-3 kcal/mol which is translated into a 100-1000 fold higher affinity of MutS for mismatched DNA (65). Mismatch recognition depends on the conserved residues Phe36 and Glu38 (*E. coli* numbering) within the *mismatch-recognition* domain of one subunit resulting in a functional asymmetric dimer upon mismatch binding (66-68) (Figure 1-6). This functional asymmetry is emphasized in human MutS homologues where only MSH6 contains the conserved Phe-X-Glu motif (69-71). Mismatch recognition and binding by a MutS dimer results in a kinked DNA with an angle of $\sim 60^\circ$, thereby forming the *initial recognition complex* (IRC) in the presence of ADP, which is indispensable for initiation of MMR (Figure 1-6A) (59,72,73). The DNA flexibility around the wobble T:G pair results in a modulation of the DNA structure by MutS and allows to stack the Phe36 from the *mismatch-recognition* domain into the DNA (Figure 1-6B). *E. coli* MutS was crystallized bound to five different mismatches: T:G, G:G, A:A, C:A and +T (60,74). In all co-crystal structures a kink of 60° occurs directly at the mismatch, however the base, recognized by Glu38, is different according to the mismatch. In the T:G and +T mismatch, the glutamate interacts with the N3 of the

pyrimidine T (Figure 1-5B) and in the C:A, A:A and G:G mismatches, MutS interacts with the N7 of the purines (A and G) (74). However, the role of Glu38 is puzzling due to the fact that a negatively charged residue is not absolutely required for initiation of MMR (75).

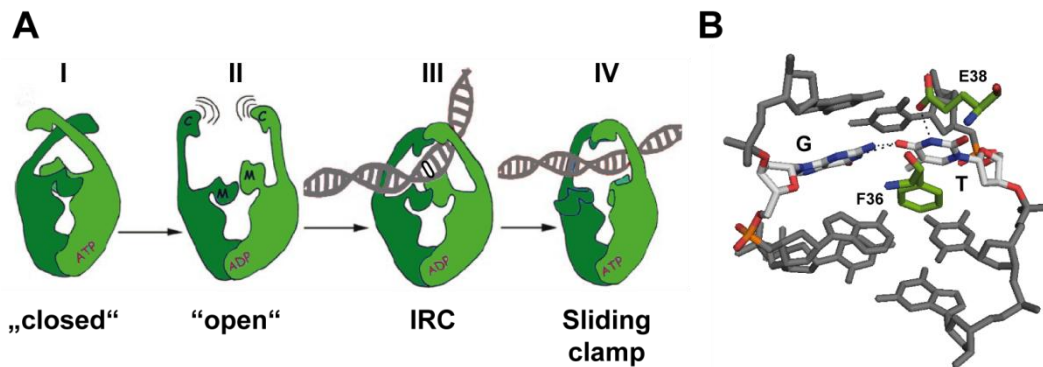


Figure 1-6: Mismatch-provoked conformational changes in MutS

A: MutS adopts a “closed” conformation after binding of ATP, due to a 25° rotation of the two monomers towards each other (I). ATP-hydrolysis results in the “open” conformation which allows DNA binding by the larger channel located between *clamp* (C) and *mismatch-recognition* (M) domain (II). Mismatch recognition by MutS induces a 60° kink within the DNA and formation of the *initial recognition complex* (IRC), which is indispensable for initiation of mismatch repair (III). Subsequent ATP binding causes a further closing of the clamp. To avoid clashing of the *mismatch-recognition* domains, they are rotated away from the DNA, leaving MutS as a *sliding clamp* on the DNA (IV). MutL is proposed to be recruited by MutS after *sliding clamp* formation, which is required for signalling the damage and activation of downstream factors. **B:** DNA kinking and mismatch recognition is achieved by intercalation of F36 within the major groove and specific interaction with the mismatched T by E38, respectively (68).

So far, it is not clear how MutS achieves such a high specificity for mismatches and it was proposed that the ATPase activity might be an answer to this question. The two ATPase domains within the homo-dimer are asymmetric in nucleotide binding and ATP hydrolysis (68,76,77). In the absence of DNA, the rate-limiting step for ATPase activity is release of ADP, whereas binding of MutS to a mismatch greatly enhances the rate of an ADP–ATP exchange (78,79). In contrast to binding to homo-duplex DNA, where ATP is hydrolyzed quickly, binding to a mismatch inhibits fast ATP-hydrolysis (80). This indicates the formation of an ATP-bound MutS state on mismatched DNA with a relatively long lifetime, which allows

mismatch-dependent recruitment of MutL and initiation of repair (8,81). Meanwhile, ATP reduces affinity of MutS for the mismatch itself and induces conversion of the protein into a *sliding clamp* that can diffuse along the DNA helix (7,63). Moreover, ATP binding to MutS induces direct dissociation of the protein from homoduplex DNA (8,82). Specific inhibition of ATP-hydrolysis in the presence of a mismatch and the different modes of dissociation from homo- and heteroduplex DNA indicate that MutS uses ATP to verify mismatch binding and initiate repair, as proposed (65,80). This may explain the high efficiency of the DNA mismatch repair process although initial discrimination between homo- and heteroduplex DNA by *E. coli* MutS is only 8- to 20-fold (83,84).

Several models exist for the role of MutS ATPase in coupling mismatch recognition and strand discrimination over a distance of 1 kb to ATP-hydrolysis (2). In the most favoured *sliding clamp* model, MutS dissociates from a mismatch upon ATP binding and slides along the DNA (7,65). As proposed, this might be the signal for MutL recruitment and therefore the ATPase-cycle regulates subsequent steps in MMR. Notably, the MutS ATPase domain is formed by two not equivalent ATP-hydrolysis pockets with different catalytic efficiency (77,85) leading to the suggestion that the MutS dimer might exist in various nucleotide-occupational states (60). Therefore, details of the MutS ATPase-cycle are still unclear and require further determination.

1.1.2 MutL – the molecular matchmaker

The homo-dimeric *E. coli* MutL couples mismatch recognition by MutS to downstream repair processes during MMR. Beside MutH and UvrD, MutL is proposed to interact with several other proteins and repair factors, not involved in the MMR pathway thereby modulating their activity (Figure 1-7) (86-89).

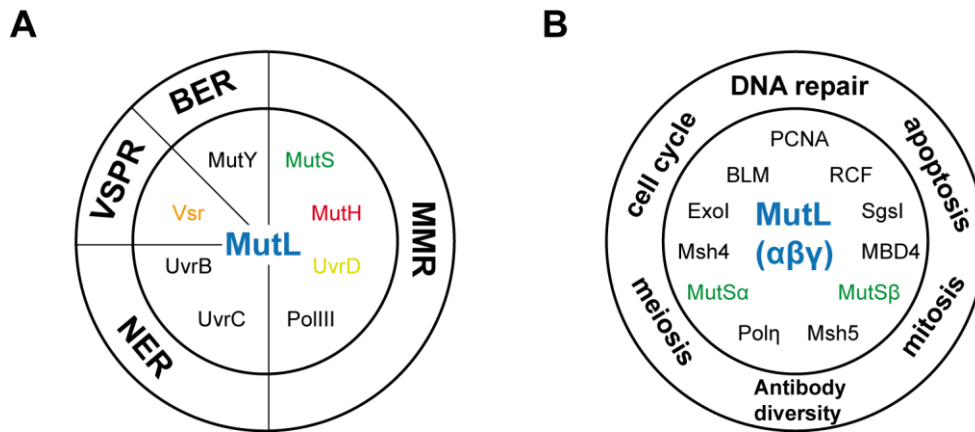


Figure 1-7: Interactions of the matchmaker MutL and their biological significance

A: Well-defined *E. coli* MutL interactions with the indicated components involved in various DNA repair processes. **B:** Involvement of eukaryotic MutL in important DNA metabolic pathways and cellular processes. In comparison to *E. coli* MutL (A), these interactions are still nebulous and not well understood (89).

The MutL monomer consists of a N-terminal domain (NTD, residues 1-349) and a C-terminal domain (CTD, residues 432-615) connected by a long flexible linker (residues 350-431) (Figure 1-8A) (90,91). The activity of MutL is modulated by an ATP-dependent dimerization of the NTD due to the intrinsic ATPase domain, which belongs to the GHKL family (Bergerat-fold) (92). This group includes type II topoisomerases (gyrases), the Hsp90 chaperone proteins, histidine kinases and MutL (93,94). As revealed by crystal structures, the N-terminal 40 kDa fragment of *E. coli* MutL (LN40) and the human homologue PMS2 are mainly in a monomeric form in solution when bound to ADP (32,91,95). On the other hand, in the presence of the non-hydrolysable ATP-analog ADPnP, the LN40 complex is a dimer in the crystal structure, indicating that the γ -phosphate of ATP induces dimerization in solution (Figure 1-8). Nucleotide binding and induced reorganization of the LN40 domain is also required for interaction with MutS, MutH, UvrD and DNA, whereas ATP-hydrolysis is proposed to induce domain dissociation and subsequent release of the interaction partner (89,96,97). The crystallized fragment of the CTD (LC20) forms a 40 kDa dimer in solution which is required for maintaining the dimeric state of MutL thereby keeping two LN40 fragments in spatial proximity (Figure 1-8) (90). However, it has been shown that LC20 by itself can physically interact with MutH

(88,98) and enhances DNA binding of full-length MutL although the CTD alone has no capability to activate MutH or to bind DNA. So far, the structure of full-length MutL remains to be determined.

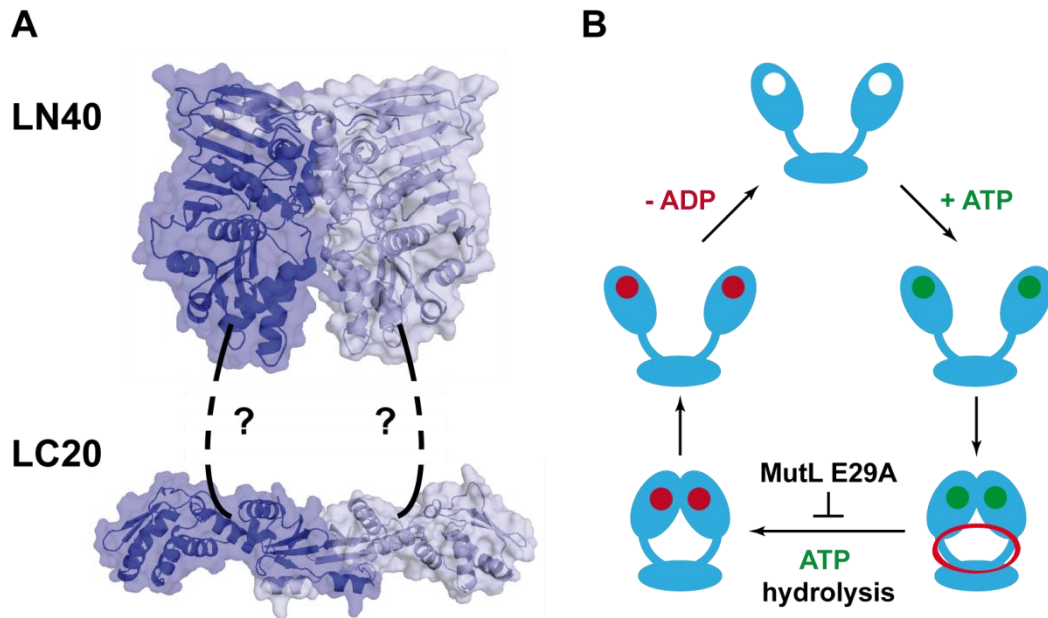


Figure 1-8 Model of full-length MutL

A: Model of full-length MutL. Side view of homo-dimeric LN40 in the presence of ADPnP (pdb code: 1b63), dashed lines show the variable linker, which connects the LN40 fragment with the MutL dimerization domain LC20 (pdb code: 1x9z). Chain A and B of MutL are coloured in dark and light blue, respectively. **B:** Simplified MutL ATPase-cycle. The NTD (LN40) of MutL dimerizes after binding of ATP (green), thereby adopting a “closed conformation”, which allows ATP-hydrolysis. The variant of MutL E29A is impaired in hydrolysis of ATP. After hydrolysis, MutL adopts an “open conformation” and releases ADP (red). The proposed region for interaction of MutL with effector proteins, such as MutH or UvrD, during the ATPase-cycle is indicated by the red circle. Modified from (95,99).

As demonstrated recently, the eukaryotic MutL homologue MutL α (MHL1-PMS2) shows an additional endonuclease activity. The active site, formed by the DQHA(X)₂E(X)₄E motif, is located within the CTD of the PMS2 monomer (100). This motif is conserved in eukaryotic PMS2 homologues and in MutL proteins of bacterial species that do not rely on GATC-site methylation for strand discrimination and therefore lack MutH. The mechanism of strand discrimination in these systems is still under investigation (2).

1.1.3 MutH – the strand discrimination endonuclease

MutH is a monomeric endonuclease that cleaves an unmethylated DNA strand 5' of a GATC-site, in a transiently hemi-methylated (N6-methyl-adenine) sequence context and therefore allows strand discrimination during MMR (Figure 1-3) (101). Mismatch-provoked activation of MutH in the presence of unmethylated GATC-sites will induce double-strand breaks by cleaving each strand independently. On the other hand, MutH does not interact with fully methylated GATC-sites (25). MutH endonuclease activity is greatly stimulated in a mismatch-dependent manner by MutS and MutL (102). Moreover, this stimulation requires ATP-hydrolysis by MutL under physiological conditions (150 mM KCl). Notably, MutL also has the capability to stimulate MutH nicking activity in a mismatch- and ATP-hydrolysis independent manner under conditions of low ionic strength (~50 mM KCl). Crystal structures of MutH from *E. coli* and a co-crystal structures with hemi-methylated DNA from *H. influenzae* were solved (Figure 1-9) (103). The *E. coli* MutH apo-enzyme resembles a clamp with a N- and a C-terminal “arm”, separated by a large cleft. Although the structure of MutH is similar to type II restriction endonucleases, such as PvuII and EcoRV, these proteins do not share significant sequence homology (104). Moreover, Sau3AI which shares sequence homology to MutH, recognizes and cleaves GATC-sites independent of the methylation state. Mutational analysis of highly conserved residues in the cleft demonstrated that Tyr212 is important for sensing the methylation state of a recognition site (105). The active site of MutH is formed by the common catalytic DX_(n)EXK sequence motif and requires Mg²⁺ for catalysis (103,106). In comparison to the apo-protein structure, binding of a cognate DNA sequence by MutH results in a rotation of both arms towards each other by an angle of 6-18° (Figure 1-9B). Helix F which contacts both arms serves as a “lever” and therefore allows the rotation resulting in an open or closed conformation of the central cleft (104).

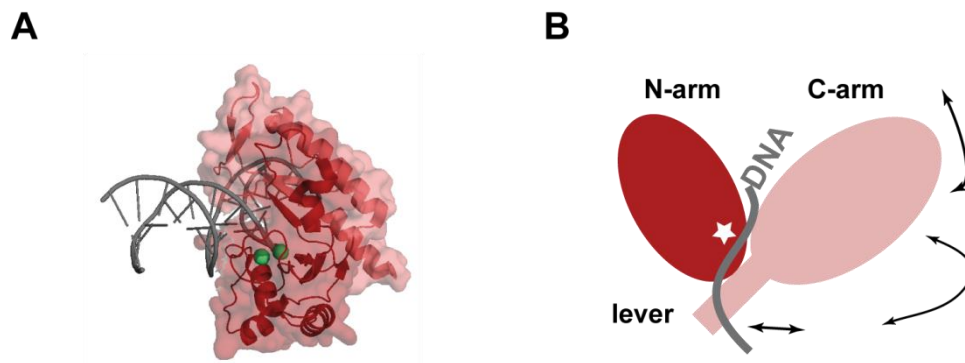


Figure 1-9: Crystal structure of the MutH-DNA complex

A: *H. Influenza* MutH bound to hemi-methylated DNA (pdb code: 2aor) in the presence of Ca^{2+} (green spheres). **B:** Simplified scheme for rotation (denoted by arrows) of the C-arm (light red) relative to the N-arm (dark red). An open conformation of the central cleft allows DNA binding by MutH. The active site of the endonuclease is indicated by the white star. Modified after (104).

However, the mechanism for activation of MutH by MutL is still unclear. MutH contains all elements sufficient for sequence-specific DNA binding and cleavage which does not explain the obvious necessity of a MutL-assistance in either DNA recognition or catalysis. Since the central cleft of MutH in the apo-crystal structure is not wide enough to bind DNA, MutL is proposed to open the central cleft via interaction with the “lever” and therefore allows DNA binding by MutH (103).

1.1.4 UvrD – the strand excision helicase

DNA helicases such as UvrD in *E. coli* are a ubiquitous class of motor enzymes that couple nucleoside-triphosphate (NTP) binding and hydrolysis to translocation along single-strand (ss) DNA as well as unwinding of double-strand (ds) DNA (107,108). These enzymes are responsible for generating the obligate ssDNA intermediates required for DNA metabolism. UvrD, also known as DNA helicase II, is the founding member of the SF1 helicase family and unwinds DNA in a 3' to 5' direction via a non-uniform translocation mechanism (109,110). As demonstrated, the helicase II rapidly translocates four to five nucleotides on ssDNA coupled to hydrolysis of one ATP followed by a small pause (109). However, UvrD is essential for the repair of UV damages by the UvrABC-mediated

nucleotide-excision repair (NER) system and plays a critical role in mismatch repair, replication and recombination (111,112).

Co-crystal structures of an UvrD monomer bound to a ss-dsDNA junction and other studies suggest that a monomer is the active helicase *in vivo* (Figure 1-10) (110,113). In contrast, self-association of UvrD in the absence of DNA, thereby forming dimers and tetramers, have led to the conclusion that at least a dimer is the active form of UvrD *in vitro* (114). Many helicases form hexameric or dimeric structures to provide the helicase with multiple potential nucleotide and DNA binding sites although members of the SF1 helicase family do not appear to form hexameric structures.

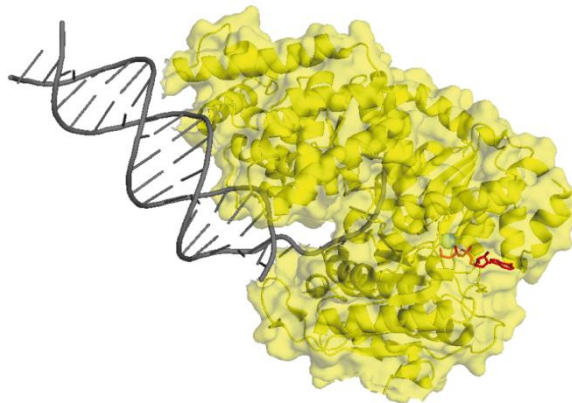


Figure 1-10: Crystal structure of the UvrD-DNA complex

UvrD bound to a ss-dsDNA junction in the presence of ADPnP (red) using a duplex DNA substrate containing a single-strand 3'-overhang (pdb code: 2is4) (110).

During MMR, UvrD is required for mismatch-provoked DNA unwinding starting at a nicked hemi-methylated GATC-site towards the recognized mismatch, regardless of the orientation (Figure 1-3). With regard fact that UvrD unwinds exclusively in a 3' to 5' direction with respect to the bound DNA strand, bi-directional unwinding from a nick requires the capability of UvrD to bind to both strands. These observations led to the conclusion that there might be a signal within the MMR system which is used to orient helicase II and therefore allows unwinding in the proper direction for mismatch excision. As proposed, MutL serves to load UvrD directly onto the nicked DNA substrate with the appropriate polarity to ensure

correction of the mismatch (38,115). The physical interaction between MutL and UvrD was demonstrated via yeast-two-hybrid and deletion analysis, thereby mapping the interaction site to a region within the flexible linker as well as the C-terminus of MutL (115). However, MutL stimulates DNA unwinding by UvrD although the mechanism and the role of ATP-hydrolysis by MutL are not fully understood (38,111). Finally, mismatch-provoked stimulation of DNA unwinding by UvrD in a MutSL-dependent manner might be the result of multiple loading during MMR (38). Considering that no homolog for UvrD has been discovered in eukaryotes so far, the mechanism of strand excision during MMR is puzzling and depends on the 5'-directed exonucleolytic activity of ExoI (116).

1.2 *Very-short patch repair - VSPR*

The very-short patch repair (VSPR) pathway is required for repair of T:G mismatches that arise spontaneously via deamination of the 5-methylcytosine (4,117,118). In *E. coli*, C5 methylation occurs at the second C within a Dcm-site (5'-CCWGG-3') which is used by this organism to distinguish between DNA from different sources, which lack this modification or as a regulatory element for gene expression (5). Vsr, the main component of the VSPR pathway, is a monomeric endonuclease which recognizes T:G mismatches preferentially within a Dcm sequence context (5,119). Mismatch recognition by the Vsr endonuclease results in a nick directly 5' of the mismatched T which serves as starting point for further repair (Figure 1-11A).

In consideration of the fact that mismatch recognition is coupled to a specific sequence context and a specific type of damage, the incorrect base pair is recognized and repaired directly. The mismatch is removed via nick-translation by DNA polII which possesses a 5' to 3' exonuclease and DNA polymerase activity, thereby restoring the Dcm-site. Finally, the nick is sealed by DNA ligase and methylation pattern is restored by the DNA cytosine methyltransferase (Dcm) (Figure 1-8B) (119,120). The absence of Vsr causes a high frequency of C:G to T:A transitions

after replication (117,121). Therefore, VSPR is required for maintaining Dcm-sites in *E. coli* (4).

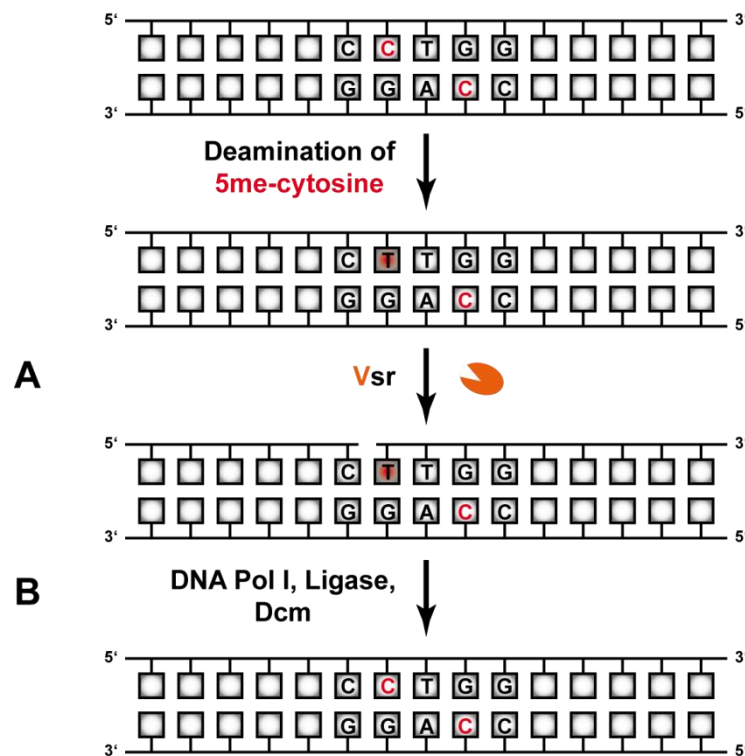


Figure 1-11: Overview of very-short patch repair in *E. coli*

A: Mismatch recognition and strand discrimination is achieved by Vsr, which introduces a nick 5' of the mismatched T (red square), thereby creating the processed VSPR intermediate. **B:** DNA is repaired via nick-translation and remaining nick is sealed by DNA polI and ligase, respectively. Finally, methylation pattern is restored by the DNA cytosine methyltransferase (Dcm). 5-methylcytosine is indicated in red.

1.2.1 Vsr – the mismatch recognizing endonuclease

The Vsr endonuclease is the main component of the VSPR pathway in *E. coli* and responsible for recognition of T:G mismatches that arise spontaneously due to deamination of 5-methylcytosine within Dcm-sites (4,122). In comparison to MMR, where MutSLH are absolutely required for mismatch recognition and strand discrimination, Vsr combines all these activities in one molecule. Therefore, coupling of mismatch recognition within a specific sequence context to strand incision 5' of the mismatched T directly allows repair via nick-translation without

previous DNA unwinding. Co-crystal structures of Vsr bound to a T:G mismatch within a Dcm sequence context (Figure 1-12A) revealed that Vsr has an overall topology comparable with type II restriction enzymes, such as PvuII, EcoRV or MutH (122).

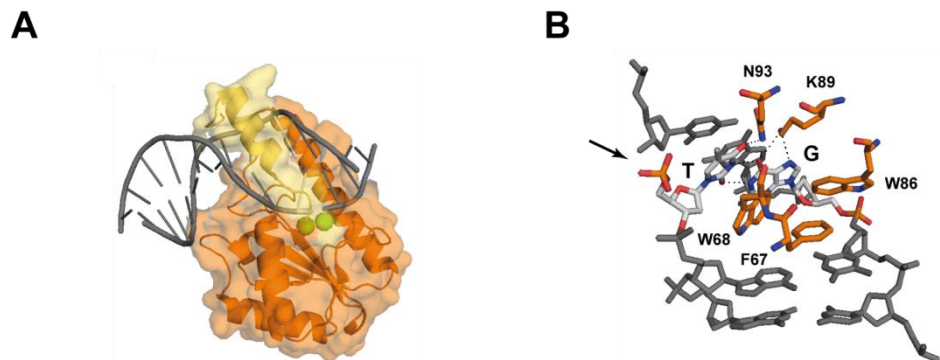


Figure 1-12: Crystal structure of the Vsr-DNA complex

A: *E. coli* Vsr bound to a T:G mismatch (light grey) in a Dcm sequence context. The N-terminal domain (light orange), which is absent in Vsr-Δ14, is important for DNA binding. Catalytic important Mg^{2+} as indicated as green spheres **B:** DNA kinking ($\sim 90^\circ$) by Vsr due to intercalation of hydrophobic residues F67, W68, W86. T:G mismatch recognition is achieved by K89 and N93. The nicking site is indicated by the arrow (122).

However, the mechanism of DNA recognition differs from that observed for type II restriction endonucleases. The DNA in the complex is kinked by an angle of $\sim 90^\circ$ upstream of the cleavage site due to intercalation of three aromatic residues into the major groove of the DNA (Figure 1-12B). The absence of a hemi-methylated recognition site reduces Vsr activity up to 60 % (123).

1.2.2 Crosstalk between MMR and VSPR

Several experimental observations have led to the conclusion that VSPR has evolved a close and well-nuanced relationship with the general mismatch repair proteins in order to assure that the two processes do not significantly interfere with each other (5,124). Strains without Vsr are completely deficient in VSPR, and therefore show a high frequency of C to T mutations at 5-methylcytosines (117,121). Earlier *in vivo* studies showed that very-short patch repair (VSPR) is reduced (125),

but not eliminated in cells, which are unable to produce MutS or MutL (5,126,127). On the other hand, overexpression of MutS also reduces VSPR, indicating MutS and Vsr compete for mismatch binding and repair (127,128). Overexpression of plasmid-borne Vsr in *E. coli* has been shown to be mutagenic (129), an effect attenuated by co-overexpression of MutL or MutH but not MutS (130,131).

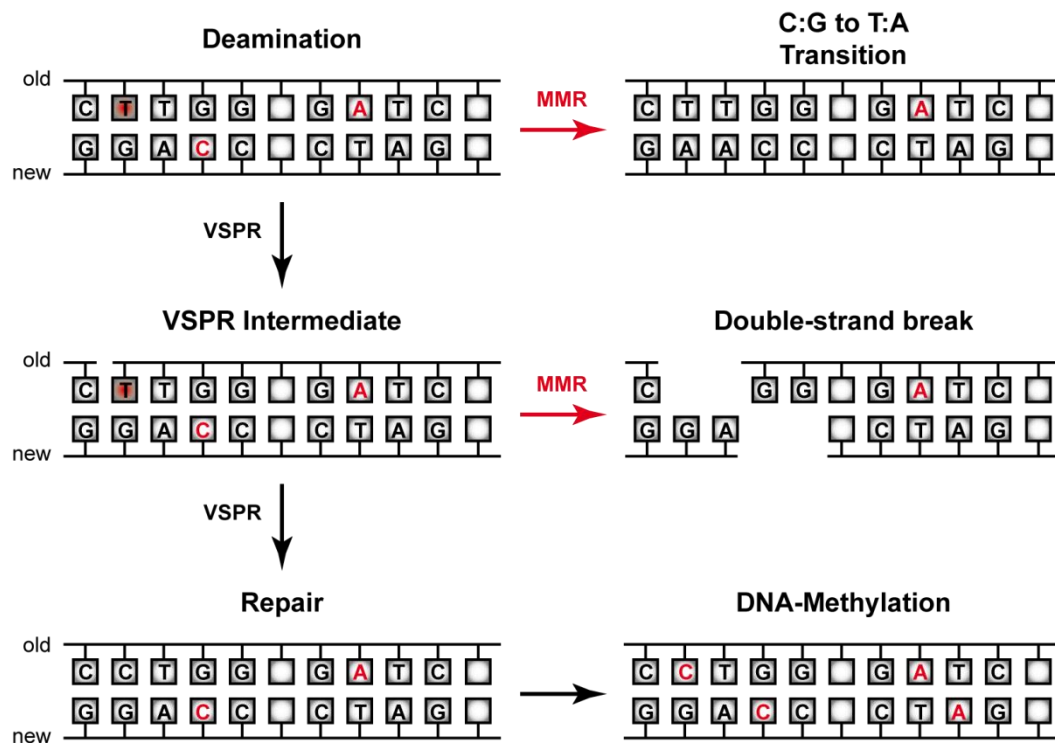


Figure 1-13: Consequences of defective crosstalk between MMR and VSPR

Spontaneous deamination of 5-methylcytosine in the parental DNA strand during replication generates T:G mismatches that are target for both MMR and VSPR in *E. coli*. Only initiation and completion of VSPR allows restoration of the original Dcm-site, whereas initiation of MMR prior to VSPR or triggered by the appearing VSPR intermediate results in a C:G to T:A transition mutation or a lethal double-strand break. Unfavoured repair processes are indicated by red arrows.

The physical interaction between MutL and Vsr has been demonstrated by bacterial and yeast-two hybrid analysis, analytical ultracentrifugation and site-directed crosslinking (132-134). The proposed model by Luis Giron-Monzon and Sven Geisler maps the interaction site of MutL for Vsr to a similar region as the MutH-MutL interaction site, supporting the proposed competition of MutH and Vsr

for binding to MutL. Moreover, a functional interaction between MutL and Vsr was shown by a slightly stimulation of Vsr DNA binding and cleavage (87). A mutant Vsr protein lacking the N-terminal 14 amino acids (Vsr- Δ 14) has diminished endonuclease and VSPR activity, but interacts with MutL as strongly as the wildtype (133). Recently, based on *in vivo* data, it has been suggested that MMR MutS and MutL collaborate with Vsr endonuclease in the repair of O⁶-methylguanine by methyltransferases, i.e. Ada and Ogt (135). However, little biochemical data is available that directly demonstrates competition or synergism between Vsr and the MMR protein MutS. Two models have been proposed for the mechanism of Vsr stimulation by the MMR machinery. The first model suggest a distortion of the DNA by MutS and MutL, facilitating Vsr binding (136), whereas the second model proposes a conformational change of Vsr from an inactive to an active form facilitated by MutL (137). The recently achieved co-crystal structure of MutH bound to DNA supports the idea that MutL facilitates DNA binding of both, MutH and Vsr. Although structural information for Vsr, MutH and MutL are available, the sites of physical interaction are still unknown. Due to the fact that MutL interacts with both MutH and Vsr, resulting in a stimulation of endonuclease activity (5), it has to be determined whether MutH and Vsr share a common MutL interaction site and/or are stimulated by a similar mechanism of activation.

Beside the information achieved from *in vivo* experiments, only little biochemical data is available about crosstalk between MMR and VSPR. Less is known about competition or synergism between both *E. coli* repair pathways in initiation of repair after a single deamination event of 5-methylcytosine *in vitro*. In contrast to replication errors, that mainly occurs in the newly synthesized DNA strand, deamination at Dcm-sites could in principle effect bases in both DNA strands. A mismatched T in the parental DNA strand is only efficiently repaired by VSPR (Figure 1-13). In contrast, repair of this mismatch by MMR will consequently result in a C:G to T:A transition due to excision of the original G, which finally eliminates the Dcm-site. Moreover, the influence on initiation of MMR by the nicked VSPR intermediate has not been investigated so far. The nick previously introduced by Vsr, has the capability to serve as an entry point for further repair by the MMR

machinery, which also allows correct repair of the parental DNA strand. On the other hand, initiation of MMR on the newly synthesized strand during ongoing VSPR might result in a DNA double-strand break (Figure 1-13). To this end, discovering and monitoring how MMR proteins hand off T:G mismatches to suitable downstream repair factors and therefore interact with the VSPR pathway remains a significant challenge.

1.3 Base-excision repair - BER

Base-excision repair (BER) is the primary DNA repair pathway that corrects base lesions that arise due to oxidative alkylation deamination and depurination/depyrimidination damages (3,138). The core BER pathway requires the function of at least four proteins, including a DNA glycosylase, an AP endonuclease or AP lyase, a DNA polymerase and a DNA ligase (139). All these proteins function in concert to remove a damaged DNA base and replace it with the correct base. In *E. coli* spontaneous deamination of cytosine to uracil generates U:G mismatches that are target of the uracil DNA glycosylase (UDG) which catalyzes the release of uracil, thereby generating an apurinic/apyrimidinic (AP) site (Figure 1-14A). In the next step this AP-site is processed by EndoVI which generates a single-nucleotide gap due to removal of the abasic patch of the DNA backbone (Figure 1-14B). Finally, the gap is filled by DNA polI thereby restoring the original C and the nick is sealed by a ligase (Figure 1-14C).

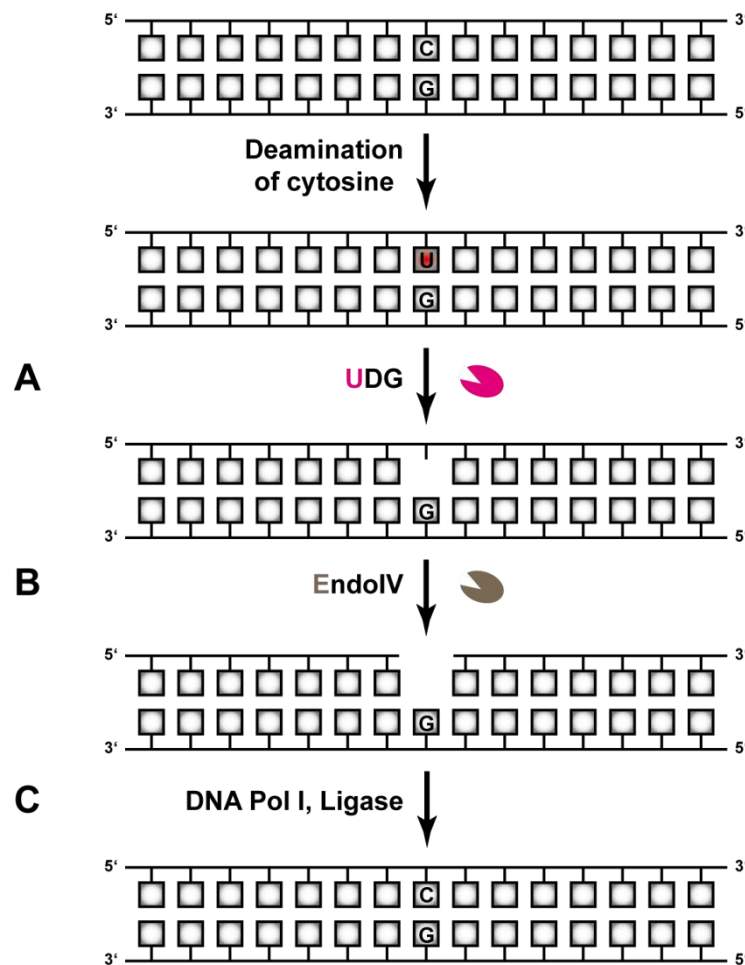


Figure 1-14: Example of base-excision repair in *E. coli*

A: Uracil containing DNA is recognized by the uracil DNA glycosylase (UDG), which catalyzes the release of the wrong nucleotide, thereby creating the BER intermediate containing an apurinic/apyrimidinic (AP) site. **B:** EndoIV, an AP-endonuclease and lyase, cleaves the DNA backbone at the AP-site, which results in a single-nucleotide gap. **C:** Original C is restored after re-synthesis of DNA by polI and the remaining nick is sealed by a ligase (see text for details).

1.3.1 UDG – the sensor of uracil

DNA glycosylases are absolutely required for BER due to the fact that they recognize specific damaged bases and excise them from the genome (reviewed). So far, several different mammalian glycosylases have been characterized. The primary function of most DNA glycosylases is to recognize their substrate (the damaged base) and catalyze the cleavage of an N-glycosidic bond, thereby releasing a free base and creating an abasic site (140). In addition to the cleavage function, some

glycosylases are bi-functional and contain an additional AP lyase activity. The uracil DNA glycosylase (UDG) was the first DNA glycosylase to be identified and cloned (Figure 1-15) (140). Uracil in DNA arises as a result of deamination of cytosine or incorporation during replication, which results in a C:G to T:A transition mutation (141). Consequently, homologous enzymes that catalyze the excision of uracil from the genome are present in almost all organisms (138).

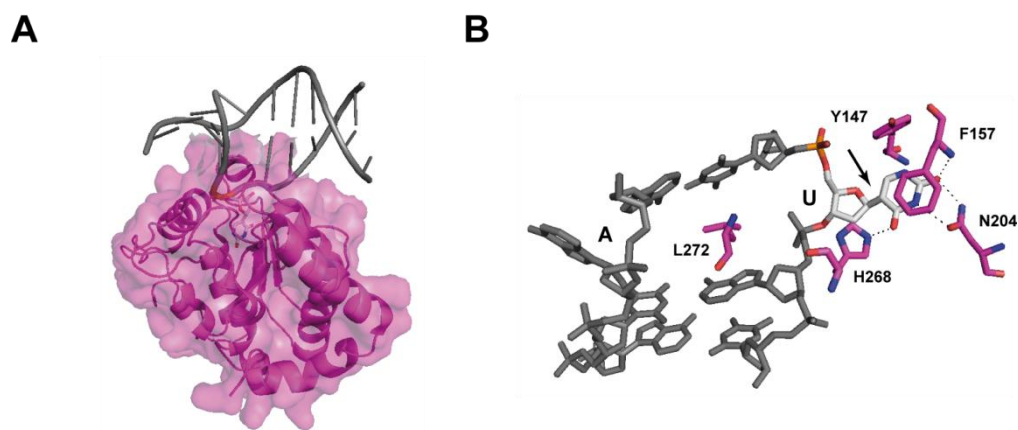


Figure 1-15: Crystal structure of the UDG-DNA complex

A: Human uracil DNA glycosylase (UDG) bound to A:U base pair containing DNA (pdb code: 1emh). UDG uses a nucleotide-flipping mechanism to recognize the damaged base. **B:** Uracil is flipped out after intercalation of L272 into DNA and bound by a recognition pocket. Specific contacts to N204 and H268 keep uracil in an position, which allows subsequent cleavage of the N-glycosidic bond of the base (arrow) (142).

In comparison to all other DNA glycosylases, UDG has a very high turnover rate and is capable to catalyze the removal of 1000 uracil residues from DNA per minute (143). Recognition of uracil by the enzyme causes helical distortions in the DNA and the damaged base is flipped out into a binding pocket followed by cleavage of the N-glycosidic bond (Figure 1-15). Moreover, UDG is also sufficient to process the excision of cytosine-derived products of oxidative DNA damage, although at lower efficiencies. Moreover, isodialuric acid, 5-hydroxyuracil and alloxan have been described as substrates for UDG (144).

1.3.2 Potential crosstalk between MMR and BER

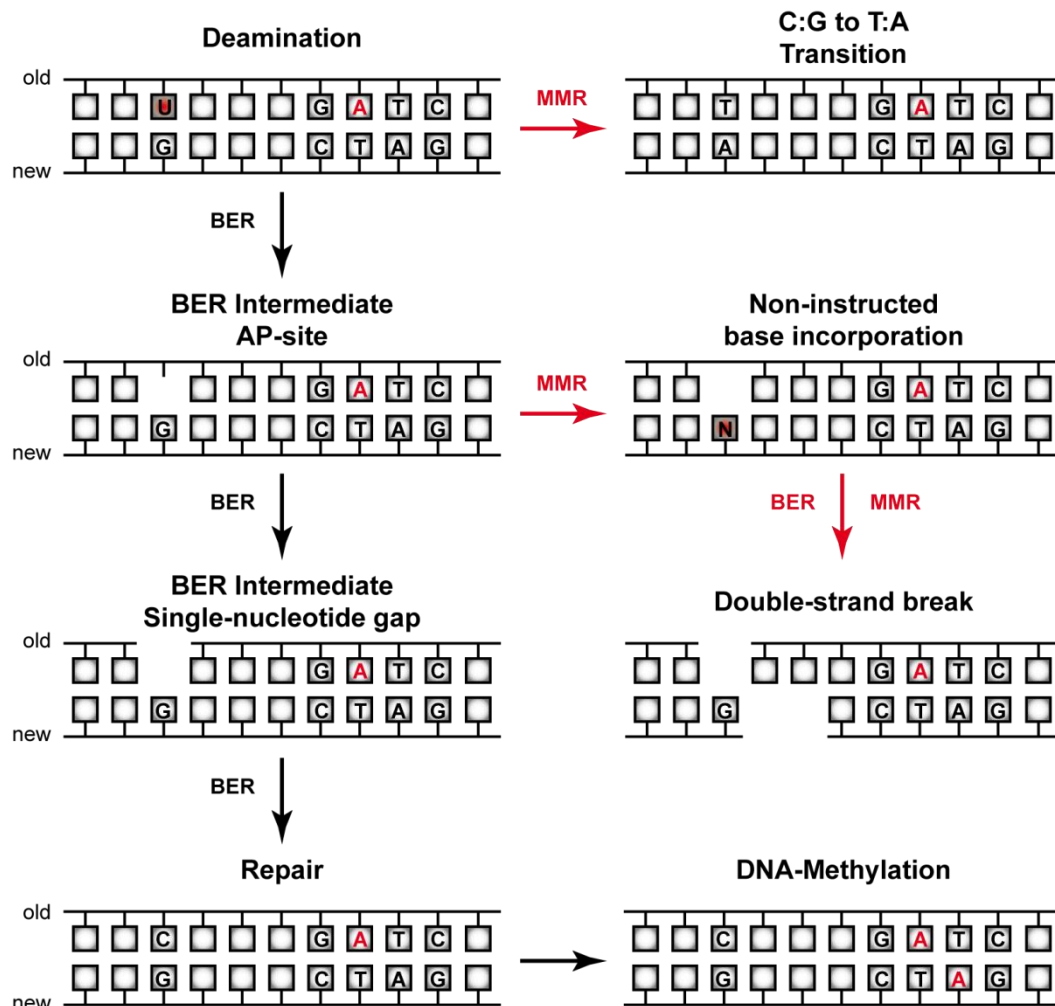


Figure 1-16: Consequences of defective crosstalk between MMR and BER

Deamination of cytosine in the parental DNA strand generates a U:G mismatch, which is only efficiently repaired by BER. However, the same damage is sufficient to trigger initiation of MMR resulting finally in a C:G to T:A transition due to excision of the original G and replacement by A. Release of uracil by UDG creates an AP-site, which might also induce MMR because of the fact that the remaining nucleotide is proposed to adopt an IDL-like structure and therefore could be recognized by MutS as a mismatch. However, initiation of MMR during ongoing BER has the capability to produce a lethal double-strand break. Unfavoured repair processes are indicated by red arrows.

Beside the activation of BER, a U:G mismatch is also recognized by MutS and therefore has the capability to induce MMR (1,2,145). Unlike DNA polymerase errors that occur mainly in the nascent strand during DNA replication, such deamination events can affect bases in both DNA strands. A single deamination

event in a transcription/replication bubble or in transiently unwound DNA would generate a uracil residue in one of the strands, which would generate a U:G mismatch after re-annealing of DNA. If not restored to the original C:G base pair by BER, the damage could result in a C:G to T:A transition mutation after initiation of MMR (Figure 1-16). However, initiation of MMR and BER on both DNA strands simultaneously may cause a double-strand break that might be lethal. Although unlikely under normal circumstances, in humans this situation may arise *in vivo* during somatic hypermutation (SHM) and class switch recombination of Ig genes, where activation-induced cytidine deaminase (AID) generates multiple U:G mismatches in the variable or switch regions and is believed to be recruited to sites of transcription (146,147).

In conclusion, the fact that the same damage is recognized by MutS and UDG, crosstalk between the two different repair pathways seems obviously. So far, almost no biochemical data is available about the capability of the AP-site containing BER intermediate to induce MMR, which might finally result in a lethal double-strand break. The remaining nucleotide after release of uracil is proposed to be recognized by MutS similar as an IDL and therefore in principle sufficient to provoke initiation of DNA mismatch repair.

1.4 Fluorescence - FRET

Fluorescence is a very useful technique to detect changes in the surrounding of a fluorophore when attached to a protein or nucleic acid (Figure 1-17) (148). In particular, *Förster Resonance Energy Transfer* (FRET) is invaluable for studying small distance changes within those molecules, from 10-100 Å. FRET requires the presence of two appropriate fluorophores, one donor and one acceptor fluorophore, within the mentioned range (149). This method is useful for both DNA as well as protein studies and the only obstacle is the coupling of a fluorescent dye to the target molecule. DNA is easy to label as it can be synthesized with site-specific reactive groups or with modified nucleotides (150). Labeling of proteins denotes the greater

challenge and is achieved by site-specific coupling of fluorophores via a number of coupling methods (149).

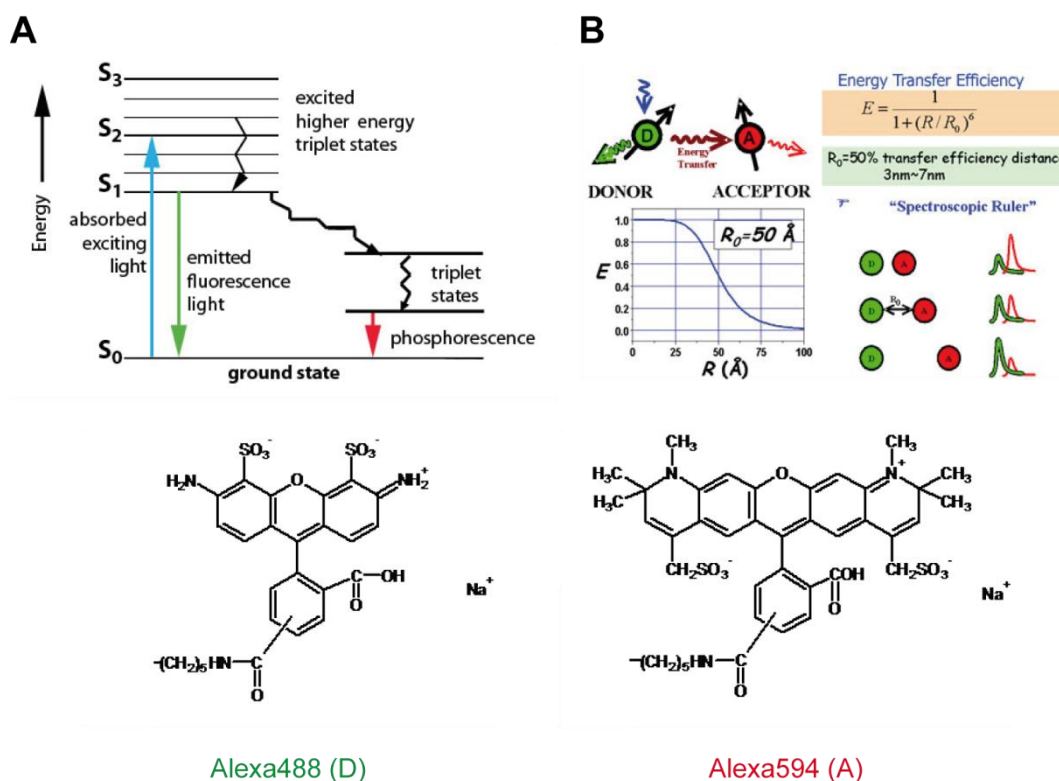


Figure 1-17: Principles of fluorescence and FRET

A: Jablonsky diagram. **B:** To measure FRET, the donor fluorophore is directly excited and the acceptor fluorophore is excited by the emission of the donor. As a result, the emission of the donor fluorophore decreases (the donor fluorescence is quenched) coupled to an increase in acceptor emission (FRET). Considering that FRET strongly depends on a change in the distance between donor and acceptor, this technique is used as spectroscopic ruler. Alexa 488 (D) and 594 (A) is a example for a suitable FRET pair (<http://bio.physics.illinois.edu>).

FRET is used to study either conformational changes of one molecule, where both donor and acceptor fluorophore are attached to the same molecule or it is utilized to study the interaction between two molecules, in which one is labeled with acceptor and one with donor fluorophore (149,151). For FRET to take place, three conditions have to be fulfilled.

1) Overlap of the emission spectrum of the donor with the excitation spectrum of the acceptor

2) The two fluorophores need to have the correct spatial orientation, in relation to each other

3) The distance between the two fluorophores should be between 10 and 100 Å. FRET is strongly dependent on the distance, being proportional to r^6 (r is the distance between Donor and Acceptor): $E = (R_0^6)/(R_0^6 + r^6)$; R_0 (in Å) is specific for each FRET-pair and has to be calculated experimentally.

The distance at which FRET efficiency is 50% is called the Förster distance (Figure 1-17B). The extreme sensitivity of FRET to small distance changes between the fluorophores and the possibility to follow the FRET signal in real-time as well as down to the single molecule level, makes this a very useful technique to understand and “see” inter and intra-protein or DNA movements.

As mentioned, specific recognition of a mismatch by MutS induces specific conformational changes towards the *initial recognition complex* (IRC), in which the bound DNA is bent by an angle up to 60° (59,72). With regard to the fact that DNA bending results in a change of distance between two points on the DNA, formation of the IRC can be directly monitored via FRET (Figure 1-18) and therefore allows the comparison of various DNA damages in recognition and binding by MutS (9).

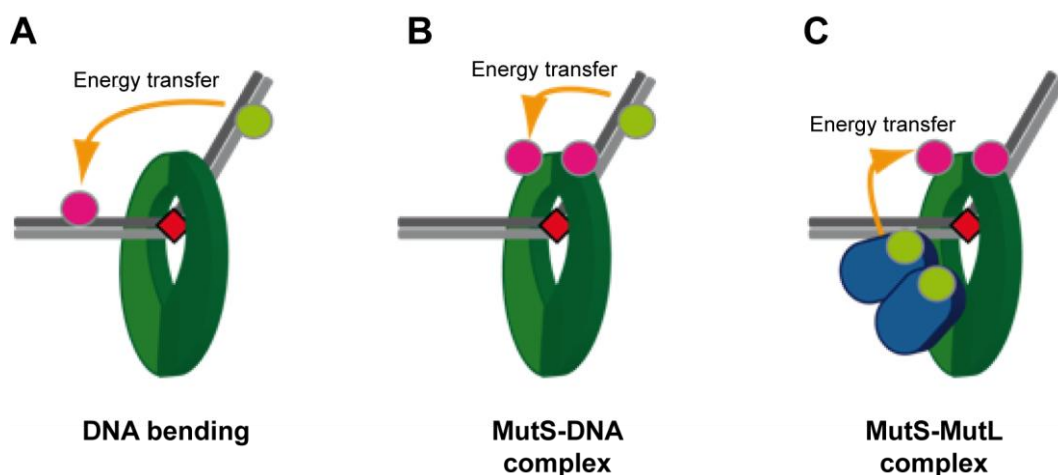


Figure 1-18: Scheme of possible FRET-systems to monitor initial steps in MMR

A: Mismatch-provoked DNA bending by MutS (IRC). **B:** Formation of the MutS-DNA complex. **C:** Formation of the *damage sensor and signalling* (MutSL) complex.

Moreover, labeling of MutS and MutL at distinct sites with suitable fluorophores in principle permits to detect the formation of transient ternary complexes such as MutSL which is proposed to play a major role in damage signalling during DNA mismatch repair (2).

1.5 Aim

Although under investigation for over 25 years, discovering and monitoring how MMR proteins hand off damages or mismatches to suitable downstream repair factors and therefore interact with components involved in other DNA repair pathways remains a significant challenge. As mentioned, MutS is able to recognize lesions that are mainly targeted by the VSPR or BER system (1). This is problematic due to the fact that initiation of an unfavoured or several repair pathways simultaneously increases the chance for arising of a mutations or a lethal double-strand break within the DNA. Beside this, the molecular matchmaker MutL, which stimulates MutH and UvrD during MMR, is proposed to interact with components of several other repair pathways, such as VSPR and BER, thereby modulating their activity (89). So far, less is known, whether these systems in principle cooperate or compete in repair, although both has been observed *in vivo* and how they assure that these processes do not significantly interfere with each other. Consequently, crosstalk in DNA mismatch repair seems obviously and the well-nuanced relationship that has evolved requires further control mechanisms that are not well understood so far.

Aim of this study was to investigate the mechanisms that regulate the crosstalk between MMR, VSPR and BER during repair of common targets *in vitro*. Therefore, it was necessary to generate suitable DNA substrates containing the desired mismatches or modifications and to develop appropriate DNA *mismatch* repair assays that demonstrate the damage-provoked initiation of these repair pathways due to specific activation of the involved components. These assays have to allow the monitoring of specific changes in the integrity and topology of the DNA substrate due to procession of distinct steps in repair, such as strand incision and excision, gap

formation or re-synthesis of DNA. Moreover, the influences on MMR by intermediates of the VSPR and BER pathway, which are proposed to trigger an unfavoured initiation of DNA mismatch repair, have not been investigated so far. In conclusion, almost complete reconstitution of MMR, VSPR and BER *in vitro* has to be attempted as starting point for detailed investigations in mutual influences by these pathways on initial steps in repair which should help to discover the mechanisms of cooperation and competition, required for efficient crosstalk in DNA mismatch repair.

As mentioned, successful mismatch recognition by MutS results in formation of the distinctive *initial recognition complex* (IRC), in which the DNA is bent up to 60° (59). These mismatch-provoked conformational changes towards the IRC can be determined using fluorescence techniques. A recently developed MutS mismatch binding and DNA bending assay (Dr. Michele Cristovao), which uses *Förster Resonance Energy Transfer* (FRET) to demonstrate small distance changes between two fluorophores attached to the DNA substrate, was adopted and optimized to monitor the induced DNA bending during formation of the IRC. Furthermore, in combination with fluorescence anisotropy measurements this assay allows the determination of the orientation in which a lesion is bound by the mismatch sensor. As revealed by crystal structures, specific recognition of only one of the mismatched bases by one subunit of the MutS homodimer results in formation of a functional hetero-dimeric protein, which is proposed to play a major role in damage signalling to downstream factors. Consequently, this assay was used to analyze the recognition of various crosstalk relevant mismatches and intermediates by MutS as the first step in MMR.

As a strategy to solve the question, whether MutS leaves the damage after recognition (mobile) or remains at the lesion (stationary), the transient MutS-DNA complex should be trapped via site-directed chemical crosslinking, thereby taking the protein on a “leash”. Crosslinking is an established method to study protein / DNA as well as protein / protein interactions or to trap transient and highly dynamic complexes for subsequent crystallization, as demonstrated previously (152,153). To this end, variants of MutS (Kind gift from Wei Yang) containing a single cysteine

within the clamp domain of the protein should be tested for mismatch and nucleotide-dependent chemical crosslinking to a short heteroduplex DNA oligonucleotide that is modified with a single thiol-group. Based on the co-crystal structure of the MutS-DNA complex (59), a cysteine within the MutS dimer is in such a close proximity to the thiol-group of the substrate during mismatch binding to allow in principle the formation of a covalent disulfide bond, thereby trapping this complex.

The chance to trap for the first time the transient MutS-DNA complex via thiol-specific crosslinking will offer new possibilities for further functional and structural studies in damage recognition and signalling by the mismatch sensor. A mismatch binding MutS on a “leash” might serve as an optimal starting point to investigate, whether the protein has to leave the damage in form of a *sliding clamp* after recognition and binding of ATP (mobile vs. stationary) to permit activation of effector proteins up to 1000 bp away from the mismatch by the *damage sensor and signalling complex* (MutSL). In contrast to other chemical crosslinking methods, disulfide bonds are cleaved by reducing agents such as DTT which allows leaving MutS from the “leash”. Finally, a covalent coupled MutS-DNA complex might be suitable for crystallization trials to solve the structure of the *sliding clamp* which is unknown so far.

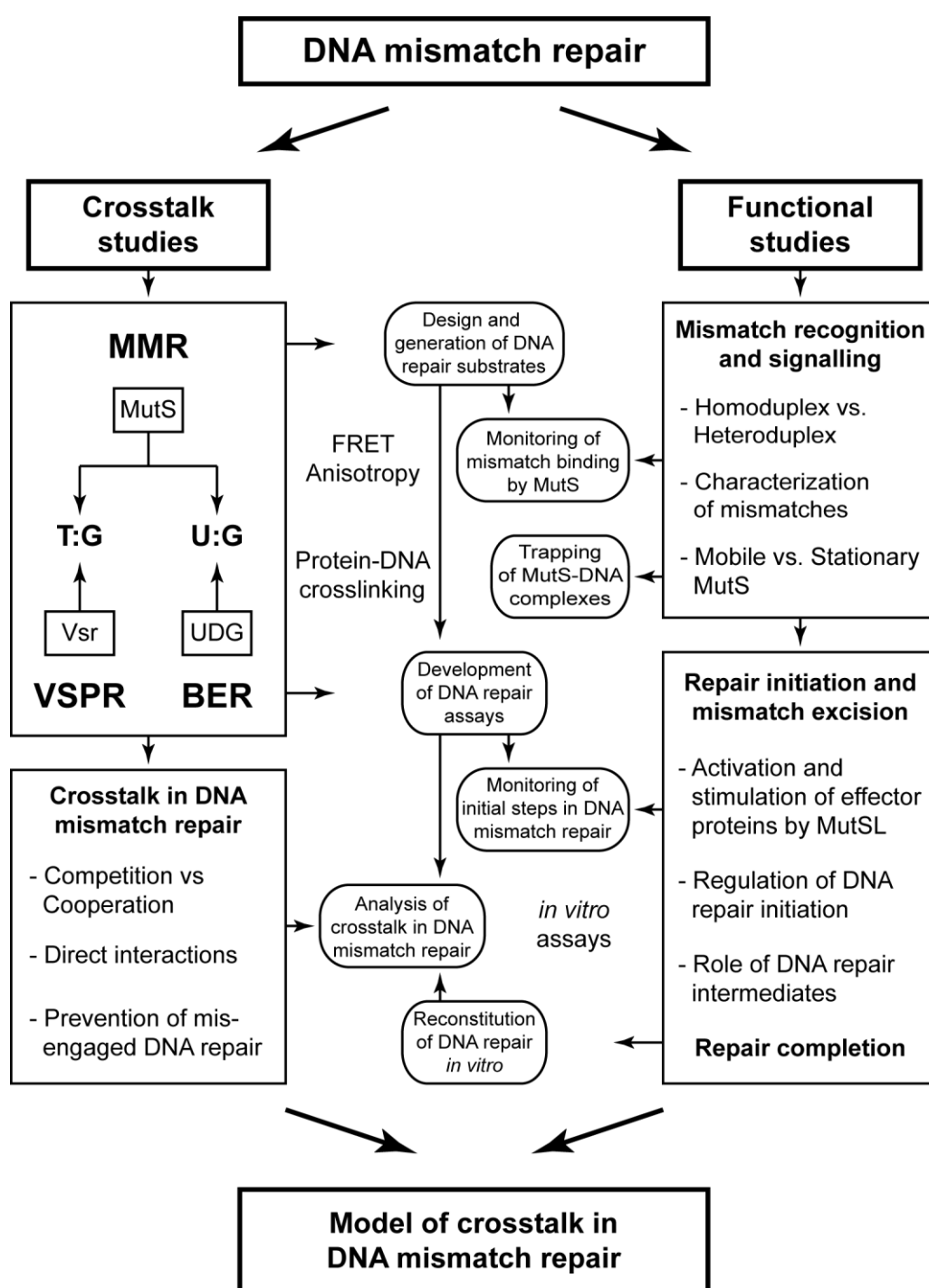


Figure 1-19: Layout of this study

2 Materials and Methods

2.1 Materials

2.1.1 Reagents

All chemicals and reagents that have been used have *pro analysi* purity grade and are listed in table 2-1. All buffers and solutions were prepared with water obtained by filtration using a Q-Gard 2 water purification system (Millipore).

Table 2-1: Chemicals and Reagents

Name	Company
Acrylamide:bisacrylamide (29:1) 40 %	AppliChem
Agar	AppliChem
Agarose	Invitrogen
Ampicillin	AppliChem
Arabinose	Sigma
ATP, ADP, ADPnP, ATP γ S	Sigma
Bromophenol blue	Merck
Coomassie Blue G250/R250	AppliChem
dNTPs	Sigma
DTT	Applichem
EDTA	AppliChem
Ethanol	Merck
Ethidium bromide	Roth
Glycerol	AppliChem
Glycine	AppliChem
HCl	Merck
HEPES	AppliChem
H ₃ PO ₄	Merck
Imidazole	AppliChem
IPTG	Roth
Isopropanol	Roth
Kanamycin	AppliChem
KCl	Merck
KOH	Merck
MgCl ₂	Merck
β -Mercaptoethanol	Merck

Name	Company
NaCl	Merck
NaOH	Merck
Ni-NTA agarose	Qiagen
PMSF	AppliChem
Rifampicin	Sigma
SDS	Roth
Sucrose	AppliChem
TEMED	Merck
Tris	Merck
Tryptone	AppliChem
Tween20	Merck
Yeast extract	AppliChem

2.1.2 Buffers

Table 2-2: Buffers and Solutions

Application	Name	Components
<u>Protein / DNA expression</u>	LB-medium	1 % Tryptone, 0.5 % Yeast extract, 0.5 % NaCl, pH 7.5
	STE buffer	10 mM Tris-HCl pH 8.0, 100 mM NaCl, 0.1 mM EDTA
<u>Protein purification</u>	Binding buffer	20 mM Tris-HCl pH 7.9, 1 M NaCl, 5 mM imidazole, 1 mM PMSF
	Washing buffer	20 mM Tris-HCl pH 7.9, 1 M NaCl, 20 mM imidazole, 1 mM PMSF
	Elution buffer	20 mM Tris-HCl pH 7.9, 1 M NaCl, 200 mM imidazole, 1 mM PMSF
	Dialysis buffer	10 mM HEPES-KOH pH 7.9, 500 mM KCl, 1 mM EDTA, 1 mM DTT, 50 % glycerol
	HPLC buffer	10 mM HEPES-KOH pH 7.9, 500 mM KCl, 1 mM EDTA, 10 % glycerol

Application	Name	Components
<u>DNA purification</u> (Wizard [®] , Promega)	Cell resuspension solution	50 mM Tris-HCl pH 7.5, 10 mM EDTA, 100 µg/ml RNase A
	Cell lysis solution	200 mM NaOH, 1 % SDS
	Neutralization solution	4.09 M guanidine hydrochloride, 759 mM potassium acetate 2.12 M glacial acetic acid
	Column wash solution	8.3 mM Tris-HCl, 0.04 mM EDTA, 60 mM potassium acetate, 60 % ethanol
<u>Substrate preparation</u>	Buffer red	10 mM Tris-HCl pH 7.9, 10 mM MgCl ₂ , 100 mM KCl, 0.1 mg/ml BSA
<u>Repair assays</u>	Buffer yellow	10 mM Tris-HCl pH 7.9, 5 mM MgCl ₂ , 150 mM KCl, 1 mM ATP, 0.1 mg/ml BSA
<u>Crosslinking / Fluorescence</u>	FB-buffer	20 mM HEPES-KOH pH 7.9, 5 mM MgCl ₂ , 125 mM KCl, 0.05 % Tween20 (v/v), 1 mM ADP
<u>Gel-electrophoresis</u>	TPE buffer	90 mM Tris-H ₃ PO ₄ pH 8.2, 2 mM EDTA
	SDS buffer	25 mM Tris-HCL pH 8.3, 190 mM glycine, 0.1 % SDS
	AAP (5x)	250 mM EDTA, 25 % sucrose, 1.2 % SDS, 0.1 % bromophenol blue
	LAP (5x)	160 mM Tris-HCl pH 6.8, 2 % SDS, 5 % β-mercaptoethanol, 40 % glycerol, 0.1 % bromophenol Blue

2.1.3 Enzymes and Proteins

Table 2-3: Enzymes and Repair components

Name	Company
BamHI	NEB
BSA	NEB
Dam	NEB
DNA ligase <i>E. coli</i>	NEB
DNA polymerase I <i>E. coli</i>	NEB
DpnI	Fermentas
EndoIV	NEB
ExoI	Fermentas
ExoIII	NEB
HindIII	NEB
MutH (and variants)	own purification
MutL (and variants)	own purification
MutS (and variants)	own purification, W. Yang
NaeI	NEB
Nb.Bpu10I	Fermentas
Nt.Bpu10I	Fermentas
PasI	Fermentas
<i>Pfu</i> -DNA polymerase	H. Büngen, Giessen
Proteinase K	Fermentas
RecJ _f	NEB
SSB	U. Curth, Hannover
T4-DNA ligase	NEB
UDG	NEB
UGI	NEB
UvrD	N. Hermans, Amsterdam
Vsr (and variants)	own purification
XbaI	NEB
XhoI	Fermentas

2.1.4 Oligonucleotides

HPLC-purified oligonucleotides were purchased from Biomers or IBA and used to generate modified circular DNA substrates or amino acid substitutions in MutL. Fluorescent-dye labeled oligonucleotides for MutS binding and DNA bending assays were obtained by IBA. Oligonucleotides for trapping transient MutS-DNA complexes were achieved from Eurogentec.

Table 2-4: Oligonucleotides and Substrate components

Application	Name	Sequence (5' – 3')
<u>Generation of pET-MMR and pUC-MMR</u>	MP-Bpu10I-I	CGTCATCCTCGGCTCAGG - CACCTGGGTGCTGAGG – GCATAGGCTT
	MP-Bpu10I-II	GCCGCGCCTGAGCCATATG – CTCGAGGATCCCTCAGCTA - ACAAAGC
	VDE-Prom	AATAGGCGTATCACGAGG – CCCTTTC
	35-Caro	CCCTCTAGAAATAATTTTG - TTTAACTTTAAGAAGG
<u>MutL mutagenesis</u>	MutL-XPXXIP	CCGCAACGGAATCGCCGCC - GGCGCGGCGCAAACGGG
	MutL-H5-Peter	CCAGAAACAGCAAGGTGAAGT
<u>DNA repair substrates</u> MMR 3' – 5' repair (long patch), BER and VSPR	Nb-HoC	P - TCAGGCACCC <u>T</u> GGGTGC
	Nb-HoC U:A	P – TCAGGCACCC <u>U</u> GGGTGC
	Nb-MM	P - TCAGGCACCC <u>T</u> GGGTGC
	Nb-MM U:G	P - TCAGGCACCC <u>U</u> GGGTGC
	Nb-MM ΔG	P – TCAGGCACCC <u>T</u> GGGTGC
	Nb-GATC	P – TGAGGGATCCTCGAGCA - TATGGC
MMR 3' – 5' repair (short patch)	Nt-HoC	P – TCAGCACCC <u>C</u> AGGGTGCC
	Nt-GATC-4	P – TGAGCCATATGCT <u>T</u> GAG - GATCCC
	Nt-GATC-12	P – TGAGC <u>T</u> ATATGCTCGAG - GATCCC

Application	Name	Sequence (5' – 3')
<u>DNA repair substrates</u> MMR 5' – 3' repair (long patch), BER and VSPR	Nt-HoC	P – TCAGCACCC <u>C</u> AGGGTGCC
	Nt-MM	P – TCAGCACCC <u>T</u> AGGGTGCC
	Nt-MM +1	P – TCAGCACCCC <u>G</u> GGGTGCC
	Nt-MM U:G	P - TCAGCACCC <u>U</u> AGGGTGCC
	Nt-MM ΔT	P - TCAGCACCC <u>-</u> AGGGTGCC
	Nt-GATC	P – TGAGCCATATGCTCGAG - GATCCC
<u>MutS binding / DNA bending (FRET)</u>	pUC-C-A488	CAAGCCTA <u>T</u> GCCCTCAGCAC – CC <u>C</u> AGGGTGCCTGAGACGAGG – ATGAC
	pUC-T-A488	CAAGCCTA <u>T</u> GCCCTCAGCAC – C <u>T</u> AGGGTGCCTGAGACGAGG – ATGAC
	pUC-U-A488	CAAGCCTA <u>T</u> GCCCTCAGCAC – C <u>U</u> AGGGTGCCTGAGACGAGG – ATGAC
	pUC-AP-A488	CAAGCCTA <u>T</u> GCCCTCAGCAC – C(AP)AGGGTGCCTGAGACGA – GGATGAC
	pUC-ΔC-A488	CAAGCCTA <u>T</u> GCCCTCAGCAC – C <u>-</u> AGGGTGCCTGAGACGAGG – ATGAC
	pUC-A-A594	GTCATCCTCG <u>T</u> CTCAGGCAC – CCT <u>A</u> GGTGCTGAGGGCATA – GGCTTG
	pUC-G-A594	GTCATCCTCG <u>T</u> CTCAGGCAC – CCT <u>G</u> GGTGCTGAGGGCATA – GGCTTG
<u>Trapping of MutS-DNA complexes</u>	pUC-T-C ₃ -SH	ATAGGACGCTGACACTG - GTGC <u>T</u> TGGCAGCT - SH
	pUC-G	AGCTGCCA <u>G</u> GCACCAGT - GTCAGCGTCCTAT

Desired double-strand oligonucleotides for FRET-assays and crosslinking experiments were achieved by annealing of corresponding complementary single-strand oligonucleotides (table). DNA sample containing the two appropriate oligonucleotides in a 1:1 ratio (molar equivalents) was heated up to 90 °C for 10 min and subsequent slowly cooled down to room temperature. Oligonucleotides were annealed to a final concentration of at least 1 µM for FRET-substrates or 40 µM for crosslink substrates and stored at -20 °C.

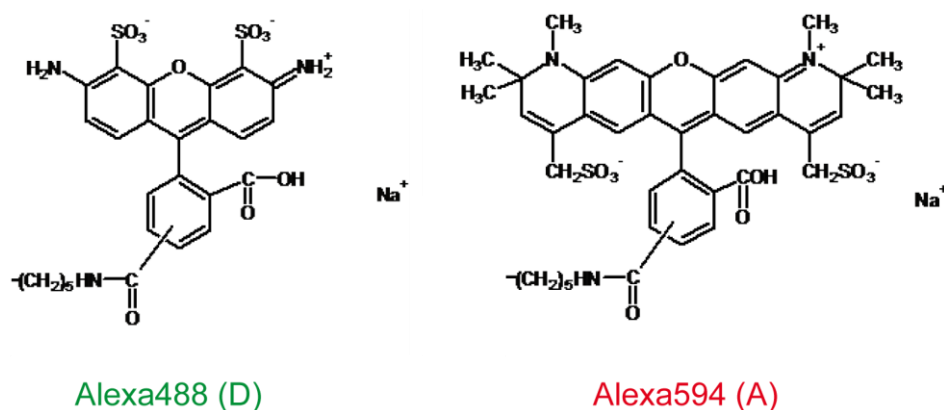


Figure 2-1: Fluorophores for FRET (attached to thymine within DNA)
(Adapted from www.nanoprobes.com)

2.1.5 Plasmids

Table 2-5: Plasmids and Expression vectors

Plasmid	Application	Reference
pTX412 (pET-15b)	His-MutS expression	Feng, 1995
pTX412 (scMutS)	His-scMutS expression	Yang, 2009
pTX418 (pET-15b)	His-MutL expression	Feng, 1995
pMQ402 (pBAD18)	His-MutH expression	Loh, 2001
pET11d-H2wt	UvrD expression	Yang, 2006
pDV111 (pET-15b)	His-Vsr expression	Cupples, 2000
pET-15b-Xh hoI	pET-MMR	Invitrogen
pBluSKP	pUC-MMR	Invitrogen

2.1.6 Strains

TX2652: This bacterial strain was used in the *in vivo* complementation assay to test the MutL-XPXXIP variant. It is a descendent of the *E. coli* strain CC106 in which the *mutL* gene has been inactivated by the insertion of a transposon. This cell line is *mutL*⁻.

Genotype: CC106 *mutL*::Ω4 (*Bsa*AI; Km^r)

HMS174(λDE3) (Novagen): HMS174(λDE3) cells were used for the expression of MutL, MutS and Vsr. They were transformed with vectors derived from pET-15b containing the *mutL*, *mutS* and *vsr* genes. It is excellent for the production of large quantities of protein because they carry the T7 RNA polymerase gene enhancing the expression of gene products under the T7 promotor.

HMS174(λDE3) cells are resistant to rifampicin and recombination deficient.

Genotype: F⁻, *recA**hdsR* (r_{K12}⁻m_{K12}⁺) (Rif^r) (DE3)

XL1 blue (Stratagene): This bacterial strain was used to express MutH, pET-MMR and pUC-MMR and as receptor of the MutL-XPXXIP plasmid, via electro-transformation (154).

Genotype: *recA1 endA1 gyrA96 thi-1 hsdR17 supE44 relA1 lac* [F' *proAB lacI^fZAM15 Tn10* (Tet^r)]

2.1.7 Protein / DNA marker

Table 2-6: Marker for gel-electrophoresis

Name	Application	Company
PageRuler™ Unstained Protein Ladder	Protein marker (10-200 kDa)	Fermentas
GeneRuler™ 1 kb Ladder	DNA marker	Fermentas
pUC 8 Mix Marker	DNA marker	Fermentas
O'GeneRuler™ Low Range Ladder	DNA Marker	Fermentas

2.2 *Methods*

Standard molecular biology methods such as preparation of electro-competent cells, electro- and heat-shock transformation were performed as described in Current Methods in Molecular Biology (154).

2.2.1 Protein expression and purification

E. coli cells carrying the desired plasmid for MutH, MutL, MutS and Vsr were grown overnight at 37° C (air shaker) in a 25 ml LB-medium culture, containing 100 µg/ml ampicillin. 10 ml of this overnight culture were transferred to 500 ml LB-medium. The cells were grown under the same conditions as described above until an OD₆₀₀ value of 0.8 to 1.0. The induction of MutL, MutS, and Vsr was started by adding IPTG to a final concentration of 1 mM, whereas the induction of MutH was induced by adding arabinose to a final concentration of 0.5 % (v/v). Growth was continued for 4 h at 28° C and afterwards cells were centrifuged at 4200 rpm (Beckmann, J6-HC) for 15 min at 4° C. Pellets were washed with 30 ml STE buffer and centrifuged again. The supernatant was discarded and pellets were stored either at -20° C or resuspended directly in binding buffer for further purification.

All purification steps were carried out at 4° C. Cell pellets obtained after protein induction were resuspended in 25 ml binding buffer in a 50 ml beaker and thawed on ice. Cells were lysed by ultra-sonification using a Branson sonifier (6 x 30 sec, Duty cycle 50 %, Output control 5). The soluble fraction was separated from cell debris by centrifugation at 20000 rpm for 30 min (Beckman, JA20). Ni-NTA (750 µl) was equilibrated with 30 ml binding buffer at 4° C for 30 min and centrifuged afterwards at 1000 rpm (Beckmann, J6-HC) for 2 min at 4° C. The supernatant from the cell lysate was incubated with Ni-NTA for 1 h and afterwards centrifuged for 2 min at 1000 rpm and 4° C. The Ni-NTA was resuspended in 50 ml washing buffer and centrifuged again at 1000 rpm for 2 min at 4° C. After each step of Ni-NTA centrifugation during protein purification the supernatant was discarded. Finally the Ni-NTA was transferred to a chromatography column (BioRad) and

proteins were eluted with 0.5 ml elution buffer. MutH and Vsr were dialyzed for 12 h in 2 l dialysis buffer. Further, MutL and MutS were purified by gel filtration using an Elite LaChrom VWR-Hitachi L-2455 HPLC system with a superdexTM 200 column 10/300 (GE Healthcare) equilibrated with HPLC buffer (flowrate 500 µl/min). Protein concentration was determined by UV-absorption at 280 nm using a UV spectrophotometer (NanoDrop ND-1000, PeqLab) and theoretical extinction coefficients.

2.2.2 DNA expression and purification

E. coli cells carrying the pET-MMR or pUC-MMR plasmid for the DNA substrates were grown in a 25 ml LB-medium culture, containing 100 µg/ml ampicillin, overnight at 37° C in a Innova[®] 40 incubator shaker. 10 ml of this overnight grown culture were transferred to 500 ml LB-medium. The cells were grown under the same conditions as described above until an OD₆₀₀ value of 1.0 to 1.2. Cells were centrifuged at 4200 rpm (Beckmann, J6-HC) for 15 min at 4° C. Pellets were washed with 30 ml STE buffer and centrifuged again. The supernatant was discarded and pellets were stored either at -20° C or resuspended directly in cell resuspension buffer (Promega) for further purification. Plasmid DNA was purified using the Wizard[®] Plus SV DNA purification system from Pomega

2.2.3 Site-directed mutagenesis of MutL

Site-directed mutagenesis reactions were carried out on the pTX418 plasmid as described (155). The mutagenesis primer (see table 2-4) that introduces a mutation at the desired codons was generated with a silent restriction marker (NaeI) in the coding sequence using VectorNTI (Invitrogen). Oligonucleotides were chosen to yield a short PCR fragment (megaprimer) during the first phase of amplification reaction (from 100 up to 700 bp). PCR was performed with 2 ng/µl DNA template, 0.2 mM dNTPs, 0.4 µM mutagenesis primer, 0.4 µM reverse primer and 1 U/µl *Pfu*-DNA polymerase in *Pfu*-DNA polymerase buffer. The megaprimer was purified using the Wizard[®] Plus SV Gel and PCR clean-up system (Promega). The amplified

megaprimer was directly used in a second “rolling circle PCR” containing 2 ng/μl DNA template, 0.4 mM dNTPs, 50 nM megaprimer and 1 U/μl *Pfu*-DNA polymerase in *Pfu*-DNA polymerase buffer to generate the MutL plasmid pTX418-XPXXIP. The “rolling circle PCR” was performed as described previously (155) with slight changes to accommodate the longer DNA template (7838 bp). The amplification program for the whole vector in one process was: 95° C for 120 sec, 16 × (95° C for 50 sec, 55° C for 55 sec, 68° C for 25 min). After all, digestion with 10 U of DpnI was performed to cleave fully and hemi-methylated GATC sites, and thus remove the parent plasmid pTX418 that was isolated from *dam*⁺ *E. coli*. The digested sample was precipitated with two volumes of ethanol and 1/10 volume of 3 M sodium acetate, resuspended in 10 μl water and used for electro-transformation. For screening, the plasmid DNA containing the putative mutated DNA region was purified (Promega) and digested with the restriction enzyme (NaeI) that corresponds to the restriction marker. Finally, the mutated plasmids were sequenced by automated methods (MWG).

2.2.4 Generation of modified circular DNA substrates

Circular DNA substrates containing various mismatches and/or modifications were necessary to study MMR, VSPR and BER *in vitro*. Therefore, pET-MMR (5708 bp) containing a single T:G or U:G mismatch within a hemi-methylated Dcm-site at position 169 and a hemi-methylated GATC site at position 356 was generated using a derivative of pET-15b-XhoI and a procedure similar to that described before (156). Plasmid pET-15b-XhoI was used to generate the plasmid pET-MMR by PCR mutagenesis. Four new sites for the nicking endonucleases Nb.Bpu10I and Nt.Bpu10I (table 2-4, underlined) were introduced using the oligonucleotides MP-Bpu10I-I and MP-Bpu10I-II. VSR-substrates containing a T:G mismatch in the sequence context of the Dcm-methyltransferase (5'-CTTGG-3'/5'-CC_{me}AGG-5') were generated using a procedure similar to that described before.

The pUC-MMR plasmid (3315 bp) was created by cloning a 405 bp DNA fragment from the low-copy pET-MMR plasmid (5708 bp) into the pBlueSKP vector (2958 bp, Invitrogen). A 472 bp DNA fragment was amplified using VDE-Prom and 35-Caro. Both the 472 bp PCR product and pBlueSKP were digested with XbaI and HindIII. The resulting 405 bp long fragment was cloned into the digested 2910 bp pBlueSKP vector fragment to form the smaller (3315 bp) high-copy pUC-MMR plasmid.

Substrates containing a T:G mismatch in the sequence context of the Dcm-methyltransferase (5'-CTTGG-3'/5'-CC_{me}AGG-3') were generated using a procedure similar to that described before . Briefly, the Dcm and Dam methylated plasmid (pUC- or pET-MMR, 100 nM) was nicked by Nt.Bpu10I (CC'TNAGC; 0.05 U/ml; 0.14 U/mg) or Nb.Bpu10I (GC'TNAGG; 0.05 U/ml; 0.14 U/mg) for 16 h at 37° C, followed by denaturation and re-annealing in the presence of the corresponding (Nt. or Nb.) 5'-phosphorylated oligonucleotides for the DNA repair substrates as mentioned in table 2-4 in 50-fold molar excess. After ligation with T4 DNA ligase (0.1 U/ml) for 8 h at 25° C, the reaction mixture was treated with ExoI (0.04 U/ml) and ExoIII (0.05 U/ml) at 37° C for 16 h to remove any remaining nicked (oc) and linear (lin) DNA fragments. Optionally, the DNA was methylated at the hemi-methylated GATC-site by Dam-methyltransferase. Additional incubation with 10 u proteinase K for 30 min at 37 °C allowed the degradation of all proteins in the reaction-mix. Finally, the DNA was precipitated with 1 volume of isopropanol and 1/10 volume of 3 M sodium acetate. The resulting covalently-closed circular (ccc) DNA containing a single hemi-methylated Dcm-site with a T:G mismatch and an additional hemi-methylated GATC site, was resuspended in 50 µl nuclease-free water (Promega) and stored at -20 °C.

All various circular DNA substrates required for crosstalk studies were generated by the same procedure using the appropriate oligonucleotides (Table 2-4).

2.2.5 Complementation mutator assay

Cells lacking a functional chromosomal *mutL* gene have an incomplete DNA mismatch repair system and show a mutator phenotype, which can be analyzed by the frequency of rifampicin-resistant clones arising from unrepaired polymerase errors in the *rpoB* gene (106). Single colonies of *mutL*-deficient TX2652 cells transformed with vector control or plasmids carrying the indicated gene were grown o/n at 37° C in 3 ml LB-medium cultures containing 100 µg/ml ampicillin. 50 µl aliquots of the undiluted culture were plated on LB-medium agar plates containing 25 µg/ml ampicillin and 100 µg/ml rifampicin. Colonies were counted after incubation o/n at 37° C. Median and range values were calculated from at least five independent experiments.

2.2.6 Mismatch-provoked MutH endonuclease assay

Mismatch-provoked MutH endonuclease activity was assayed on various generated circular DNA substrates containing a T:G mismatch with different orientation and distance to a single hemi-methylated GATC-site. If not stated otherwise, 25 nM of the circular DNA substrate was incubated with 200 nM MutS, 200 nM MutL and 50 nM MutH (monomer equivalents) in buffer yellow for 1 to 30 min at 37°C. Reaction was stopped by adding 4 µl AAP and 15 U/µl proteinase K to a 15 µl reaction mix. Activation of MutH, resulting in a nick 5' of the unmethylated GATC-site, was demonstrated by the transition from cccDNA (covalently closed circle) to nicked ocDNA (open circular). An 1 % agarose gel, pre-stained with ethidium bromide, allows separation of these both DNA forms because intercalation of ethidium bromide leads to a supercoiled-like structure of the cccDNA which migrates faster during gel-electrophoresis.

2.2.7 Mismatch-provoked UvrD unwinding assay

Mismatch-provoked UvrD helicase activity was assayed indirectly via exonucleolytic digestion of appearing single-stranded DNA by ExoI or RecJ, both members of the *E. coli* MMR system, after unwinding by UvrD. If not stated otherwise, 25 nM of the circular DNA substrate was incubated with 200 nM MutS, 200 nM MutL, 50 nM MutH and 100 nM UvrD (monomer equivalents) in the presence of 400 nM SSB (tetramer) and 0.1 U/μl ExoI or RecJ in buffer yellow for 1 to 30 min at 37°C. Reaction was stopped by adding 4 μl AAP and 15 U/μl proteinase K to a 15 μl reaction mix. UvrD unwinding activity was demonstrated by the transition from cccDNA over ocDNA, due to described MutH activity, to circular DNA containing a single gap or single-stranded circular DNA. In comparison to cccDNA, single-strand circular DNA migrates faster during gel-electrophoresis using EtBr pre-stained agarose gels.

Due to the fact that DNA with a short single-strand gap is not efficiently separated from ocDNA via gel-electrophoresis, restriction analysis was used to demonstrate UvrD helicase activity. Appearing of a single-strand patch within a double-strand DNA after strand-excision avoids cleavage by a restriction enzyme at these sites. Therefore, the reaction mix was treated with 0.4 U/μl BamHI or XhoI for 15 min at 37° C. Reaction was stopped and cleavage products analyzed as mentioned above.

2.2.8 Vsr endonuclease assay

Vsr endonuclease activity and therefore initiation of VSPR *in vitro* was assayed on circular DNA substrates containing the T:G mismatch within a hemi-methylated Dcm-site. If not stated otherwise, 25 nM of the circular DNA substrate was incubated with various concentrations of Vsr in the presence or absence of 200 nM MutS and 200 nM MutL (monomer equivalents) in buffer yellow for 1 to 30 min at 37°C (134). Reaction was stopped by adding 4 μl AAP and 15 U/μl proteinase K to a 15 μl reaction mix. Vsr activity was demonstrated by the

transition from cccDNA to the nicked (oc) VSPR intermediate due to strand incision 5' of the mismatched T within the hemi-methylated Dcm-site.

2.2.9 Base-excision repair assay

Circular DNA substrates containing either a single U:G mismatch or a U:A base pair as homoduplex control (Table 2-4) were used to study BER and the crosstalk with DNA mismatch repair (MMR) *in vitro*. Initiation of BER was demonstrated by appearing of ocDNA, indicating the generation of a single-nucleotide gap, in a two-step process strictly depending on UDG and EndoIV (NEB). Although UDG catalyzes the release of uracil, thereby generating an abasic-site (AP-site), the resulting BER intermediate adopts an equal supercoiled-like structure as the circular substrate during gel-electrophoresis due to the intact DNA backbone. Consequently, AP-lyase activity of EndoIV was utilized to show previous actions by UDG via generation of the proposed single-nucleotide gap. If not stated otherwise, 25 nM of the circular DNA substrate was incubated with 0.05 U/μl UDG for 5 min at 37° C followed by treatment with 0.1 U/μl EndoIV for 5 min at 37° C. Reaction was stopped by adding 4 μl AAP and 15 U/μl proteinase K to a 15 μl reaction mix and analyzed as mentioned above.

2.2.10 MutS binding and DNA bending assay (FRET)

The 45 bp substrate used for this study consists a mismatch or corresponding processed intermediate in a central position flanked by Alexa488 as donor in the top strand and Alexa594 as acceptor in the bottom strand (Figure ..). Moreover, each fluorophores was attached to a thymine 12 bp away from the damage. To measure fluorescence, the excitation wavelength for donor and acceptor was 470 nm and 575 nm, respectively. Emission was detected at 517 nm (Alexa488) and 617 nm (Alexa595). To measure FRET, the donor fluorophore is directly excited and the acceptor fluorophore is excited by the emission of the donor. As a result, the emission of the donor fluorophore decreases (the donor fluorescence is quenched) coupled to an increase in acceptor emission (FRET). This process does not involve

the emission or re-absorption of a photon but is the result of long-range dipole-dipole interactions. All fluorescence measurements were performed with the FluoroMax-4 Spectrofluorometer from HORIBA Jobin Yvon. If not stated otherwise, mismatch binding by MutS was tested using 50 nM of the 45 bp double-labeled DNA substrate and increasing amounts of wildtype MutS as indicated in the presence of 1 mM ADP at 20 °C.

Beside FRET, Fluorescent anisotropy is a useful technique to determine protein-protein or DNA-protein interaction in solution due to the molecular rotations that the fluorophore undergoes during its excited state which depolarizes its fluorescence. When a sample is excited with polarized light, the emission of light can also be polarized. The extent of the emission polarization is defined as anisotropy (r). Anisotropy depends on the transition moments for absorption and emission that lie along specific directions within the fluorophore structure. In a homogeneous solution, the fluorophores are randomly oriented. When they are exposed to polarized light, the fluorophores with their dipoles oriented along the vector of the light source are preferentially excited, conferring an average anisotropy to the solution.

All fluorescence anisotropy measurements were performed with the polarization module of the Steady State Benchtop Spectrofluorometer Fluoromax 4 from HORIBA Jobin Yvon. Slits were kept constant at 4nm and the samples were excited at 470 nm (Alexa488) or 575 nm (Alexa594). For each anisotropy measurement, the fluorescence spectrum was also recorded, excited at the same wavelength. Anisotropy measurements were taken simultaneously to FRET experiments.

2.2.11 Site-directed crosslinking of MutS to DNA

Crosslinking is an established method to study protein / DNA as well as protein / protein interactions or to trap transient and highly dynamic complexes for subsequent crystallization, as demonstrated previously (152,153).

Single-cysteine (sc) variants of MutS N468C and N497C (expression constructs achieved from Wei Yang) were purified as mentioned above and used in

this study for trapping transient MutS-DNA complexes via thiol-thiol specific crosslinking. To attempt covalent coupling of scMutS variants to DNA, a 30 bp heteroduplex DNA substrate was designed containing a single thiol-group linked to the 3'-end (C3-linker). Similar to the co-crystal structure, a T:G mismatch was generated 9 bp away from the modified 3'-end and should in principle allow crosslinking of MutS while sitting at the mismatch. As demonstrated by the co-crystal structure, during mismatch binding always one cysteine of each scMutS dimer is pointed towards the modified 3'-end and in such a close proximity (1-1.2 nm) to the thiol-group of the DNA substrate to allow formation of a covalent disulfide bond.

The desired modified heteroduplex dsDNA substrate with similar sequence context as used for *in vitro* repair assays (pUCMMR) was obtained after annealing of the two corresponding single-strand oligonucleotides (Table 2-4). Therefore, a DNA sample containing both oligonucleotides in a 1:1 ratio (molar equivalents) was heated up to 90 °C for 10 min and subsequent slowly cooled down to room temperature. Single-strand Oligonucleotides were annealed to a final concentration of at least 40 µM and stored at -20 °C.

To test the nucleotide-dependence of the crosslink reaction, 5 µM (monomer equivalent) of the tested scMutS variant N468C or N497C was incubated in FB-buffer with 5 µM of the modified 30 bp heteroduplex DNA substrate in the absence or presence of 1 mM ADP, ATP or ADPnP for 10 min at 37 °C. Reaction was stopped by adding 4 µl LAP without any disulfide bond reducing agent to a 10 µl reaction mix. Crosslinking yield was analyzed via SDS-PAGE using a 6 % separation gel or a 4-20 % gradient gel. Subsequent staining with EtBr allowed visualization of the shifted DNA in the covalent-coupled MutS-DNA complex. To detect crosslinked and free MutS the gel was additionally stained with coomassie. In contrast to the free protein, the crosslinked complex is shifted because of the bigger mass. Notably, due to the fact that in principle only one subunit of the MutS dimer is coupled to the DNA substrate, 50 % of crosslinked MutS-DNA complex is the highest yield that can be achieved under the used experimental conditions.

2.2.12 Purification of trapped MutS-DNA complexes

Purification of covalent coupled MutS-DNA complex via gel-filtration (HPLC) was performed as described for proteins used in DNA repair assays.

3 Results

3.1 *Generation of circular DNA repair substrates*

Numerous DNA repair systems have evolved to guarantee the integrity and stability of a genome which is jeopardized by a much broader repertoire of possible lesions. However, some induced or spontaneously appearing damages and mismatches have the capability to trigger initiation of more than one DNA repair pathway concurrently. Consequently, distinct control mechanisms are required to avoid unfavoured actions on DNA by perhaps misengaged repair systems. The repair of T:G and U:G mismatches either by MMR, VSPR or BER falls into this category (see Introduction).

For investigations in DNA repair and the proposed crosstalk between different repair pathways directed to a common target *in vitro*, it was indispensable to generate suitable DNA substrates containing appropriate mismatches and/or modifications at defined positions. Both, a single T:G mismatch and a hemi-methylated Dam-site (5'-GATC-3'/5'-GA_{me}TC-3') with a distinct distance below 1 kb to each other, are required and sufficient for initiation of methyl-directed mismatch repair (MMR) in *E. coli* (2). The same mismatch located within a hemi-methylated Dcm-site (5'-CTAGG-3'/5'-CC_{me}TGG-3') as result of deamination at 5-methylcytosine (5meC) represents the best substrate for very-short patch repair (VSPR) (4). Finally, a U:G mismatch which might appear after deamination of cytosine is either processed by base-excision repair (BER) or targeted by the MMR machinery. Furthermore, it has been shown that linear DNA substrates are insufficient to study MMR *in vitro* due to the fact that DNA-ends are sensitive for UvrD unwinding (157). Beside this, MutS has been reported to show a strong affinity for DNA ends (158). Consequently, suitable circular DNA substrates were designed to surmount these problems, although it denoted a big challenge to introduce different mismatches

and/or modifications at defined positions into a plasmid. To generate the required features such as a single hemi-methylated site or a single uracil within circular DNA, a recently developed method (156) was adapted and optimized (Figure 3-1; see Materials and Methods).

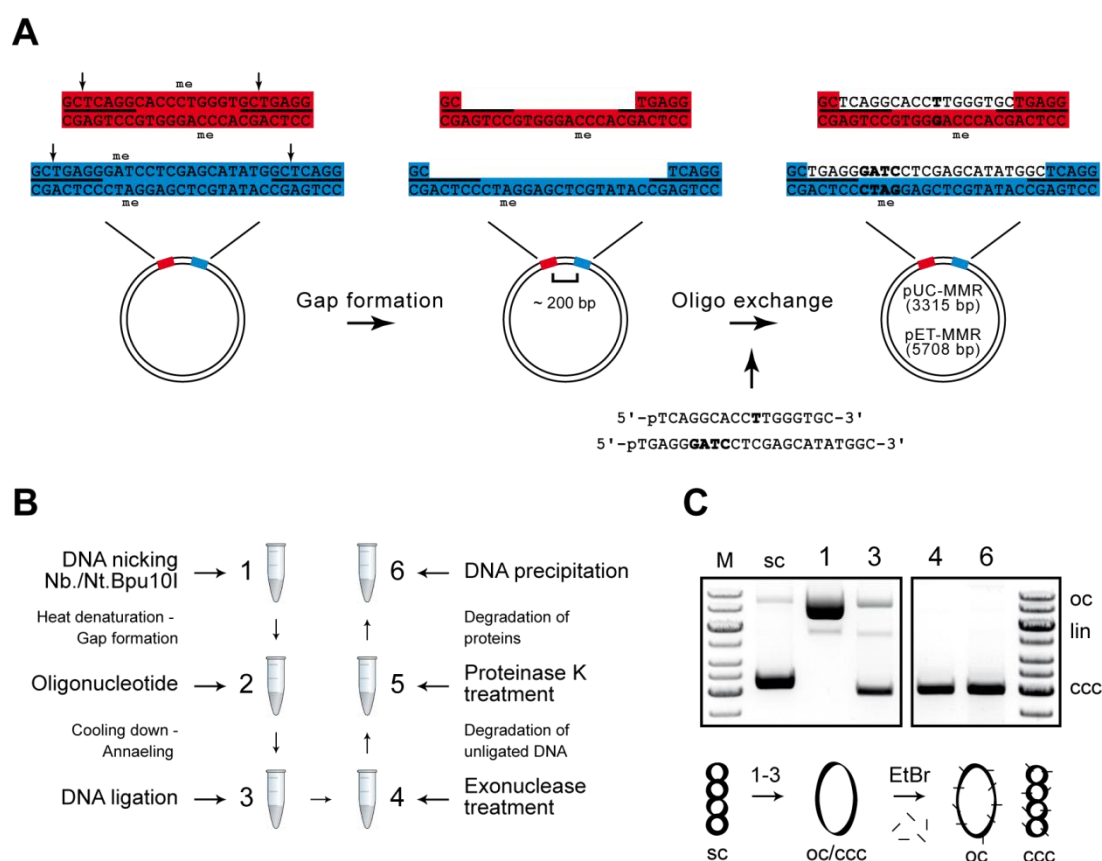


Figure 3-1: Generation of modified circular DNA repair substrates

A: Scheme for generation of circular DNA repair substrates. Specific strand incisions (arrows) by a nicking enzyme (NEB, Fermentas) around a Dcm-site (red fragment) as well as around a Dam-site (blue fragment) allow the exchange of two short oligonucleotides in one reaction to introduce mismatches and/or modifications at defined positions. **B:** Developed procedure for generation of all required circular DNA repair substrates (see Materials and Methods). **C:** Monitored steps during generation of circular substrates using an EtBr pre-stained agarose gel. Indicated numbers are equivalent to steps in B (see text for details). In contrast to ocDNA appearing after nicking of scDNA (1), intercalation of the dye into cccDNA which is achieved after oligonucleotide exchange and ligation promotes a supercoiled-like structure which migrates faster during gel-electrophoresis (1). This effect is used to discriminate between unprocessed DNA repair substrates and appearing intermediates containing a nick or single-nucleotide gap.

To create a suitable blueprint which offers the flexibility to generate various DNA substrates with this method, four recognition sites for the nicking enzyme pair Nt./Nb.Bpu10I (Fermentas) were introduced into a fully methylated starting plasmid at defined positions via site-directed mutagenesis (155). Two of them were introduced around a Dcm-site (5'-CC_{me}AGG-3'/5'-CC_{me}TGG) with a distance of 17 bp to each other. The other two sites were introduced around Dam-site (5'-GA_{me}TC-3'/5'-GA_{me}TC-3') ~200 bp downstream of the mentioned Dcm-site (Figure 3-1A). The capability to choose whether the top or bottom strand should be modified increased the number of possible DNA substrates (Figure 3-2). However, nicking of the blueprint and partial denaturation in the presence of molar excess of short synthetic oligonucleotides allowed the exchange of two short DNA fragments in one reaction (Figure 3-1B). To achieve for example a T:G mismatch within the Dcm-site, the incorporated 17 bp oligonucleotide contained a T instead of the original 5meC, thereby creating the designated recognition site for Vsr (5'-CTAGG-3'/5'-CC_{me}TGG-3'). A hemi-methylated GATC-site for MutH was generated in the same way using an unmethylated complementary 23 bp oligonucleotide. Optionally, the DNA substrate was fully methylated again to avoid nicking at the GATC-site by MutH. The designated circular substrate was achieved after complete ligation of modified DNA. Finally, treatment with a specific set of exonucleases allowed a first purification step due to elimination of unligated products and remaining oligonucleotides (Figure 3-1C).

Notably, the old DNA fragment can always re-anneal during this procedure, thereby creating homoduplex DNA or a fully methylated GATC-site resulting in incompletely processed repair substrates. However, the fact that intercalation of ethidium bromide (EtBr) into cccDNA promotes a supercoiled-like structure which migrates faster during gel-electrophoresis, was utilized to discriminate between an unprocessed substrate (ccc) and the appearing intermediate for example after strand incision or gap formation (both oc) indicating initiation of DNA repair (see Introduction). To this end, DNA repair was demonstrated by restriction cleavage analysis (linearization) due to restoration of an additional recognition site for a restriction enzyme such as MvaI or PstI.

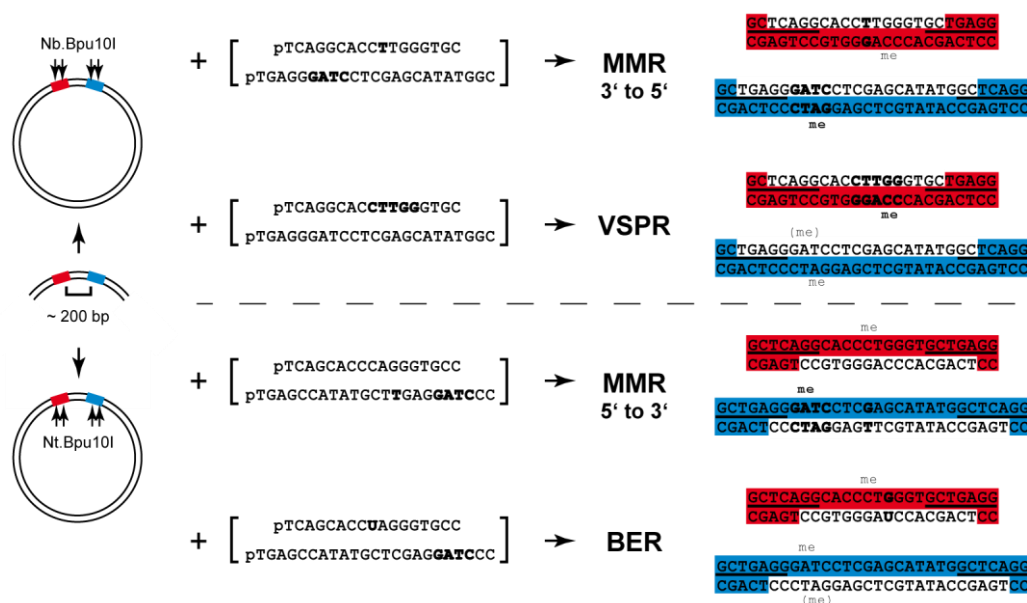


Figure 3-2: Selection of modified circular DNA repair substrates

The developed procedure allows the exchange of two short DNA fragments covering a Dcm-site (17 bp, red fragment) and a Dam-site (23 bp, blue fragment), respectively, either in the top or bottom strand in one reaction. The possibility to introduce various mismatches and/or modification (bold) at defined positions with different orientations permits to generate all required circular substrates to study crosstalk in DNA repair *in vitro*. Optionally, DNA is fully methylated at hemi-methylated GATC-sites by the Dam methyltransferase (NEB).

In conclusion, the developed procedure described here allowed the efficient generation of suitable DNA repair substrates indispensable to study crosstalk in DNA mismatch repair. To this end, several different DNA substrates and almost all proposed components of the MMR, VSPR and BER pathway were used to develop appropriate DNA repair assays and to attempt partial reconstitution of these systems *in vitro*. Finally, the distinction between unprocessed DNA substrates and appearing repair intermediates via gel-electrophoresis made it possible to monitor initial steps in DNA mismatch repair such as strand incision or gap formation. The possibility to generate a brought repertoire of different circular DNA substrates containing various damages and/or modification permits to analyze the crosstalk of DNA repair systems involved in repair of lesions that appear after oxidation or methylation of bases (see Introduction).

3.2 Monitoring methyl-directed mismatch repair (MMR) *in vitro*

The initial steps in DNA methyl-directed mismatch repair (MMR) from *E. coli* require actions and enzymatic activities of at least seven components. During replication, MMR is triggered by mismatch-provoked activation of the latent endonuclease MutH by MutS and MutL. MutH introduces a nick 5' of an unmethylated GATC-site within the newly replicated and erroneous daughter strand that serves as entry point for subsequent mismatch-provoked strand excision by UvrD and an appropriate exonuclease. Considering that MMR is a bi-directional process, depending on the orientation of a mismatch to the introduced nick, several single-strand (ss) specific exonucleases such as ExoI (3' to 5') or RecJ (5' to 3') are required for degradation of the appearing erroneous ssDNA. Furthermore, SSB is involved to avoid procession or degradation of the parental DNA strand and has been reported to stimulate processivity of UvrD. Finally, all these proteins function in concert to carry out recognition and excision of DNA mismatches thereby allowing a new round of DNA synthesis (see Introduction).

In this work initial steps in MMR were reconstituted *in vitro* and monitored via specific procession of heteroduplex DNA by the repair machinery. Mismatch-provoked strand discrimination in the presence of MutSLH was demonstrated by mismatch-provoked nicking of a circular DNA substrate resulting in the corresponding open circular (oc) MMR intermediate (Figure 3-3). Subsequent mismatch-provoked strand unwinding was assayed via excision of the erroneous DNA strand and appearing of single-strand gaps or single-strand circular (ssc) DNA in the presence of MutSLH, UvrD, ExoI/RecJ and SSB (Figure 3-4). Finally, repair of a single mismatch by MMR *in vitro* was demonstrated by restriction cleavage analysis due to restoration of a recognition site for a restriction enzyme such as MvaI or PstI.

3.2.1 Mismatch-provoked strand discrimination by MutH

The flexibility in generation of various suitable DNA repair substrates (Table 2-4) offered the possibility to study initiation of MMR *in vitro* depending on orientation and distance of a T:G mismatch related to a single hemi-methylated GATC-site. To this end, efficient initiation of DNA mismatch repair was monitored by appearing of the proposed nicked MMR intermediate in the presence or absence of the required components involved in this pathway.

Specific initiation of MMR *in vitro* was analyzed using a circular DNA substrate containing both a T:G mismatch and a hemi-methylated GATC-site, ~200 bp downstream of the damage as well as all proposed components required for strand discrimination. As expected, mismatch-provoked activation of MutH by MutS and MutL in the presence of ATP resulted in the nicked (oc) MMR intermediate, indicating strand incision 5' of the unmethylated GATC-site (Figure 3-3; compare lane 2 and 7). However, in the absence of MutS, MutL, MutH or ATP strand incision was avoided, demonstrating that strand discrimination during MMR strictly requires MutS, MutL, MutH and hydrolysis of ATP (Figure 3-3; compare lane 7 and 8-11) under the used conditions *in vitro*. Moreover, initiation of MMR was also observed, independent whether the lesion was upstream or downstream located of the strand discrimination signal and therefore the results are in agreement with the described bi-directionality of this process *in vivo* (Figure 3-6).

Interestingly, strand incision by MutH also occurred efficiently when T:G mismatch and hemi-methylated GATC-site were separated by a distance of only 4 bp (Figure 3-8). However, the fact that simultaneous binding to overlapping DNA regions by MutS and MutH is mutual exclusive, strand incision directly next to a mismatch suggests rather a mobile than a stationary MutS, which leaves the mismatch after recognition allowing MutH to bind at its target site and perform strand discrimination. Finally, DNA substrates without a mismatch or a hemi-methylated GATC-site prevented initiation of MMR and strand incision, as expected (Figure 3-17).

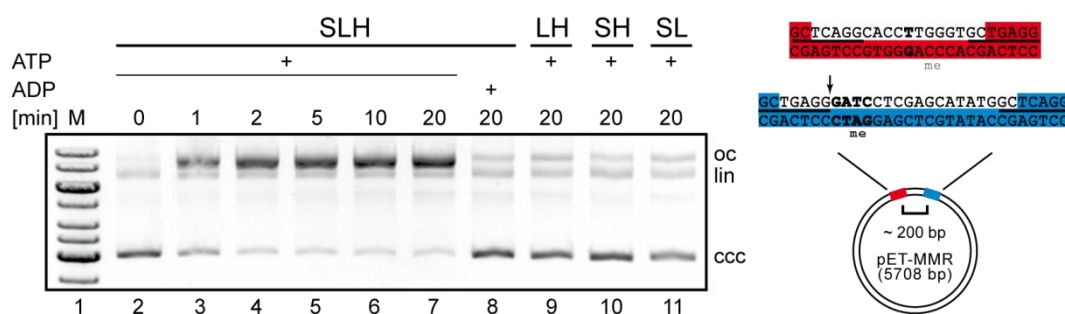


Figure 3-3: Mismatch-provoked strand discrimination by MutH

Incubation of heteroduplex cccDNA (20 nM) containing a single hemi-methylated GATC-site ~200 bp downstream of a T:G mismatch with MutS (200 nM), MutL (200 nM) and MutH (50 nM) in the presence of ATP (1 mM) results in the nicked MMR intermediate, as expected (compare lane 2 and 7). No strand incision is observed after 20 min in the absence of MutS, MutL, MutH or ATP, respectively, demonstrating the specificity of mismatch-provoked and ATP-hydrolysis dependent initiation of MMR *in vitro* (compare lane 7 and 8-11). Samples were taken at time points as indicated. T:G mismatch and hemi-methylated GATC-site are shown in bold. The MutH nicking site is indicated by the arrow.

In conclusion, these results demonstrate that the generated modifications within the used circular DNA substrate were necessary and sufficient to trigger specific initiation of MMR *in vitro*. The described MutSLH assay allowed monitoring of the strand discrimination step due to mismatch-provoked activation of the MutH-endonuclease by MutS and MutL in an ATP-hydrolysis dependent manner resulting in the nicked MMR intermediate. Consequently, this DNA repair assay was used for investigations in subsequent steps of the MMR pathway such as mismatch-provoked strand excision by UvrD. Moreover, the MutSLH assay was utilized to study influences on initial steps in MMR as a possible consequence of the crosstalk between MMR and VSPR for repair of T:G mismatches that appear after deamination of 5-methylcytosine within a Dcm-site (see Introduction).

3.2.2 Mismatch-provoked strand excision by UvrD

In *E. coli*, mismatches proficient to initiate MMR can arise up to 1000 bp away from the next strand discrimination signal (hemi-methylated GATC-site) to be efficiently repaired. However, to avoid fixing of mutations, the erroneous DNA strand has to be removed in a proper way. Therefore, UvrD is proposed to be

recruited by MutL directly to the nick, previously introduced by MutH, and starts unwinding of DNA towards the mismatch. Subsequent degradation of the excised DNA strand by direction-dependent exonucleases such as ExoI or RecJ results in a single-strand gap and permits a new round of DNA synthesis. During excision, UvrD processivity is stimulated by SSB which protects the parental unprocessed DNA strand (see Introduction). Notably, details in the hand-off between MutH and UvrD both stimulated by MutSL for actions at a hemi-methylated GATC-site are still unclear. Consequently, after establishing the mismatch-provoked strand discrimination assay it was attempted to reconstitute the strand excision step in the presence of all proposed components *in vitro*. To this end, generation of a single-strand gap containing MMR intermediate was assayed via restriction cleavage analysis as well as by appearing of single-strand circular (ssc) DNA due to complete excision of the erroneous strand.

As shown in this work, it was possible to reconstitute initial steps in MMR *in vitro* using a circular DNA substrate containing a single T:G mismatch ~200 bp upstream of a hemi-methylated GATC-site and all proposed components of this repair pathway (Figure 3-4). As expected, initiation of MMR strictly required MutSLH for mismatch-provoked strand discrimination and incision (Figure 3-4A; lane 7, 10 and 13). The generated nick served as entry point for subsequent DNA unwinding and excision (Figure 3-4A; compare lane 2-4 and 5-13). In the absence of either UvrD or ExoI no strand excision or gap formation was observed due to the missing unwinding activity by a helicase as well as re-annealing of partially unwound DNA in the absence of an appropriate exonuclease (Figure 3-4A; lane 14-19). Moreover, SSB was used to stimulate and therefore visualize strand excision due to the fact that the MMR intermediate with a short gap was not separated from ocDNA during gel-electrophoresis (Figure 3-4A; compare lane 2-4 and 20-22). Consequently, short-patch strand excision was monitored via restriction cleavage analysis because ssDNA is proposed to be insensitive for double-strand cleavage (Figure 3-5). Finally, mismatch-provoked unwinding was also observed when the mismatch was located ~200 bp downstream of the MutH recognition site and RecJ

was used for 5' to 3' degradation of the appearing ssDNA, demonstrating the bi-directionality of the MMR system (data not shown).

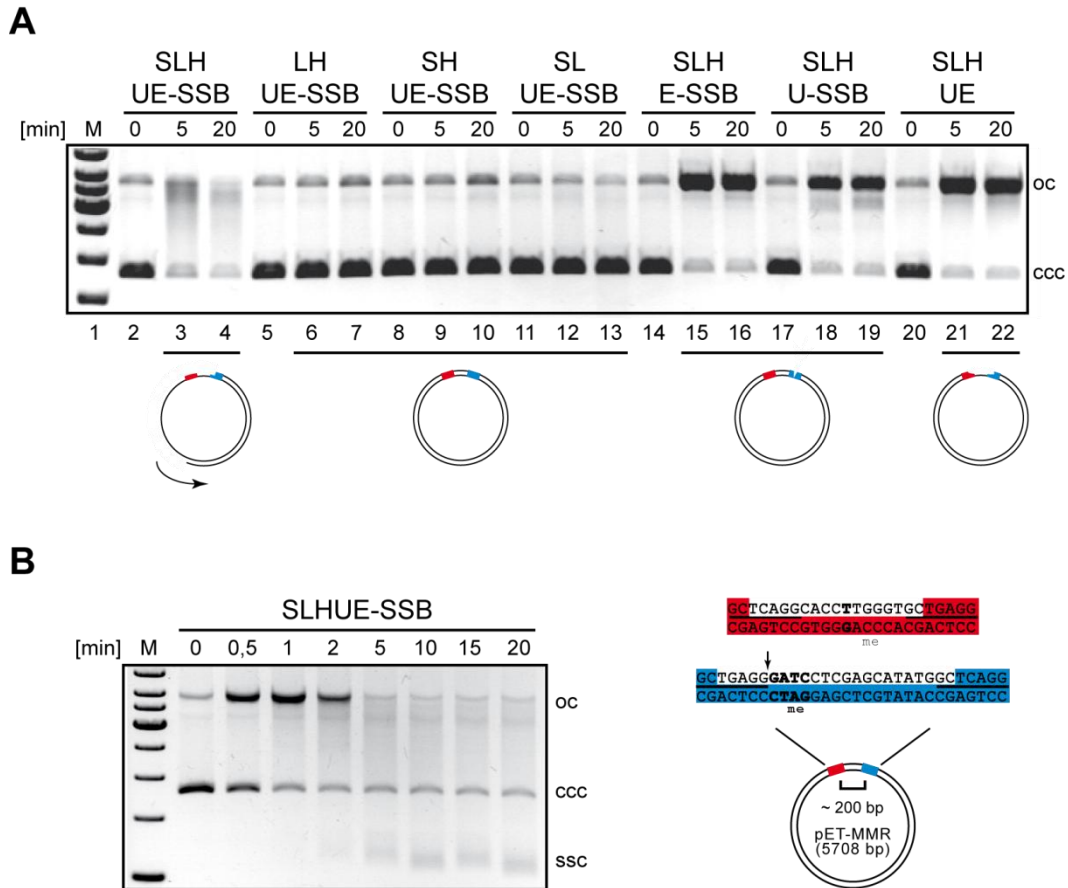


Figure 3-4: Mismatch-provoked strand excision by UvrD

A: Heteroduplex cccDNA (20 nM; B) containing a single T:G mismatch ~200 bp upstream of a hemi-methylated GATC-site was incubated with all proposed components required for strand discrimination and excision. In the presence of MutS (200 nM), MutL (200 nM), MutH (50 nM), UvrD (50 nM), ExoI (0.1 u/μl) and SSB (300 nM) the circular substrate is specifically processed, thereby creating repair intermediates containing a long single-strand region of undefined length (lane 2-4). In the absence of MutS, MutL or MutH initiation of MMR is prevented, as expected (lane 5-13). Without UvrD or ExoI, cccDNA containing a nick 5' of the mismatched T (arrow) is not further processed after strand incision (lane 14-19). Lacking SSB results in a MMR intermediate with a short single-strand gap which is not separated from cccDNA via gel-electrophoresis (compare lane 2-4 and 20-22). Therefore, SSB-independent short-patch unwinding was monitored via restriction cleavage analysis (Figure 3-5). **B:** Kinetic of complete processon of the circular DNA substrate (20 nM) to sscDNA after mismatch-provoked strand discrimination and excision in presence of MutSLH, UvrD and ExoI, stimulated by SSB (400 nM).

Further analysis revealed that strand incision does not strictly depend on MutH to allow initiation of mismatch-provoked strand excision *in vitro* (Figure 3-5). To demonstrate that MutH is replaceable by any other nicking enzyme, the heteroduplex circular DNA substrate was pre-incubated with Nt.BbvCI, thereby generating a nick 18 bp downstream of the T:G mismatch. To this end, SSB-independent short-patch unwinding and excision towards the mismatch starting from this nick was monitored via restriction cleavage analysis using BamHI (5'-GGATCC-3'). As expected, UvrD was able to perform short-patch excision in a MutSLE-dependent manner in order to remove the mismatch. Consequently, generation of the single-strand gap containing MMR intermediate avoided subsequent linearization by BamHI (Figure 3-5; lane 3). In the absence of MutS, only little inhibition in double-strand cleavage by the enzyme was observed due to unspecific recruitment of UvrD by MutL (Figure 3-5; lane 5). Almost complete linearization of the substrate was detected after incubation without UvrD demonstrating that strand excision was prevented in the absence of helicase activity *in vitro*, as expected (Figure 3-5; compare lane 3 and 7). Finally, indeed similar results were obtained with the same circular DNA substrate when the desired nick was introduced by MutH (Figure 3-8).

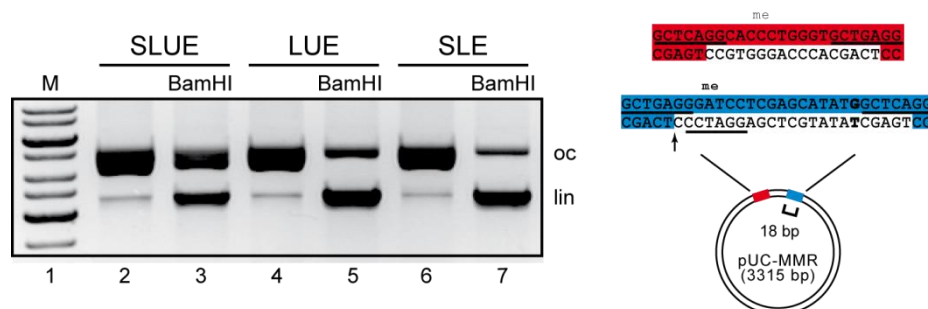


Figure 3-5: MutH-independent short-patch strand excision by UvrD

Incubation of a pre-nicked (Nt.BbvCI, arrow) heteroduplex DNA substrate (20 nM, oc) with MutS (200 nM), MutL (200 nM), UvrD (100 nM) and ExoI (0.1 u/μl) allows MutH-independent short-patch strand unwinding and excision. The achieved MMR intermediate contains a short single-strand gap that prevents linearization by BamHI, as expected (lane 3). In the absence of MutS only little inhibition in BamHI cleavage is observed as a consequence of unspecific recruitment of UvrD by MutL (lane 5). Without UvrD the DNA substrate is almost complete linearized demonstrating the absence of a short single-strand gap (compare lane 3 and 7). The T:G mismatch and BamHI recognition site (5'-GGATCC-3') are indicated in bold and underlined, respectively.

3.2.3 Reconstitution of UvrD/RecJ-independent MMR *in vitro*

After successful reconstitution of the initial steps in MMR it was attempted to reconstitute also the final step of this DNA repair pathway *in vitro*. As mentioned, this step includes DNA re-synthesis by polIII and DNA ligation after excision of the erroneous strand. However, due to the fact that DNA polIII was not available, polI was used to complete MMR *in vitro*. PolI is suggested as a member of the VSPR and BER pathway in *E. coli* and responsible for DNA repair via nick-translation (5' to 3' exonuclease and polymerase activity) after strand incision by Vsr or gap formation by UDG/EndoIV (see Introduction). Consequently, it was attempted to repair a circular heteroduplex DNA substrate via nick-translation in the absence of UvrD and RecJ the proposed components for 5' to 3' MMR. Notably, because 5' to 3' polarity of nick-translation, only substrates containing a hemi-methylated GATC-site upstream of the mismatch were suitable for UvrD/RecJ-independent MMR via nick-translation *in vitro*. Finally, DNA repair was demonstrated by restriction cleavage analysis using PstI (5'-CCCTGGG-3'). In contrast to homoduplex DNA, linearization of heteroduplex DNA substrates is proposed to be avoided by a T:G mismatch located within the recognition sequence for this restriction enzyme (5'-CCTTGGG-3'; Figure 3-6).

As expected, incubation of the a circular DNA substrate containing the hemi-methylated GATC-site ~200 pb upstream of a single T:G mismatch with MutSLH allowed strand discrimination and resulted in the nicked MMR (Figure 3-6B; lane 4). Beside this, the remaining T:G mismatch within the PstI recognition site successfully prevented linearization of the substrate by the restriction enzyme (Figure 3-6B; lane 5). However, addition of polI to the reaction obviously allowed subsequent linearization of the substrate by PstI indicating restoration of the original C:G base pair within the recognition site (Figure 3-6B; lane 6 and 7). These data demonstrate that DNA repair after strand discrimination indeed was achieved via nick-translation by polI and in an UvrD/RecJ-independent manner. Finally, addition of DNA ligase resulted in covalent closed circular DNA that was completely linearized by PstI but not further processed by MutSLH indicating absence of the

mismatch and reconstitution of MMR *in vitro* (Figure 3-6B; compare lane 6 and 8). Under the conditions used, the DNA ligase was not able to avoid nicking by MutH when the T:G mismatch was present (data not shown). Finally, it was demonstrated that the repair mix containing MutSLH, DNA polII and ligase efficiently repaired the used MMR substrate within a few minutes *in vitro* (Figure 3-6B; lane 10 and 11).

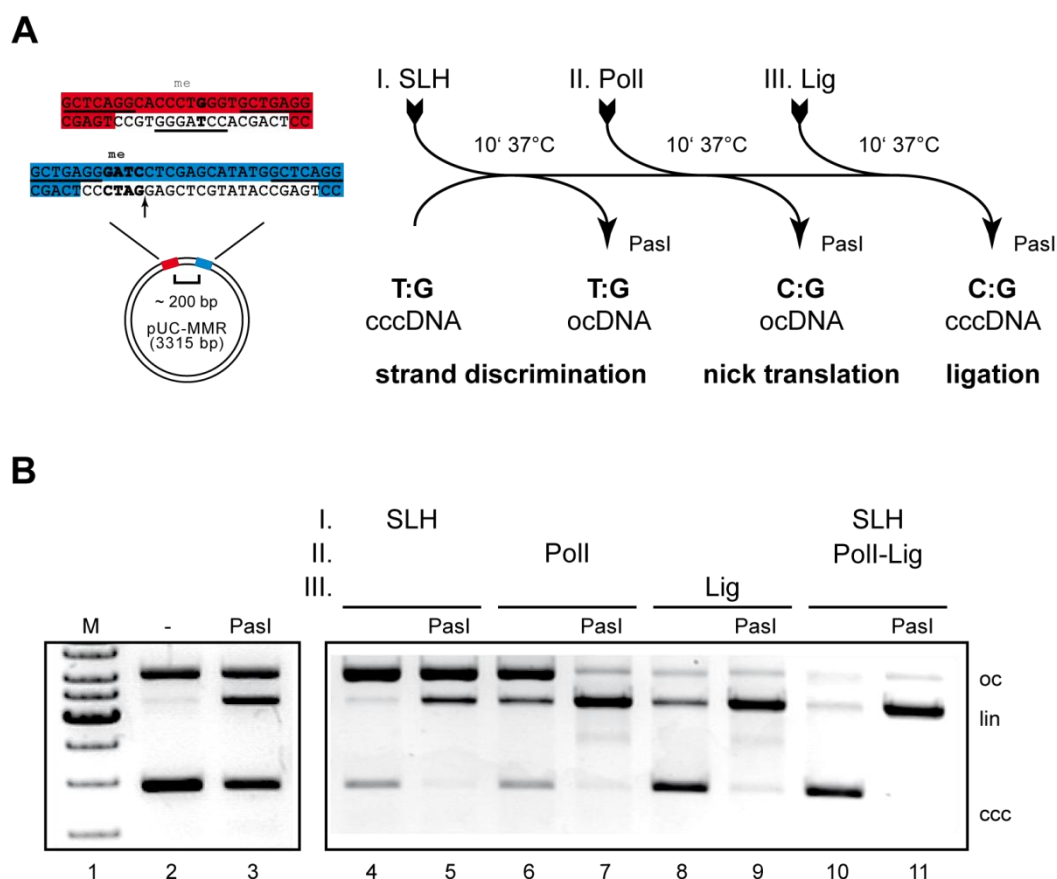


Figure 3-6: Reconstitution of UvrD/RecJ-independent MMR *in vitro*

A: Scheme for stepwise reconstitution of 5'-3' MMR via nick-translation *in vitro*. The required nick (arrow) achieved after strand discrimination is introduced ~200 bp upstream of a T:G mismatch (bold). DNA repair and reconstitution of a single PasI recognition site (underlined) is demonstrated by restriction cleavage analysis using the corresponding restriction enzyme. **B:** Incubation of the heteroduplex circular DNA substrate (20 nM; A) with MutS (200 nM), MutL (200 nM) and MutH (50 nM) results in strand incision, as expected (compare lane 2 and 4). Moreover, neither the heteroduplex DNA substrate nor the nicked MMR intermediate are linearized by PasI (lane 3 and 5). However, after stepwise addition of polII and ligase (0.1 u/μl each; 1 mM) to the reaction as shown in A, treatment with PasI results in almost complete linearization of the DNA substrate (lane 7 and 9), indicating restoration of the original C:G base pair and finally reconstitution of MMR *in vitro* via nick-translation in an UvrD/RecJ-independent manner (see text for details).

In conclusion, the results demonstrate that efficient 5'-directed DNA repair *in vitro* can be achieved by DNA polII suggesting a possible alternative route for 5'-3' MMR *in vivo*. In order to repair a mismatch that is located downstream of a processed strand discrimination signal, DNA pol is suitable for MMR in *E. coli* via nick-translation without the requirement for UvrD and an appropriate 5'-3' exonuclease such as RecJ. Notably, there is no evidence for a mismatch-dependent recruitment of DNA polII by MutS and MutL as shown for UvrD and therefore DNA repair might be the positive consequence of initiated nick-translation towards the damage as suggested for VSPR.

3.3 Crosstalk between MMR and VSPR in *E. coli*

Methylation of cytosine to 5-methylcytosine (5meC) is used by many organisms as a chemical tag to discriminate between DNA from different sources that lack this modification and/or to regulate transcriptional activity. In *E. coli*, MMR and VSPR are directed to repair T:G mismatches that arise after deamination of 5meC within a Dcm-site. Earlier *in vivo* studies and several experimental observations have demonstrated the obvious requirement for crosstalk between both systems in order to prevent misengaged repair as well as to assure that these two processes do not significantly interfere with each other. The fact that both competition and cooperation between components of these repair systems have been reported to regulate actions in DNA mismatch repair reveals a puzzle in the crosstalk required for maintaining Dcm-sites (see Introduction).

In this work, the crosstalk between MMR and VSPR was studied *in vitro* using circular DNA substrates sufficient to trigger initiation of both pathways concurrently. To this end, a Vsr endonuclease assay was developed that allowed to monitor the generation of a nicked VSPR intermediate as consequence of the proposed mismatch-provoked strand incision 5' of the mismatched T. For investigations in the crosstalk with MMR, Vsr endonuclease activity was analyzed in the presence or absence of factors responsible for initiation of MMR. On the other hand, the

influence on initial steps in MMR such as strand discrimination and excision by Vsr was investigated in detail.

Beside this, no data is available that directly demonstrates a requirement for crosstalk between both repair systems after strand incision by Vsr. Misengaged MMR induced by the nicked VSPR intermediate ('T:G) increases the chance for arising of a double-strand break within the DNA under unfavourable conditions (Figure 1-13). To provoke initiation of MMR, MutS has to recognize and to bind the processed intermediate in similar way as the T:G mismatch prior to nicking by Vsr. Consequently, VSPR substrate and corresponding *in situ* generated intermediate were compared in mismatch binding by MutS using fluorescence techniques such as FRET and anisotropy measurements. FRET assays were performed to monitor mismatch-provoked conformational changes by MutS towards the *initial recognition complex* (IRC) which is indispensable for initiation of MMR. Due to the fact that mismatch recognition and binding by MutS induces specific bending of DNA, FRET is a powerful tool to detect these changes using fluorophore double-labeled DNA substrates. Moreover, anisotropy measurements were performed to achieve information about the orientation in which the mismatch is bound by MutS (see Materials and Methods).

3.3.1 Initiation of very-short patch repair (VSPR) *in vitro*

The VSPR system from *E. coli* is the major pathway responsible for repair of T:G mismatches that appear after deamination of 5-methylcytosine within a regulatory Dcm-site. In contrast to MMR where mismatch-provoked strand discrimination strictly depends on MutSLH, the Vsr endonuclease alone is required and sufficient for mismatch recognition and generation of a nick 5' to the mismatched T.As mentioned, the introduced nick serves as entry point for subsequent repair by DNA polI via nick-translation (see Introduction).

In this work, VSPR was studied on a generated circular DNA substrate containing a T:G mismatch within a hemi-methylated Dcm-site which represents the natural substrate for the Vsr endonuclease *in vivo* (Figure 3-7). Consequently,

initiation of VSPR and therefore Vsr activity was demonstrated by mismatch-provoked nicking of the circular DNA substrate resulting in the proposed VSPR intermediate due to strand incision 5' of the mismatched T. Appearing of the intermediate was monitored via gel-electrophoresis as described previously for the MutH endonuclease assay (see Materials and Methods).

Incubation of the heteroduplex circular DNA substrate with the mismatch recognizing Vsr endonuclease resulted in strand incision, indicating initiation of VSPR *in vitro* and generation of the proposed intermediate (Figure 3-7; lane 2-6). In contrast, the corresponding homoduplex circular DNA substrate containing the original C:G base pair instead of a mismatch was not processed by Vsr, demonstrating that initiation of VSPR is mismatch-dependent under the used conditions, as expected (Figure 3-7; compare lane 6 and 11). Finally, DNA substrates with a mismatch in a different sequence context were not cleaved by Vsr indicating the observed DNA nicking was specific for the mismatch recognizing endonuclease (Figure 3-8).

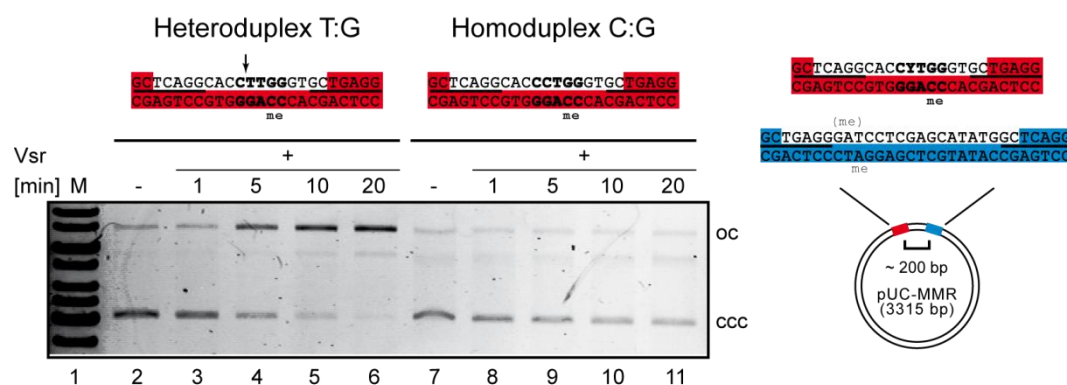


Figure 3-7: Mismatch-provoked activation of Vsr

Incubation of the heteroduplex circular DNA substrate (15 nM) containing a single T:G mismatch within a hemi-methylated Dcm-site (bold) with Vsr (50 nM) results in the desired nicked VSPR intermediate (compare lane 2 and 6) due to strand incision 5' of the mismatched T (arrow). No VSPR intermediate is observed after 20 min, when homoduplex DNA was used, demonstrating that initiation of VSPR *in vitro* is mismatch-dependent, as expected (compare lane 6 and 11). Samples were taken at time points as indicated and strand incision by Vsr was monitored via gel electrophoresis using an EtBr pre-stained 1 % agarose gel as described previously.

In conclusion, the possibility to generate the natural occurring recognition site for the Vsr endonuclease within a circular DNA substrate allowed successful development of a Vsr endonuclease assay and therefore to monitor initiation of VSPR *in vitro*. Moreover, the fact that the same damage also triggers initiation of MMR, offered the chance to investigate mutual influences by components of both DNA mismatch repair systems as a possible consequence of crosstalk required for repair of a common target.

3.3.2 Vsr inhibits mismatch-provoked activation of MutH by MutS and MutL

Various experimental observations have led to the conclusion that crosstalk between MMR and VSPR does not only rely on competition between MutS and Vsr for mismatch binding and subsequent initiation of repair, but also includes specific interactions of components involved in both repair systems. Especially MutL the molecular matchmaker in MMR is proposed to play a role in VSPR due to modulating the activity of Vsr. The previous demonstrated physical interaction between MutL and Vsr using bacterial and yeast-two hybrid analysis, was recently confirmed via analytical ultracentrifugation (AUC) and site-directed crosslinking by Sarah L. Elliot and Luis Giron-Monzon (134). The proposed model by Luis Giron-Monzon and Sven Geisler maps the interaction site of MutL for Vsr to a similar region as the MutH-MutL interaction site, supporting the proposed competition of MutH and Vsr for binding to MutL.

To investigate whether the physical interaction between Vsr and MutL is sufficient to explain the inhibitory effect on MMR *in vivo*, the influence of Vsr on initial steps in MMR, i.e. the mismatch-provoked activation of the MutH endonuclease by MutS and MutL, was tested *in vitro*. DNA mismatch repair substrates containing a T:G mismatch in a different sequence context, that are not cleaved by Vsr were used to study the crosstalk between methyl-directed mismatch repair (MMR) and very-short patch repair (VSPR), indicating the observed nicking was specific for MutH. Heteroduplex circular DNA substrates containing a T:G

mismatch only 4 bp away from the hemi-methylated GATC-site was nicked by MutH in a MutSL-dependent manner, as expected (Figure 3-8A; lane 2-5). However, in the presence of Vsr strand discrimination by MutSLH was obviously inhibited *in vitro* (Figure 3-8A; compare lane 2-5 and 6-9).

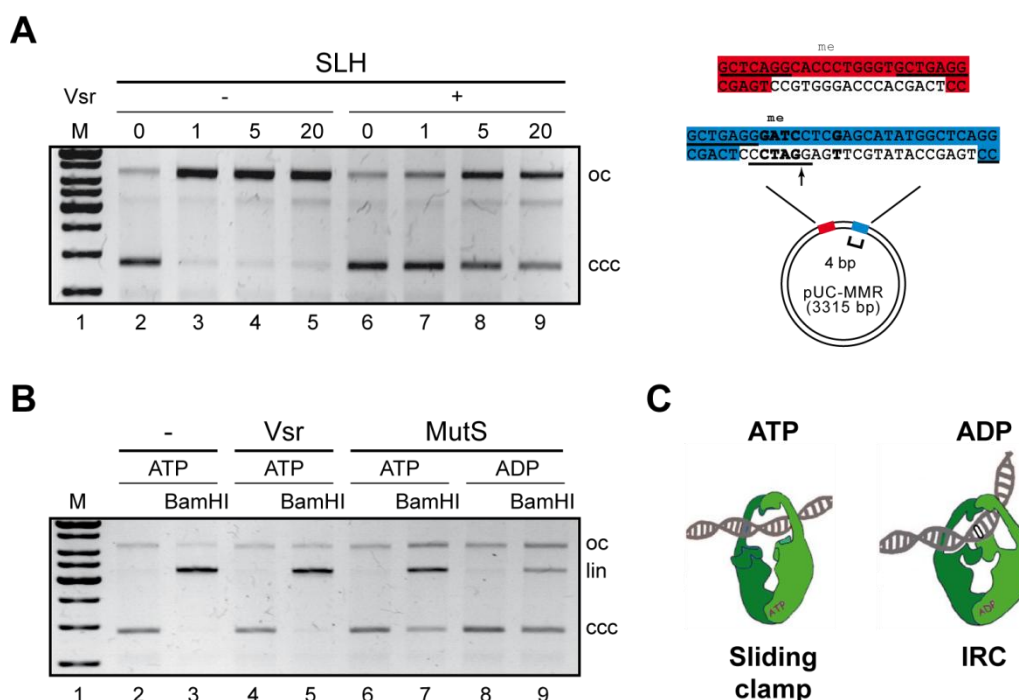


Figure 3-8: Vsr inhibits mismatch-provoked activation of MutH

A: Heteroduplex circular DNA (20 nM) containing a T:G mismatch 4 bp upstream of a hemi-methylated GATC-site was incubated with MutS (400 nM), MutL (1 μM), MutH (200 nM) and ATP (1 mM) in the presence or absence of Vsr (3 μM) at 37 °C for the indicated time. Mismatch-provoked activation of MutH by MutSL is obviously inhibited by Vsr under the conditions used *in vitro* (compare lane 2-5 and 6-9). **B:** To rule out unspecific mismatch recognition by Vsr, the circular DNA substrate (20 nM) was incubated with either Vsr (5 μM) or MutS (5 μM) in the presence of the indicated nucleotide (1 mM each) for 5 min at 37 °C, followed by addition of BamHI (5 U) for 10 sec. As expected, no or little BamHI blocking is observed in the presence of Vsr or MutS, incubated with ATP (lane 5 and 7). Mismatch binding by MutS in the presence of ADP avoids linearization by BamHI due to formation of the *initial recognition complex* (IRC) (lane 9; see text for details). **C:** Model for mismatch and nucleotide induced conformational changes in MutS towards the *sliding clamp* and the IRC in the presence of ATP and ADP, respectively.

Restriction cleavage analysis revealed that binding of MutS in the presence of ADP is blocking the action of BamHI whereas Vsr is not, indicating that Vsr is not strongly binding to this mismatch (Figure 3-8B; compare lane 5 and 9). As proposed, mismatch recognition by MutS in the presence of ADP results in formation of the *initial recognition complex* (IRC) thereby blocking linearization by BamHI (Figure 3-8C). Moreover, in the presence of ATP only little blocking of DNA cleavage was observed, which suggests *sliding clamp* formation by MutS, leaving the mismatch after recognition and thereby allowing MutH (Figure 3-8A; lane 5) or BamHI to act at their target site (Figure 3-8B; compare lane 7 and 9). On the other hand, influence on Vsr activity by components of the MMR system was studied using the natural Vsr substrate containing a T:G mismatch within the hemi-methylated Dcm-site (Figure 3-9). To indicate that the observed nicking was specific for the Vsr endonuclease competition assays were performed in the presence of the catalytic inactive variant MutH E77A. To this end, this MutH variant indeed inhibited strand incision by Vsr under the conditions used *in vitro* when MutS and MutL were present (data not shown).

In conclusion, these results demonstrate that competition between Vsr and MutS for mismatch binding is not necessary to inhibit mismatch-provoked activation of MutH which is a consequence of competition between Vsr and MutH for binding to MutL. Moreover, these results confirm the model in which the molecular matchmaker MutL is involved in crosstalk between MMR and VSPR due to interaction with effector proteins of both repair pathways. Interestingly, Vsr endonuclease activity was stimulated in the presence of MutS and MutL, an effect which was subsequently investigated in detail.

3.3.3 Vsr endonuclease activity is stimulated by MutS and MutL

As mentioned, efficiency of VSPR *in vivo* is influenced by the presence of both MutS and MutL. The present and previous studies have provided the evidence for a physical and functional interaction between Vsr and MutL, but little *in vitro* data is available for the role of MutS in this pathway. Therefore, the role of MutS, MutL and

ATP-hydrolysis on the activity of Vsr was analyzed using the heteroduplex circular DNA substrate containing a single T:G mismatch within the hemi-methylated Dcm-site (Figure 3-9).

Analysis of crosstalk between components of the VSPR and MMR pathway demonstrated that endonuclease activity of Vsr is greatly stimulated in the presence of both MutS and MutL in an ATP-hydrolysis dependent manner (Figure 3-9; lane 7). Under the experimental conditions used, neither MutL nor MutS alone were able to stimulate the Vsr endonuclease activity (Figure 3-9; compare lane 3-5 and 7). Moreover, this stimulation was dependent on the presence of ATP which cannot be substituted by ADP (Figure 3-9; compare lane 7 and 9). In the absence of Vsr, no strand incision was observed with MutS, MutL and ATP, as expected (Figure 3-9; lane 11). Furthermore, DNA substrates without a mismatch or a mismatch in a different sequence context were not cleaved by Vsr indicating the observed DNA nicking was specific for the mismatch recognizing endonuclease (Figure 3-8).

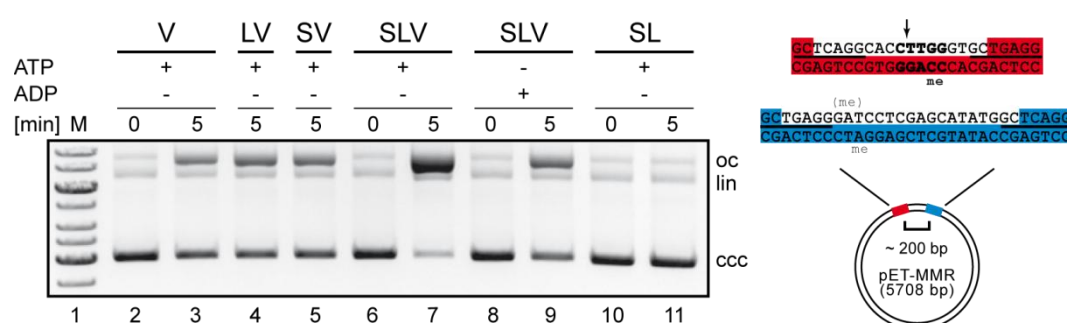


Figure 3-9: Mismatch-provoked stimulation of Vsr by MutSL

Vsr endonuclease activity is greatly stimulated by MutS and MutL in an ATP-hydrolysis dependent manner (lane 7). Compared to Vsr activity alone (lane 3), only a small stimulation is observed when Vsr was incubated either with MutL or MutS (lane 4 and 5). In the presence of ADP no obvious increase in stimulation of Vsr activity by MutSL is detected, indicating that stimulation of the endonuclease requires ATP-hydrolysis (lane 9). MutS and MutL in the absence of Vsr are not sufficient to initiate VSPR, as expected (lane 11). Strand incision by Vsr, resulting in a nick 5' of the mismatched T (arrow), was monitored after incubation of the circular DNA substrate (15 nM) containing a T:G mismatch within the Dcm-site (bold) for 5 min at 37 °C in the presence or absence of the following compounds: Vsr (75 nM), MutS (400 nM), MutL (400 nM) and ATP or ADP (1 mM).

AUC and crosslinking experiments revealed that the physical interaction between Vsr and MutL requires nucleotide binding but not hydrolysis (134). Consequently, the ATP-binding proficient but ATPase impaired variant MutL E29A was tested for the ability to stimulate Vsr endonuclease activity *in vitro*. In contrast to the results obtained with wildtype MutL little or no stimulation of DNA nicking by Vsr was observed with MutL E29A suggesting that ATP-hydrolysis by MutL is required for a functional interaction with Vsr under physiological conditions (Figure 3-10; compare circles and triangles).

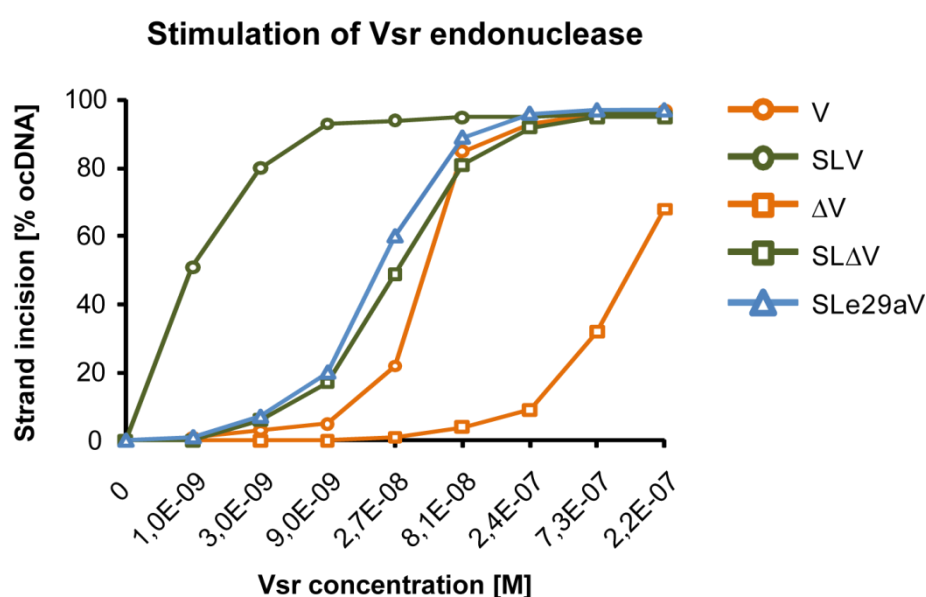


Figure 3-10: Kinetic studies in Vsr endonuclease activity

Strand incision by Vsr and Vsr-Δ14 was monitored via nicking of heteroduplex circular DNA (15 nM, Figure 3-9) after incubation for 5 min at 37° C in the presence or absence of MutS (100 nM), MutL wild type or E29A (200 nM) and ATP (1 mM). Compared to Vsr (orange circles), Vsr-Δ14 alone shows diminished endonuclease activity (orange squares), as expected. However, both endonucleases are greatly stimulated by MutS and MutL (green circles and squares). Only little stimulation of Vsr activity is observed when MutL E29A (blue triangles) was used, indicating that the functional interaction between MutL and Vsr requires ATP-hydrolysis.

Beside this, stimulation of Vsr-Δ14 was analyzed in the presence or absence of MMR components. Compared to wildtype Vsr, the truncated variant showed diminished endonuclease activity. This was not surprising because the crystal structure of the Vsr-DNA complex revealed that the missing N-terminal part contains

amino acid residues important for DNA recognition and binding (Figure 1-12). However, Vsr- Δ 14 endonuclease activity was also greatly stimulated by MutS and MutL *in vitro* (Figure 3-10; compare circles and squares).

These results demonstrate that both MutS and MutL are necessary and sufficient for the stimulation of Vsr endonuclease *in vitro* resulting obviously in enhanced VSPR. Moreover, this functional interaction requires ATP-hydrolysis by MutL which is similar to the mismatch-provoked activation of MutH during MMR. In conclusion these data suggest that the transient MutSL complex, which is formed after mismatch recognition, has the capability to stimulate effector proteins of at least two repair pathways, MMR and VSPR, which explains the results observed *in vivo*. As mentioned, the absence of MutS or MutL decreases the efficiency of VSPR in *E. coli* and therefore demonstrates that cooperation plays a role in the crosstalk of both DNA repair pathways. Finally, since simultaneous mismatch binding by MutS and Vsr is mutually exclusive, only models involving a mobile rather a stationary MutS are consistent with the demonstrated MutSL-dependent activation of Vsr. As demonstrated recently, MMR is also efficient when mismatch and GATC-site are separated by only 4 bp, a distance which is too short to allow simultaneous binding of MutS at the T:G mismatch and MutH at the GATC-site (Figure 3-8).

3.3.4 Reconstitution of enhanced VSPR *in vitro*

After demonstrating the stimulation of Vsr activity by MutS and MutL in an ATP-hydrolysis dependent manner, the whole VSPR pathway was reconstituted *in vitro*. Beside MutS, MutL and Vsr (MutSLV), the VSPR pathway in *E. coli* requires activities of DNA polI and ligase. After strand incision by Vsr, polI is required for DNA repair via nick-translation and ligase for subsequent nick sealing, as described (see Introduction).

As shown here, it was possible to repair a T:G mismatch within a Dcm-site in the presence of all proposed components required for enhanced VSPR *in vitro* (Figure 3-11). DNA repair and restoration of the original C:G base pair was verified via linearization of the generated homoduplex DNA by PasI (5'-CCCAGGG-3'). As

mentioned, the Vsr recognition site (5'-CCTAGGG-3') is included within the recognition sequence for PstI and therefore avoids linearization of heteroduplex DNA by the restriction enzyme (Figure 3-11B). Mismatch-provoked initiation of VSPR was monitored via appearing of the nicked VSPR intermediate ('T:G) as the consequence of strand incision 5' of the mismatched T within the Dcm/PstI-site (Figure 3-11B; lane 5). Subsequent incubation with PstI resulted only in a little increase of linear DNA due to cleavage of homoduplex DNA that was not processed by Vsr. Notably, small amounts of homoduplex circular DNA substrate are achieved from time to time due to the procedure of substrate generation, as mentioned (Figure 3-11B; lane 6). However, addition of DNA ligase to the MutSLV reaction mix and subsequent PstI treatment showed no significant change in the DNA procession and restriction pattern (Figure 3-11B; lane 7 and 8), demonstrating the incapability of the ligase for nick sealing directly next to a T:G mismatch or repair, as expected. Moreover, a perhaps ligated mismatch was still a target for enhanced VSPR and therefore prevented efficient ligation of the substrate. Finally, subsequent incubation of the nicked VSPR intermediate with DNA polI in the presence of the ligase resulted in a circular DNA substrate which was not further processed by MutSLV (Figure 3-11B; lane 9). Moreover, treatment with PstI showed almost complete linearization of the DNA substrate indicating restoration of the original C:G base pair within the Dcm/PstI and DNA repair via nick-translation by polI after initiation of VSPR *in vitro* (Figure 3-11B; lane 10).

In conclusion, these results reveal for the first time that initiation of VSPR *in vitro* is indeed enhanced by a mismatch-provoked stimulation of the Vsr endonuclease activity by MutS and MutL which demonstrates the proposed cooperation in the crosstalk between MMR and VSPR *in vivo*. Moreover, restoration of the Dcm-site is efficiently achieved via nick-translation in the absence of factors required for strand excision as important for MMR. However, the enhanced VSPR pathway is obviously similar to the MMR pathway. The only difference between both systems relies on the recruited effector protein that introduces a nick into DNA serving as entry point for subsequent steps in DNA repair.

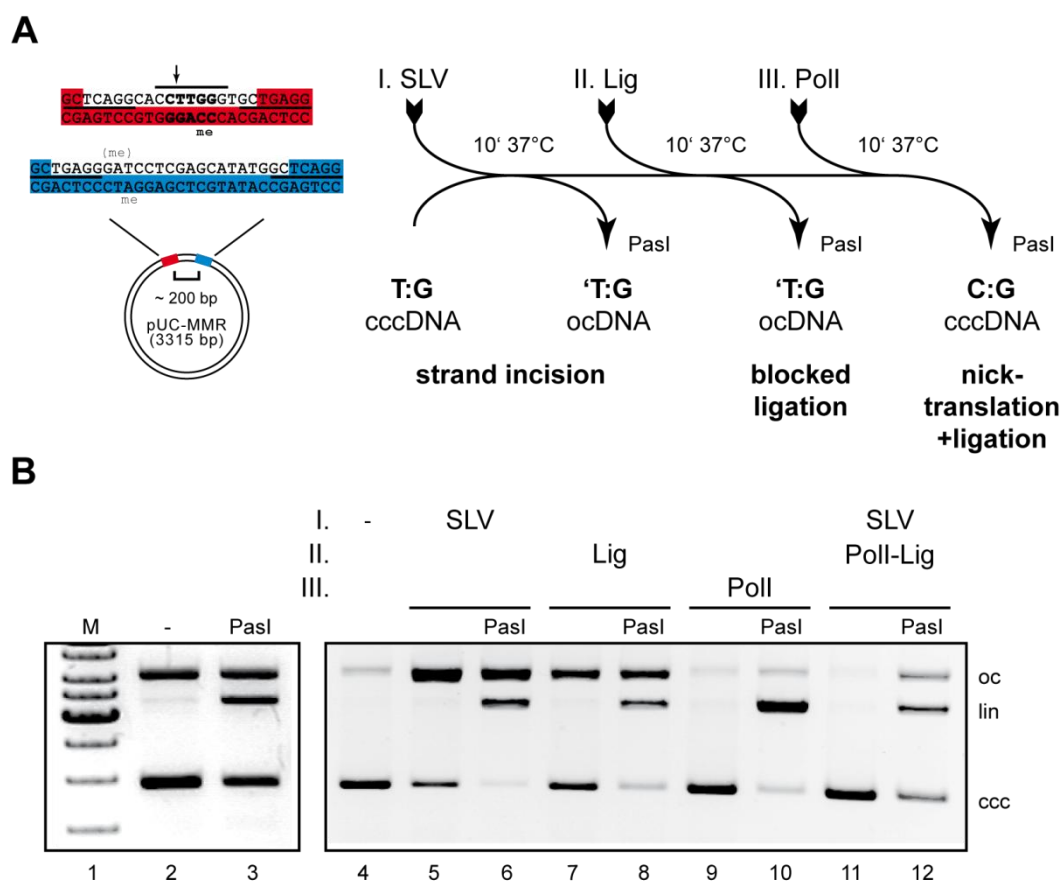


Figure 3-11: Reconstitution of enhanced VSPR *in vitro*

A: Scheme for stepwise reconstitution of enhanced VSPR *in vitro*. Repair of the T:G mismatch within the Dcm-site (bold) is demonstrated by restriction cleavage analysis using *PasI* due to restoration of the original C:G base pair within the corresponding recognition site (underlined). **B:** Heteroduplex circular DNA substrate (20 nM; B) was incubated with MutS (200 nM), MutL (200 nM) and Vsr (50 nM) followed by stepwise addition of DNA ligase and polI (0.1 u/μl each), as indicated in A. Neither heteroduplex circular DNA nor the nicked VSPR intermediate, achieved after strand incision by MutSLV (lane 4), is linearized by *PasI* (lane 3 and 6). Addition of DNA ligase to the nicked intermediate has almost no effect on DNA repair, explained by incapability of the ligase to seal a nick directly next to a mismatch as well as further activation of MutSLV by the mismatch (lane 7 and 8). In the presence of polI and dNTP's (1 mM), DNA is efficiently repaired via 5' to 3' nick-translation activity, thereby restoring the single recognition site for *PasI* (compare lane 6 and 10). PolI and ligase alone are not sufficient to repair the VSPR substrate, as expected (lane 11 and 12).

3.3.5 Intermediate of VSPR triggers initiation of MMR

As demonstrated, arising of a T:G mismatch within a Dcm-site due to spontaneous deamination of 5-methylcytosine or incorporation of T opposite G during replication triggers in principle initiation of at least two repair pathways, MMR and VSPR, in *E. coli*. Additionally, both DNA repair systems include mismatch recognition and subsequent activation or stimulation of downstream effector molecules, such as MutH, UvrD and Vsr, by a MutSL complex. However, simultaneous initiation of MMR and VSPR *in vivo* may cause lethal double-strand breaks within DNA under unfavourable conditions (see Introduction). Moreover, an influence by the nicked intermediate of the VSPR pathway on MMR has not been investigated so far. Therefore, the capability of MutS for binding to a T:G mismatch after strand incision by Vsr was tested *in vitro*. To investigate MutS binding specificity for the VSPR substrate as well as intermediate ('T:G), mismatch recognition and thereby induced conformational changes in the DNA were analyzed via FRET using double-labeled oligonucleotides. The MutS binding and bending assay, developed by Michele Cristovao, allows monitoring the formation of the IRC, which is indispensable for initiation of MMR. Finally, anisotropy measurements were performed to test the influence of the IRC on the free rotation of the fluorophores attached to the substrates, which provides information about the orientation in which the mismatch is bound by MutS (see Materials and Methods).

A great increase in FRET between Alexa 488 and Alexa 594 was observed after incubation of the heteroduplex VSPR substrate with MutS and ADP, indicating mismatch binding and formation of the IRC (Figure 3-12A). DNA kinking which decreased the distance between the FRET pair was monitored by an increase of emission by the acceptor (Alexa 594) during excitation of the donor (Alexa 488). In contrast, homoduplex DNA containing a C:G base pair within the same sequence context was not kinked by MutS, as expected. In the absence of a mismatch, formation of the IRC is avoided and therefore no significant increase in FRET was detected (Figure 3-12B). These results demonstrate the specificity of mismatch recognition and binding by MutS required for initiation of MMR.

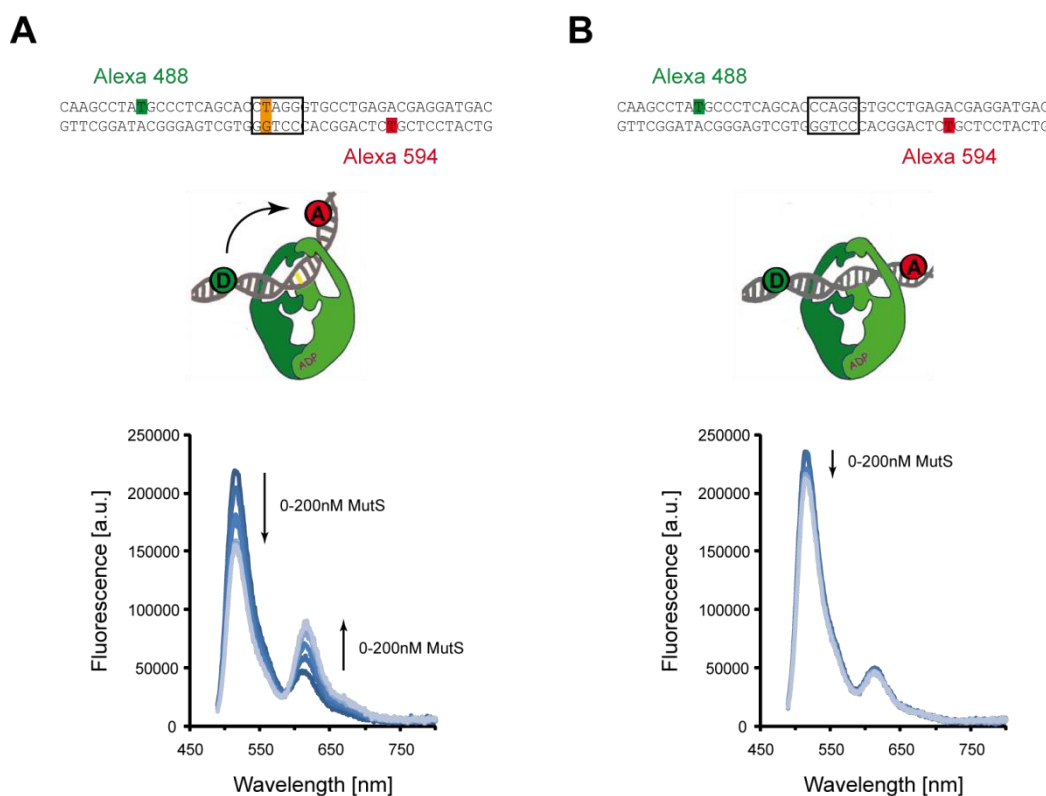


Figure 3-12: Monitoring mismatch-provoked formation of the IRC via FRET

Emission spectra of double-labeled VSPR/MMR (A) and homoduplex DNA (B) substrate titration with MutS in the presence of ADP. **A:** Increasing amounts of MutS (0-200 nM) were added to the 45 bp VSPR substrate (50 nM) and ADP (1 mM), resulting in the decrease of donor (D; Alexa 488) fluorescence coupled to an increase of acceptor (A; Alexa 594) fluorescence (FRET, indicated by the arrow). **B:** In contrast to A, no change of the acceptor fluorescence and therefore no FRET is observed in the presence of homoduplex (C:G) DNA. The small decrease of donor fluorescence (quench) in the presence of MutS indicates unspecific DNA binding (scanning) or interaction with DNA ends.

As mentioned, DNA binding by MutS and especially formation of the IRC in the presence of a mismatch in principle changes the environment and reduces the rotational freedom of the two fluorophores, attached to the DNA substrate (see Introduction). Therefore, fluorescence anisotropy measurements were performed to monitor influences on both donor (D; Alexa 488) and acceptor (A; Alexa 594) fluorophores caused by MutS in the presence or absence of a mismatch. Moreover, this assay was used to determine, in which the orientation the mismatch is bound by MutS (see Materials and Methods).

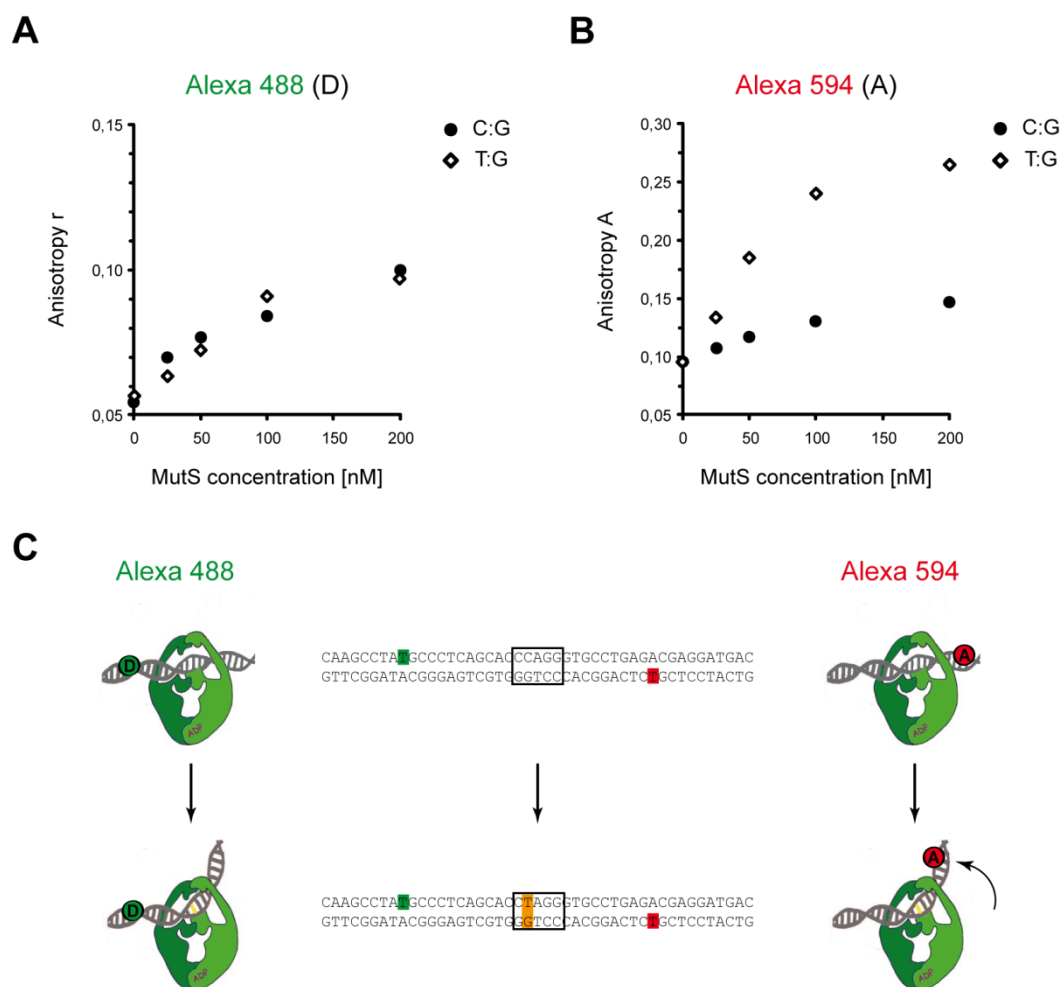


Figure 3-13: Monitoring DNA binding and kinking by MutS via anisotropy

A: Comparison of effects on donor anisotropy (Alexa 488; green) by increasing amounts of MutS (0-200 nM) binding to the T:G (open squares) or C:G (closed circles) substrate (50 nM; C). Formation of the IRC shows almost no influence on the fluorophore attached to the top strand, 12 bp away from the mismatched T (C). **B:** In contrast to A, the acceptor anisotropy (Alexa 594; red) for the VSPR substrate is greatly increased in a MutS-dependent manner. This indicates DNA kinking and suggests movement of the acceptor, which is attached to the bottom strand, 12 bp away from the mismatched G (C), towards the clamp (indicated by the arrow) thereby reducing the rotational freedom of the fluorophores. **C:** Scheme for DNA kinking after T:G mismatch recognition by MutS and influence on donor and acceptor anisotropy, respectively, due to formation of the IRC.

Anisotropy measurements revealed that MutS in principle had an influence on the rotational freedom of the fluorophores attached to DNA substrates either by unspecific binding, interaction with DNA ends or specific kinking after mismatch recognition. Although the donor fluorophore (Alexa 488) is almost not influenced

during MutS binding to both DNA substrates (Figure 3-13A), a dramatic MutS-dependent increase in anisotropy of the acceptor fluorophore (Alexa 594) was observed for the heteroduplex VSPR substrate (Figure 3-13B). These data indicate that T:G mismatch binding by MutS occurred in an orientation which will only influence the rotational freedom of the acceptor fluorophore during DNA kinking and formation of the IRC. The small increase in anisotropy of the donor fluorophore which is similar for both substrates is caused by unspecific DNA binding (scanning), interaction with DNA ends and the fact that in principle two MutS molecules can bind to a single double-labeled DNA substrate. Recent FRET studies in mismatch recognition during MMR carried out by Michele Cristovao demonstrated that a significant increase of either donor or acceptor anisotropy directly provides an information about the orientation of MutS mismatch binding. In the FRET system used for studies in crosstalk during DNA repair, binding of the mismatched base in the donor-strand, which is the case for T:G, reduces the rotational freedom of the acceptor (Figure 3-13) whereas binding of the mismatched base in the acceptor strand, which was shown for C:A, effects the anisotropy of the donor (Figure 3-21).

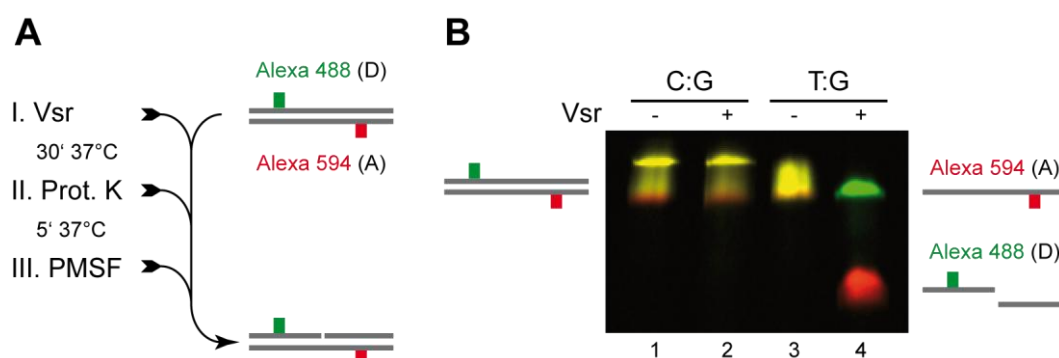


Figure 3-14: *In situ* generation of the VSPR intermediate

A: Scheme for *in situ* generation of the 45 bp double-labeled VSPR intermediate. Proteinase K (2 U) and PMSF (1 mM; proteinase inhibitor) were stepwise added to avoid blocking of MutS mismatch binding by Vsr after strand incision. **B:** Control for complete procession of the VSPR substrate (1 μ M) by Vsr (200 nM) to generate the VSPR intermediate for MutS binding and bending experiments via FRET. After nicking 5' of the mismatched T, the 21 bp single-strand fragment, labeled with Alexa 488 (green) is separated from the unprocessed strand, labeled with Alexa 594 (red) via denaturing gel-electrophoresis (lane 4). Homoduplex DNA substrate is not processed by the endonuclease, as expected (compare lane 2 and 4).

To investigate whether MutS has the capability to interfere with the VSPR pathway after strand incision 5' of the mismatched T ('T:G), the double-labeled VSPR intermediate was generated *in situ* and analyzed for MutS binding and bending in the FRET assay. To demonstrate complete procession of double-labeled VSPR substrate by the Vsr endonuclease, mismatch-provoked DNA nicking was confirmed via denaturing gel-electrophoresis (Figure 3-14B). The FRET efficiency, which was calculated by the F_A/F_D ratio (see Materials and Methods) was used to compare VSPR substrate and intermediate in mismatch binding and DNA bending by MutS.

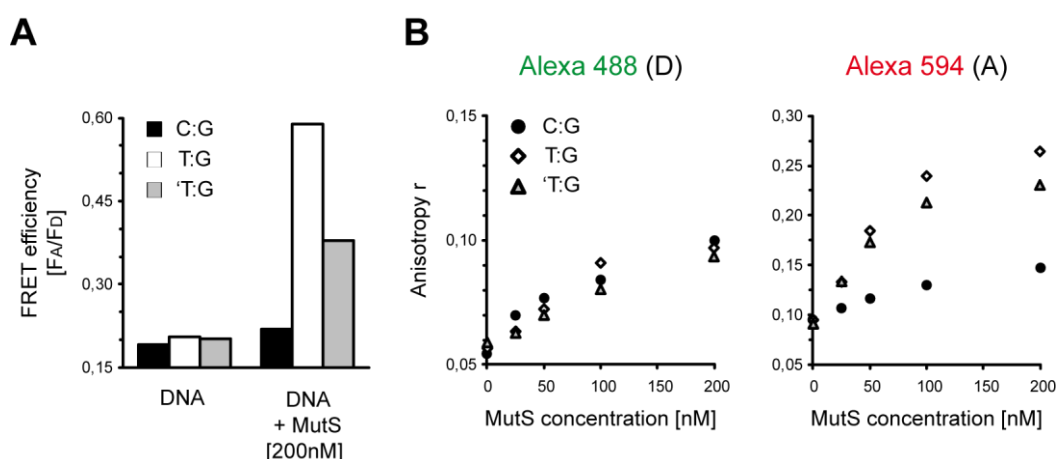


Figure 3-15: The VSPR intermediate triggers formation of the IRC

A: Comparison of FRET efficiencies (F_A/F_D ratio) for double-labeled homoduplex DNA (C:G; black), VSPR substrate (T:G; white) and intermediate ('T:G; grey; 50 nM each) in the absence and presence of MutS (200 nM) and ADP (1 mM), respectively. Previous strand incision by Vsr results in ~50 % decreased FRET compared to the unprocessed substrate (compare white and grey bars). However, MutS has the capability to recognize the 'T:G mismatch and to induce conformational changes towards the IRC. **B:** Comparison of change in donor (Alexa 488; D) and acceptor (Alexa 594; A) anisotropy for C:G, T:G and 'T:G substrates, respectively, induced by increasing amounts of MutS (0-200 nM). The greatly increase of acceptor anisotropy coupled to almost no change in the rotational freedom of the donor fluorophore for both VSPR substrate (open squares) and intermediate (open triangles), at high MutS concentrations indicates mismatch binding by MutS in the same orientation. The difference in acceptor anisotropy between both substrates, suggests less DNA bending in the IRC, which results in the decreased FRET shown in A.

Although FRET efficiency was decreased ~50 % after strand incision by Vsr the double-labeled VSPR intermediate was still kinked by MutS, indicating recognition of the 'T:G mismatch and formation of the IRC (Figure 3-15A). Finally, Anisotropy measurements revealed that mismatch binding by MutS occurred in the same orientation as shown for the substrate, demonstrated by almost no change in anisotropy of the donor (Alexa 488) coupled to a great increase in acceptor (Alexa 594) anisotropy (Figure 3-15B). However, the difference between T:G and 'T:G in acceptor anisotropy reached at high MutS concentrations (Figure 3-15B; compare triangles and squares) suggests a smaller angle of the induced DNA kink provoked by formation of the IRC in the presence of the VSPR intermediate, which consequently results in decreased FRET (Figure 3-15A; compare white and grey bars).

3.4 *Crosstalk between MMR and BER in E. coli*

Several *in vivo* studies and experimental observations demonstrated the obvious requirement for crosstalk between MMR and BER to assure that these two processes do not significantly interfere with each other during repair of uracil containing mismatches (see Introduction). In this work, the crosstalk between *E. coli* MMR and BER was studied *in vitro* using adequate mismatch substrates and all proposed components for initiation of both repair pathways. Therefore, a BER assay was developed and U:G mismatch-provoked initiation of MMR in the presence or absence of the uracil DNA glycosylase (UDG) was analyzed in detail. Due to the fact that the mismatch is converted into an AP-site after procession by UDG, it has to be determined whether the resulting BER intermediate is still recognized by MutS and therefore has the capability to initiate MMR. However, simultaneous initiation of both repair pathways *in vivo* may cause mutations or lethal double-strand breaks within DNA under unfavourable conditions (see Introduction). Finally, fluorophore double-labeled BER substrate and intermediate were used to compare mismatch binding and DNA bending by MutS via FRET and anisotropy measurements (see Materials and Methods). The recently developed FRET assay allowed monitoring the

formation of the *initial recognition complex* (IRC) in the presence of a mismatch, which is indispensable for initiation of MMR. Anisotropy measurements were performed to achieve information about changes in the rotational freedom of the fluorophores due to the IRC and the orientation in which U:G mismatch and AP-site are bound by MutS.

3.4.1 Initiation of base-excision repair (BER) *in vitro*

In this work, initial steps in BER were studied on circular DNA substrates containing a U:G mismatch or a U:A base pair, which represents the natural substrate for UDG *in vivo*. UDG catalyzes the release of uracil, thereby creating an AP-site followed by cleavage of the DNA backbone by EndoIV, which finally results in a single-nucleotide gap (see Introduction). Due to the fact that generation of an AP-site does not influence the integrity of the DNA backbone, EndoIV was directly used to demonstrate and visualize UDG activity *in vitro* via generation of ocDNA and agarose gel-electrophoresis (Figure 3-16).

Initiation of BER, resulting in ocDNA was only observed after incubation of cccDNA substrates with UDG and EndoIV (Figure 3-16B; lane 4). Neither UDG nor EndoIV alone were sufficient to generate ocDNA indicating specific procession of cccDNA during BER and appearing of a single-nucleotide gap under the conditions used *in vitro* (Figure 3-16B; lane 2 and 3). As expected, cccDNA retained after the release of uracil by UDG and the *E. coli* AP-endonuclease EndoIV catalyzed the cleavage of the DNA backbone only after specific release of uracil from DNA by UDG (Figure 3-16B; compare lane 2, 3 and 4). Furthermore, circular DNA substrates containing a T:G mismatch, such as used for VSPR, were not processed by UDG and therefore no ocDNA was observed after treatment with EndoIV, which demonstrates substrate specificity of the glycosylase (data not shown). Finally, the presence of the specific UDG inhibitor (UGI) completely prevented the initiation of BER *in vitro* (Figure 3-16B; compare lane 4 and 7).

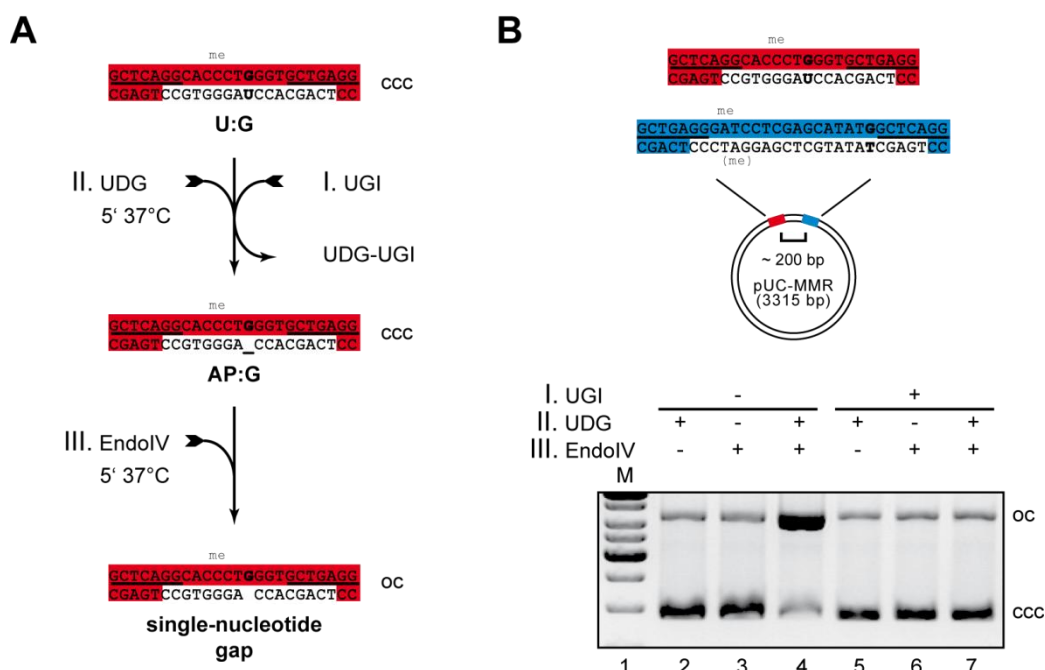


Figure 3-16: Initiation of BER *in vitro*

A: Scheme for stepwise processing of circular DNA substrates during BER by UDG and EndoIV, which allows monitoring the initial steps in BER via agarose gel-electrophoresis.

B: Monitoring single-nucleotide gap formation during BER. Incubation of circular uracil containing DNA substrate (25 nM, top) with UDG (0.05 U/ μ l) and EndoIV (0.2 U/ μ l) results in ocDNA indicating appearing of a single-nucleotide gap after specific release of uracil by UDG and DNA backbone cleavage by EndoIV (lane 4). Neither treatment with UDG nor EndoIV alone generates ocDNA (lane 2 and 3), as expected. Generation of an AP-site has no influence on the integrity of the DNA backbone and therefore cccDNA is maintained in the presence of UDG. Addition of UGI (0.2 U/ μ l) prior to incubation with the glycosylase avoids initiation of BER due to inhibition of UDG (compare lane 4 and 7).

3.4.2 Intermediate of BER inhibits initiation of MMR

Crosstalk between BER and MMR for repair of a common target was studied using various circular DNA substrates containing a single uracil either opposite A or G and a hemi-methylated GATC-site as well as all proposed components to initiate both repair pathways *in vitro*. To investigate mutual influences on initiation of MMR repair, mismatch-provoked activation of MutH was analyzed in the presence or absence of UDG, which converts a U:G mismatch into an AP-site. As described, initial steps in BER were monitored via single-nucleotide gap formation in the

presence of UDG as well as EndoIV and initiation of MMR was demonstrated by strand discrimination by MutSLH (Figure 3-17A).

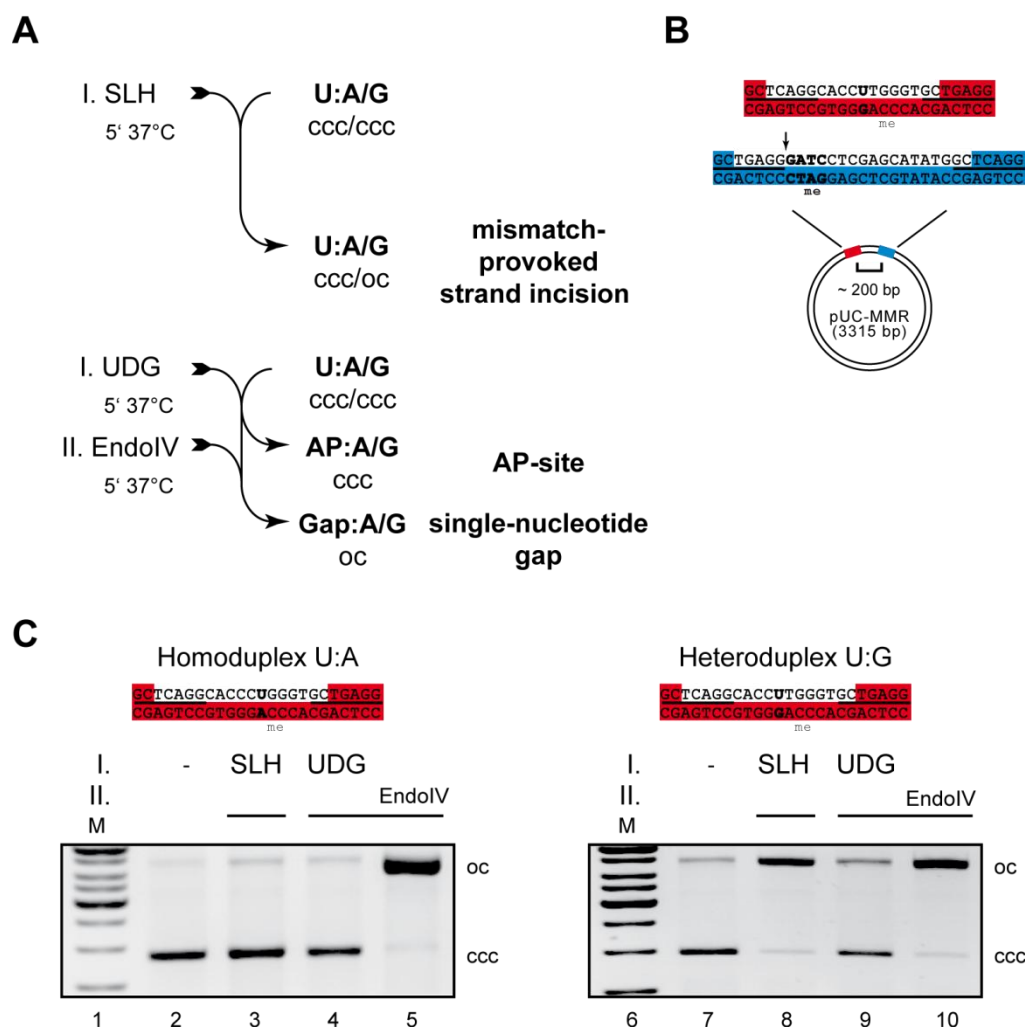


Figure 3-17: Monitoring U:G mismatch-provoked initiation of MMR and BER

A: Scheme for treatment of circular uracil containing DNA substrates with components required for initiation of either MMR or BER resulting in the corresponding intermediates monitored via agarose gel-electrophoresis (C). **B:** Heteroduplex circular DNA substrate sufficient to study crosstalk between both repair pathways *in vitro*. U:G mismatch and hemi-methylated GATC-site (both in bold) are separated by ~200 bp. Nicking site for MutH is indicated by the arrow. **C:** Mismatch-provoked initiation of MMR by the heteroduplex BER substrate. Circular DNA substrate (25 nM) containing either a U:G mismatch or a U:A base pair were incubated with MutS (200 nM), MutL (200 nM) and MutH (50 nM) in the presence of ATP (1 mM) as indicated in A. Strand incision by MutH is only observed for heteroduplex cccDNA resulting in ocDNA (compare lane 3 and 8), thereby demonstrating the specificity for initiation of MMR under the conditions used *in vitro*. Appearing of ocDNA after stepwise incubation of the uracil containing substrates with UDG and EndoIV as shown in A, indicates gap formation and initiation of BER (lane 5 and 10).

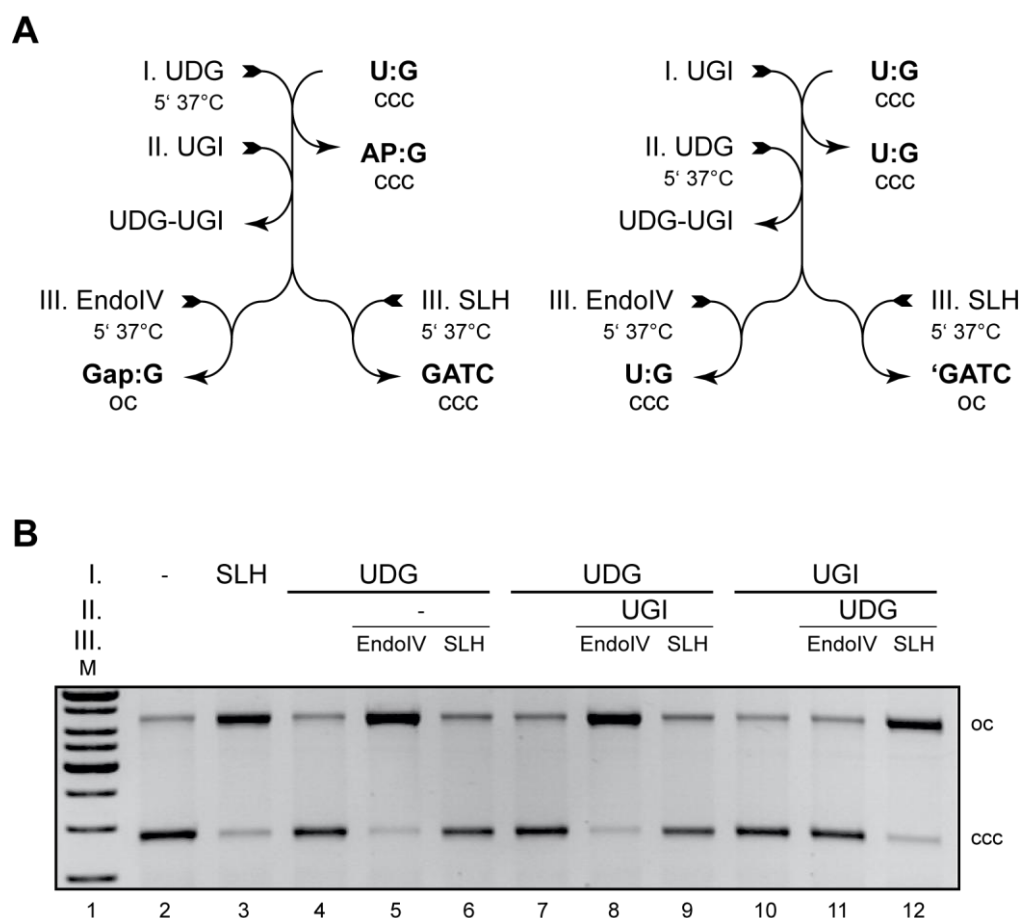


Figure 3-18: Inhibition of MMR after initiation of BER

A: Scheme for stepwise incubation of heteroduplex circular DNA substrate containing a single U:G mismatch and a hemi-methylated GATC-site (Figure 3-17) with components required for initiation of BER and MMR as indicated. To investigate whether the first intermediate of the BER pathway triggers initiation of MMR, mismatch-provoked strand incision after release of uracil was monitored via agarose gel-electrophoresis (**B**). **B:** MMR is inhibited after initiation of BER. Incubation of the circular DNA substrate (25 nM) with MutS (200 nM), MutL (200 nM), MutH (50 nM) and ATP (1 mM) results in ocDNA, as expected (lane 3; 'GATC). Although unexpected, the release of uracil, which was demonstrated by EndoIV (lane 4 and 5), avoids strand incision by MutH under the conditions used *in vitro* (compare lane 3 and 6). To rule out blocking of MutS binding to the generated AP-site by UDG, UGI was added after treatment with the glycosylase as indicated in A. However, no ocDNA, which indicates strand incision, is observed after incubation of the BER intermediate with MutSLH (compare lane 4-6 and 7-9). On the other hand, inhibition of UDG prior to incubation with the substrate, as indicated in A, avoids generation of an AP-site and allows subsequent initiation of MMR (compare lane 7-9 and 10-12).

To investigate whether the AP-site containing BER intermediate is sufficient to trigger initiation of MMR, UDG treated circular DNA substrate was subsequently incubated with MutSLH. Specific release of uracil by UDG was again demonstrated

via treatment with EndoIV resulting in ocDNA (Figure 3-18B; lane 4 and 5). Although unexpected, strand incision was avoided after release of uracil and generation of the AP-site (Figure 3-18B; compare lane 3 and 6). To rule out blocking of mismatch or AP-site accessibility for MutS by UDG, the glycosylase inhibitor UGI was added before incubation with MutSLH. However, initiation of MMR was still avoided when the glycosylase was able to process the substrate and inhibited afterwards (Figure 3-18; compare lane 4-6 and 7-9). On the other hand, addition of UDG to the inhibitor prior to incubation with the circular DNA substrate (Figure 3-18B) avoided initiation of BER and allowed subsequent mismatch-provoked strand incision by MutH (Figure 3-18; compare lane 7-9 and 10-12).

These data demonstrate that initiation of MMR *in vitro* is prevented after generation of an AP-site during the first step in BER, which suggests a possible incapability for MutS to recognize the BER intermediate as a mismatch, to induce conformational changes towards the IRC or to signal the damage after mismatch binding. FRET experiments were performed to analyze whether mismatch recognition by MutS is affected after initiation of BER.

3.4.3 AP-sites prevent formation of the IRC

Although unexpected, initiation of MMR during BER was inhibited *in vitro* after the release of uracil by UDG, which creates an AP-site. To analyze whether mismatch recognition is affected after procession of the initial step in BER, induced conformational changes towards the *initial recognition complex* (IRC), which is indispensable for initiation of MMR, were monitored via FRET, as mentioned above. MutS binds to U:G and T:G mismatches in an orientation in which Glu38 of the mismatch binding monomer makes special contacts to U and T, respectively (see Introduction). Consequently, release of uracil results in a type of damage, which obviously requires binding by MutS in a different orientation compared to the unprocessed substrate. Therefore it was analyzed whether an AP-site is bound by MutS in a similar way as demonstrated for an insertion or deletion (IDL) of a single nucleotide, due to the retaining single G within the unprocessed strand, which might

trigger initiation of MMR. Finally, double-labeled oligonucleotides containing either a single U:G mismatch, an AP-site (e.g. AP:G) or a single-nucleotide deletion (e.g. Δ U:G) within the same sequence context as used for the *in vitro* repair assays were tested for mismatch binding and induced conformational changes towards the *initial recognition complex* (IRC). Furthermore, anisotropy measurements were performed to test the influence of the IRC on the free rotation of the fluorophores attached to the DNA substrates, which provides information about the orientation in which the mismatch is bound by MutS (see Materials and Methods).

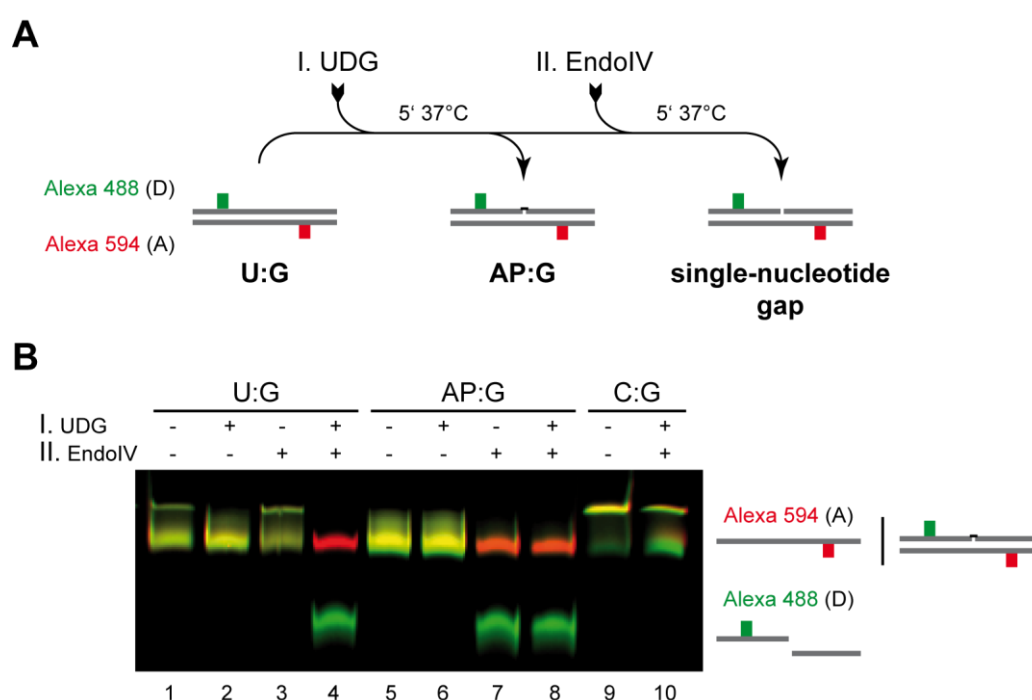


Figure 3-19: Quality control of BER substrate and intermediate

A: Scheme for stepwise monitoring of initial steps in BER on double-labeled DNA substrates used for MutS binding and bending studies via FRET. BER substrate and intermediate (1 μ M) were incubated with UDG and EndoIV (5 U each), as indicated (B) to demonstrate the presence of U:G mismatch and AP-site, respectively. **B:** Quality control of the BER substrate and intermediate. Formation of a single nucleotide gap is only observed after treatment of double-labeled BER substrate with UDG and EndoIV, as expected (compare lane 1-4). Release of uracil and subsequent cleavage of the DNA backbone results in a 21 bp single-strand DNA fragment, labeled with Alexa 488 (green), separated from the unprocessed and Alexa 594 (red) labeled oligonucleotide via denaturing gel-electrophoresis (lane 4). Appearing of the short fragment after procession of the BER intermediate by EndoIV in a UDG independent manner demonstrates the presence of the required AP-site (compare lane 3 and 7). Finally, homoduplex DNA substrate is not processed by UDG and EndoIV, as expected (compare lane 4 and 10).

To test the quality of the required double-labeled DNA substrates, initiation of BER was analyzed as described and monitored via denaturing gel-electrophoresis (Figure 3-19). As expected, generation of a single-nucleotide gap only occurred after specific release of uracil by UDG and subsequent cleavage of the DNA backbone in the presence of EndoIV, resulting in a 21 bp single-strand DNA fragment, labeled with Alexa 488 (green), separated from the unprocessed and Alexa 594 (red) labeled oligonucleotide (Figure 3-19B; compare lane 1-4). Furthermore, the BER intermediate was almost completely processed by EndoIV in the absence of UDG, demonstrating the required AP-site (Figure 3-19B; compare lane 3 and 7). In contrast, the homoduplex DNA substrate was not sufficient to trigger initiation of BER, as expected (Figure 3-19B; compare lane 4 and 10). Finally, FRET experiments revealed that U:G mismatch binding by MutS induces DNA kinking, which indicates formation of the IRC (Figure 3-20). Moreover, the double-labeled BER substrate was bound by MutS in the same orientation, recently shown for the T:G and 'T:G mismatch (Figure 3-15), which was demonstrated by an increase of acceptor anisotropy coupled to almost no change for the donor fluorophore at high MutS concentrations in comparison to homoduplex DNA (Figure 3-20; compare circles and squares).

Although the effects were not as dramatic as observed for VSPR substrate and intermediate, mismatch-provoked conformational changes towards the IRC in the presence of a heteroduplex BER substrate were sufficient to trigger initiation of MMR, as shown recently (Figure 3-17). However, no change in FRET efficiency was detected for the BER intermediate compared to homoduplex DNA indicating no kinking of DNA after incubation with MutS (Figure 3-20; compare white and grey bars). Furthermore, no increase in either donor or acceptor anisotropy in comparison to homoduplex DNA was monitored after incubation of the BER intermediate with MutS (Figure 3-20B; compare circles and triangles), demonstrating no formation of the IRC after release of uracil during BER, which finally avoids initiation of MMR *in vitro* (Figure 3-17).

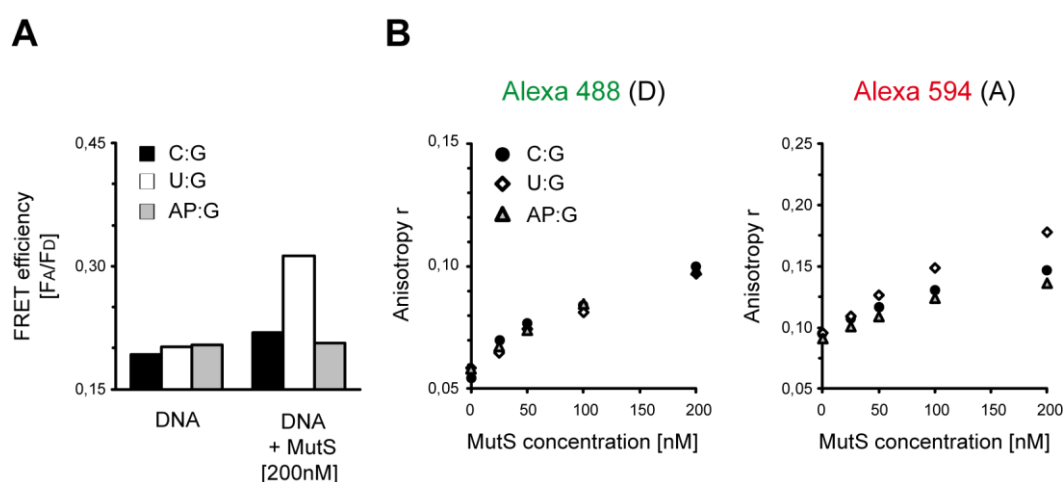


Figure 3-20: AP-sites avoid formation of the IRC

A: Comparison of FRET efficiencies (F_A/F_D ratio) for double-labeled homoduplex DNA (C:G; black), BER substrate (U:G; white) and intermediate (AP:G; grey; 50 nM each) in the absence and presence of MutS (200 nM) and ADP (1 mM), respectively. An increase in FRET is observed for the BER substrate (white bars) after addition of MutS, demonstrating formation of the IRC, as expected. However, almost no change in the FRET efficiency is monitored for the AP-site containing intermediate of the BER pathway in the presence of MutS indicating that the DNA is not kinked (compare white and grey bars). **B:** Comparison of change in donor (Alexa 488; D) and acceptor (Alexa 594; A) anisotropy for C:G, U:G and AP:G DNA substrates (50 nM), respectively, induced by increasing amounts of MutS (0-200 nM). Increase of acceptor anisotropy coupled to almost no change for the donor fluorophore of the BER substrate (open squares) at high MutS concentrations compared to homoduplex DNA (closed circles) reveals mismatch binding in an orientation, recently shown for the T:G mismatch (Figure 3-15). Although not as dramatic as observed for T:G, the induced conformational changes towards the IRC monitored via FRET result in mismatch-provoked strand incision by MutH (Figure 3-18). However, no change in either donor or acceptor anisotropy at high MutS concentrations is detected for the BER intermediate in comparison to homoduplex DNA, indicating that formation of the IRC is not occurring in the presence of an AP-site (compare circles and triangles).

To investigate whether an AP-site is recognized as a single-nucleotide deletion (IDL), as proposed, several MMR substrates and BER intermediates were compared in MutS mismatch recognition and binding orientation via FRET and anisotropy measurements, as mentioned above. Co-crystal structures of MutS bound to T:G or G:T revealed that Glu38 of the mismatch binding subunit makes special contacts to the T during formation of the IRC (see Introduction). Consequently, either the donor or acceptor labeled strand is specifically bound by MutS, depending on the experimental set up or orientation of the mismatch related to the fluorophores (see Materials and Methods). As demonstrated, U:G and T:G mismatch are bound in the

same way by MutS under the conditions used *in vitro* (Figure 3-20). Due to the fact that initiation of BER results in the release of uracil, it is obviously that the generated AP-site requires a change in the mismatch binding orientation of MutS to be recognized as damage. To this end, a heteroduplex double-labeled MMR substrate containing C:A instead of a T:G mismatch was used to monitor and compare a possible change in the binding orientation of MutS in the presence of the BER intermediate or IDL. Co-crystal structures revealed that Glu38 specifically interacts with the A of a C:A mismatch, corresponding to a binding orientation in which MutS would specifically interact with the G of a T:G mismatch, using this experimental set up.

Anisotropy measurements revealed that mismatch recognition by MutS and subsequent formation of the IRC obviously has different effects on the rotational freedom of the fluorophores, depending on the mismatch binding orientation (Figure 3-21). As demonstrated recently, T:G mismatch binding by MutS within the IRC resulted in an increase of acceptor (Alexa 594) anisotropy coupled to almost no change for the donor (Alexa 488) fluorophore compared to homoduplex DNA substrates (Figure 3-21A). In contrast to T:G, the opposite effect was observed for the C:A mismatch. Incubation of this MMR substrate with MutS induced conformational changes, in which the donor anisotropy was greatly increased, whereas almost no change for the acceptor fluorophore was detected (Figure 3-21). These data suggest that in this mismatch binding orientation the donor is moved towards the clamp due to DNA kinking during formation of the IRC. However, an increase in FRET was observed for both heteroduplex DNA substrates due to mismatch-provoked kinking of DNA during formation of the IRC. In contrast, no change in FRET was detected for homoduplex DNA substrates in the presence of MutS, as expected (Figure 3-21B). Moreover, almost no influences on either donor or acceptor anisotropy by MutS demonstrated that conformational changes towards the IRC are avoided in the absence of a mismatch.

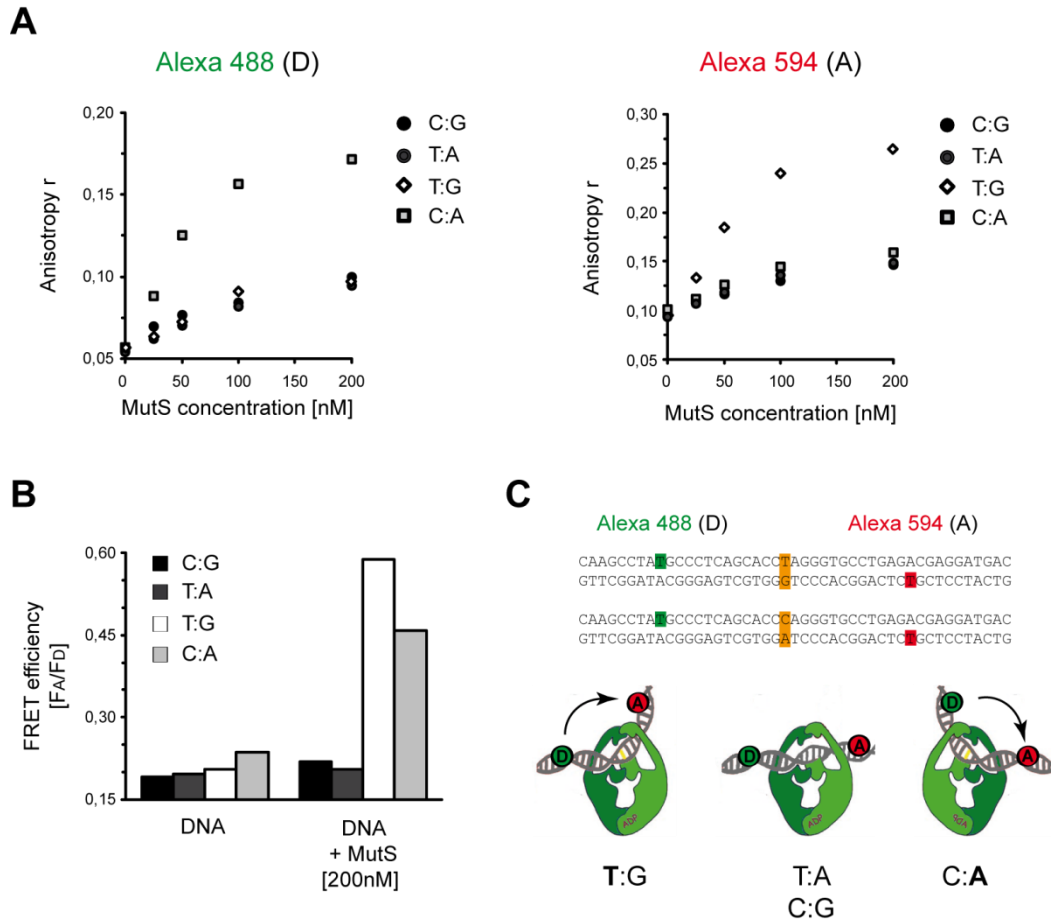


Figure 3-21: Determination of mismatch binding orientation by MutS

A: Discrimination between mismatch binding orientations of MutS during formation of the *initial recognition complex* (IRC) via anisotropy measurements. Changes in donor (Alexa 488; D) and acceptor (Alexa 594; A) anisotropy induced by increasing amounts of MutS (0-200 nM) were analyzed for the indicated double-labeled DNA substrates, as described before. As expected, almost no change in either donor or acceptor anisotropy at high MutS concentrations is observed for homoduplex DNA substrates (C:G and T:A), demonstrating that formation of the IRC is avoided in the absence of a mismatch. However, a greatly MutS-dependent increase in anisotropy of the acceptor coupled to almost no change for the donor fluorophore is detected for the MMR substrate containing the T:G mismatch. In contrast, C:A mismatch binding by MutS results in an increase of donor anisotropy, whereas almost no change is observed for the acceptor fluorophore indicating that C:A binding by MutS occurs in a different orientation, as observed for the T:G and U:G mismatch (Figure 3-19). **B:** Comparison of FRET efficiencies (F_A/F_D ratio) for double-labeled DNA substrates (50 nM), as indicated, in the absence and presence of MutS (200 nM) and ADP (1 mM), respectively. In contrast to homoduplex DNA (C:G and T:A), mismatch (T:G and C:A) recognition by MutS, independent of the binding orientation, results in an increased FRET, demonstrating DNA kinking and mismatch-provoked formation of the IRC. **C:** Model for mismatch-provoked conformational changes towards the IRC due to specific interactions of MutS with the mismatched base (bold) either in the donor or acceptor labeled DNA strand. FRET between both fluorophores is indicated by the arrow.

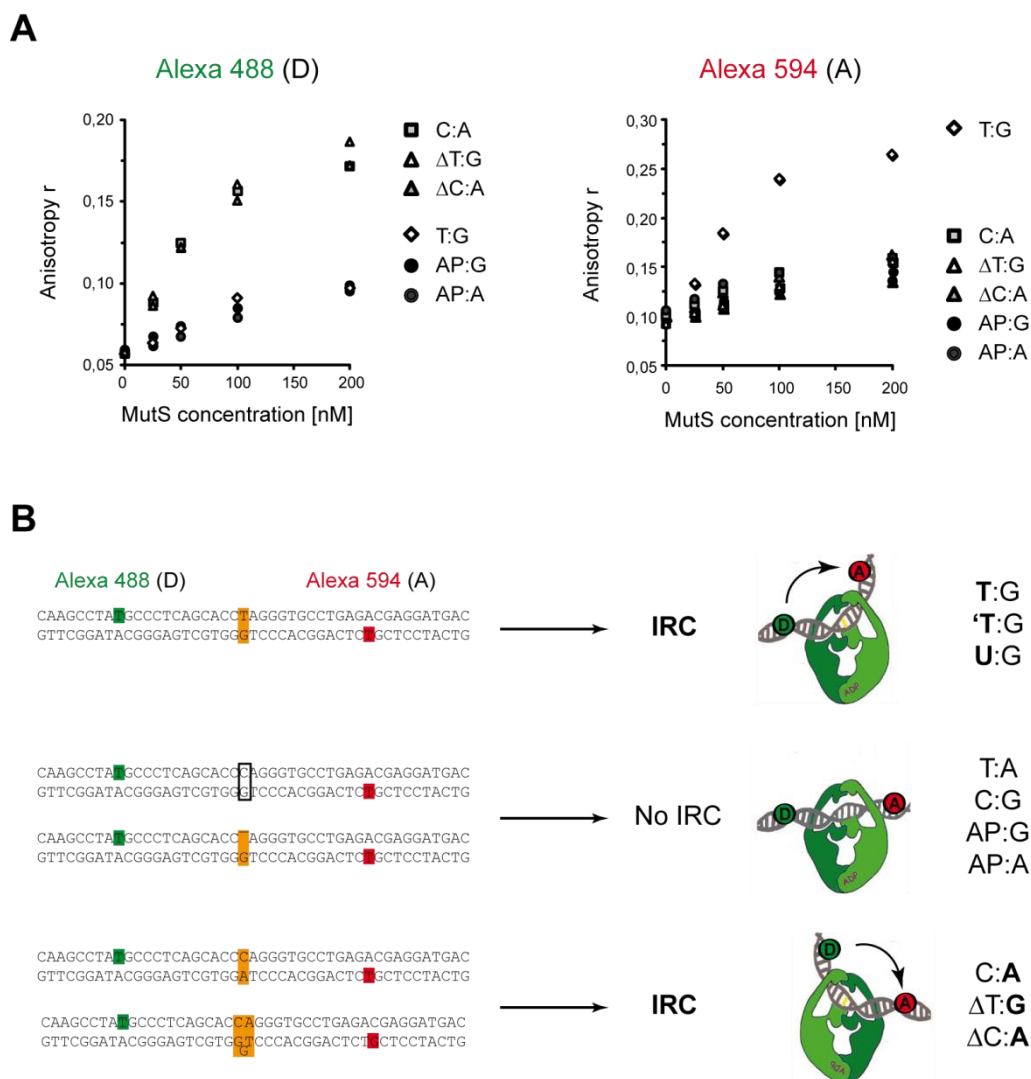


Figure 3-22: AP-sites are not recognized as IDL's

A: Comparison of BER intermediates and IDL's in mismatch binding orientation due to MutS dependent changes in fluorophore anisotropy during formation of the *initial recognition complex* (IRC). MMR substrates (50 nM) containing the deletion of a single nucleotide within the donor (Alexa 488; D) labeled strand are bound in the same orientation as a C:A mismatch using this experimental set up. Specific interactions of MutS with the mismatched base in the acceptor (Alexa 594; A) labeled strand results in an increase of donor anisotropy, as demonstrated recently (Figure 3-21). However, no change in either donor or acceptor anisotropy induced by increasing amounts of MutS (0-200 nM) compared to homoduplex DNA was monitored for the double-labeled substrates containing the AP-site, indicating no switch in the binding orientation after release of uracil. Finally, neither the remaining A nor G is recognized by MutS as a mismatch in this sequence context, consequently initiation of MMR is avoided by the BER intermediate (Figure 3-18).

Anisotropy measurements with MMR substrates containing a single-nucleotide deletion instead of an AP-site revealed that the extra nucleotide in the acceptor labeled strand was bound by MutS in the same orientation as shown recently for the C:A mismatch within the same sequence context (Figure 3-22A; compare triangles and squares). Finally, the BER intermediate showed almost no change in either donor or acceptor anisotropy in the presence of MutS, which indicates no switch in the mismatch binding orientation after release of uracil and therefore no recognition of the remaining A or G, opposite of an abasic site, in this sequence context (Figure 3-22A; compare circles and triangles).

In conclusion these results demonstrate that initiation of MMR is triggered by a U:G mismatch but immediately avoided after the initial step in BER, which changes the type of the damage by release of the mismatched uracil into an IDL-like lesion. Surprisingly, initiation of MMR is avoided at this point of ongoing BER due to the fact that an AP-site is not recognized by MutS, neither as a mismatch nor as IDL. MutS is not capable to bind the remaining base by changing the mismatch binding orientation, which consequently avoids conformational changes towards the IRC, indispensable for activation of MMR. Moreover, these data indicate that crosstalk between MMR and BER is directly controlled on the DNA level by the type of damage and not by competition between factors of both repair pathways for initiation of repair. So far, the reason for the failure of AP-site recognition by MutS requires further analysis.

3.5 *Trapping of transient MutS-DNA complexes*

As described, several models exist how mismatch recognition and strand discrimination is coupled over a distance of up to 1000 bp by combined actions of MutSLH during MMR in *E. coli*. In contrast to the model which prefers induced DNA looping by a stationary MutS remaining at the mismatch, the most prominent model proposes a mobile MutS which leaves the damage after successful recognition in form of a *sliding clamp* diffusing along the DNA (Figure 1-4). These conformational changes are induced by binding of ATP and indispensable for

recruitment of MutL resulting in formation of a transient mobile *damage sensor and signalling complex* (MutSL) which is proposed to recruit MutH to its target site for strand discrimination (see Introduction).

To answer the question whether MutS indeed leaves the mismatch after recognition, trapping of the transient MutS-DNA complex via site-directed crosslinking appears to be a promising strategy. Crosslinking is an established method to study protein / DNA as well as protein / protein interactions or to trap transient and highly dynamic complexes for subsequent crystallization, as demonstrated previously (152,153). Consequently, it was attempted to couple MutS during mismatch binding covalently to a heteroduplex DNA substrate via thiol-specific crosslinking. In theory, two thiol-groups within the same or in different molecules that are in an appropriate distance to each other should form a covalent disulfide bond (159). Additionally, both reactive groups can be coupled in a distance and length-dependent manner by thiol-specific crosslinker containing maleimide or methanthiosulfonate groups as demonstrated in numerous crosslink experiments (160,161). Based on the crystal structure of MutS bound to a T:G mismatch containing DNA oligonucleotide (pdb code: 1e3m), a single cysteine within MutS at a suitable position and a single thiol-group attached to the DNA substrate, both in a close proximity to each other, should form a stable MutS-DNA complex due to the crosslink reaction. To this end, two different single-cysteine (sc) variants of MutS (N468C and N497C) were tested in this study to attempt analytical and preparative trapping of a desired MutS-DNA complex. To this end, two different single-cysteine (sc) variants of MutS (N468C and N497C) were tested in this study to attempt analytical and preparative trapping of a desired MutS-DNA complex (Figure 3-23).

Both scMutS variants that contain the cysteine within the *clamp domain* which is involved in DNA binding and proposed to undergo conformational changes required for *sliding clamp* formation upon mismatch-provoked ATP-binding, are fully active *in vitro* (data not shown). Expression constructs for these variants were achieved from Wei Yang and previously generated via site-directed mutagenesis (155) from a cysteine free variant of MutS. Finally, a 30 bp heteroduplex DNA oligonucleotide containing a T:G mismatch 9 bp away from the 3'-end which was

modified with a single thiol-group was chosen for first crosslink experiments (Figure 3-23).

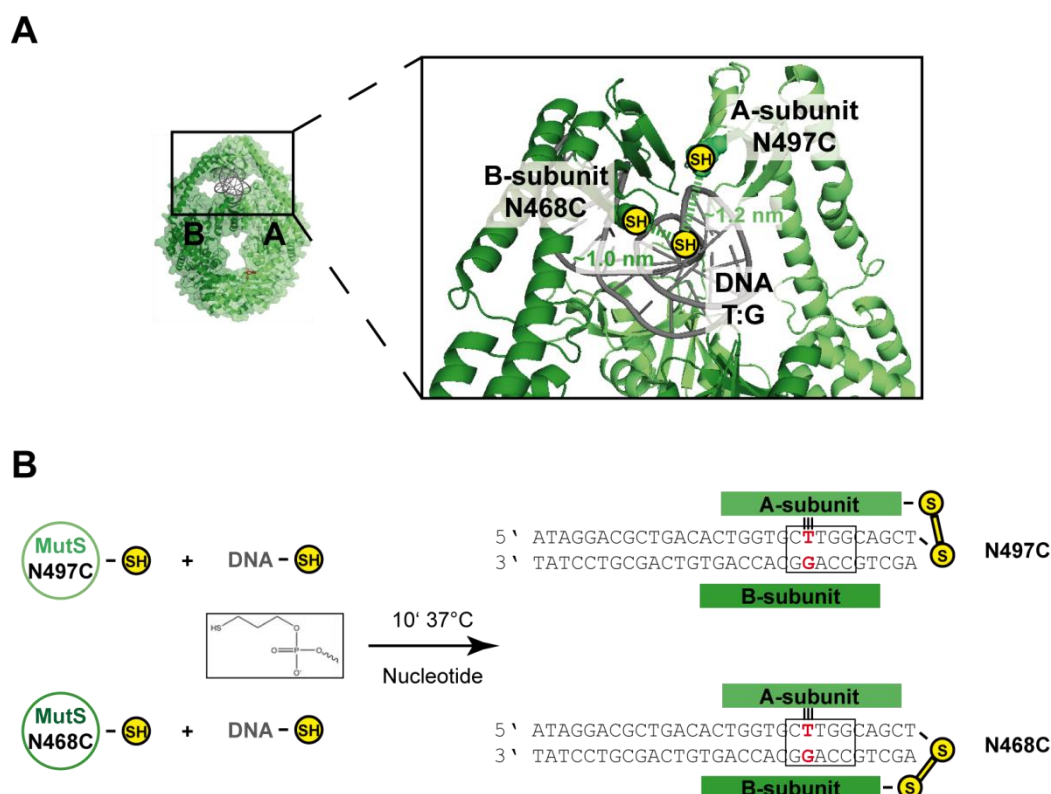


Figure 3-23: Strategy of trapping transient MutS-DNA complexes via crosslinking

A: Simplified model of single-cysteine (sc) variants of MutS, N468C and N497C, bound to a double-strand DNA oligonucleotide containing a T:G mismatch and a single thiol-group linked to the 3'-end of the T-strand. In the crystal structure of the MutS-DNA complex each introduced cysteine is in a close proximity to the thiol-group linked to the DNA (yellow) that allows in principle trapping of the transient complex by formation of a covalent disulfide bond. Notably, the second cysteine within the MutS homodimer is located at the opposite side of the protein during mismatch binding (not shown here) and therefore suggested not to be important for the crosslink reaction. **B:** Scheme for trapping the MutS-DNA complex. Depending on the used single-cysteine variant of MutS either the mismatch binding A-subunit (N497C) or the unspecific bound B-subunit (N468C) is proposed to crosslink to a 30 bp DNA oligonucleotide while the protein is sitting at the mismatch 9 bp away from the modified 3'-end in a distinct orientation as seen in the crystal structure.

With regard to the orientation in which MutS binds to this damage (specific recognition of T), these variants were suggested to crosslink either with the mismatch binding A-subunit using scMutS N497C or the unspecific bound B-subunit using scMutS N468C to the DNA substrate (Figure 3-23B). The fact that in both cases the

cysteine is pointed towards the modified 3'-end with a distance of only 1-1.2 nm increases the change for trapping the complex without the requirement of any additional crosslinker. Notably, the second cysteine within each homodimer is always located at the opposite site of the protein during mismatch binding and therefore proposed not to be suitable and important for crosslinking to the substrate.

To investigate whether mismatch binding and subsequent crosslinking is influenced by the added nucleotide, each scMutS variant was incubated with the modified DNA substrate in the absence or presence of ADP, ATP or the non-hydrolyzable ATP-analogue ADPnP (Figure 3-24). Crosslinking of MutS to DNA was visualized and monitored by denaturing SDS-PAGE as indicated. Due to the fact that covalent coupling of MutS to the DNA results in a complex with bigger mass compared to protein alone, the crosslinked MutS migrates slower during gel-electrophoresis. Subsequent staining either with coomassie or ethidium bromide allowed identification of the MutS-DNA complex, MutS and DNA as well as quantification of the achieved crosslink yield (Figure 3-24).

In contrast to scMutS N468C, the N497C variant was able to form a covalent coupled MutS-DNA complex with a yield of ~50 % crosslinked MutS in the absence of any additional nucleotide (Figure, compare lane 2 and 7). Notably, 50 % is the highest crosslinking yield that could be achieved in this kind of experiment because MutS consists of two subunits but only one is covalent coupled to the DNA. The fact that the functional MutS is a dimer these result indicates that almost all MutS was crosslinked to the substrate in a 1:1 stoichiometry in solution. The unexpected high yield of the achieved MutS-DNA complex in a nucleotide-independent manner using N497C suggests that the protein contained already a bound ADP molecule within the A-subunit which allowed mismatch binding and specific crosslinking. As revealed by the co-crystal structure and numerous studies MutS contains a single high affinity site for this nucleotide in solution which was obviously co-purified with the protein (59,68,77).

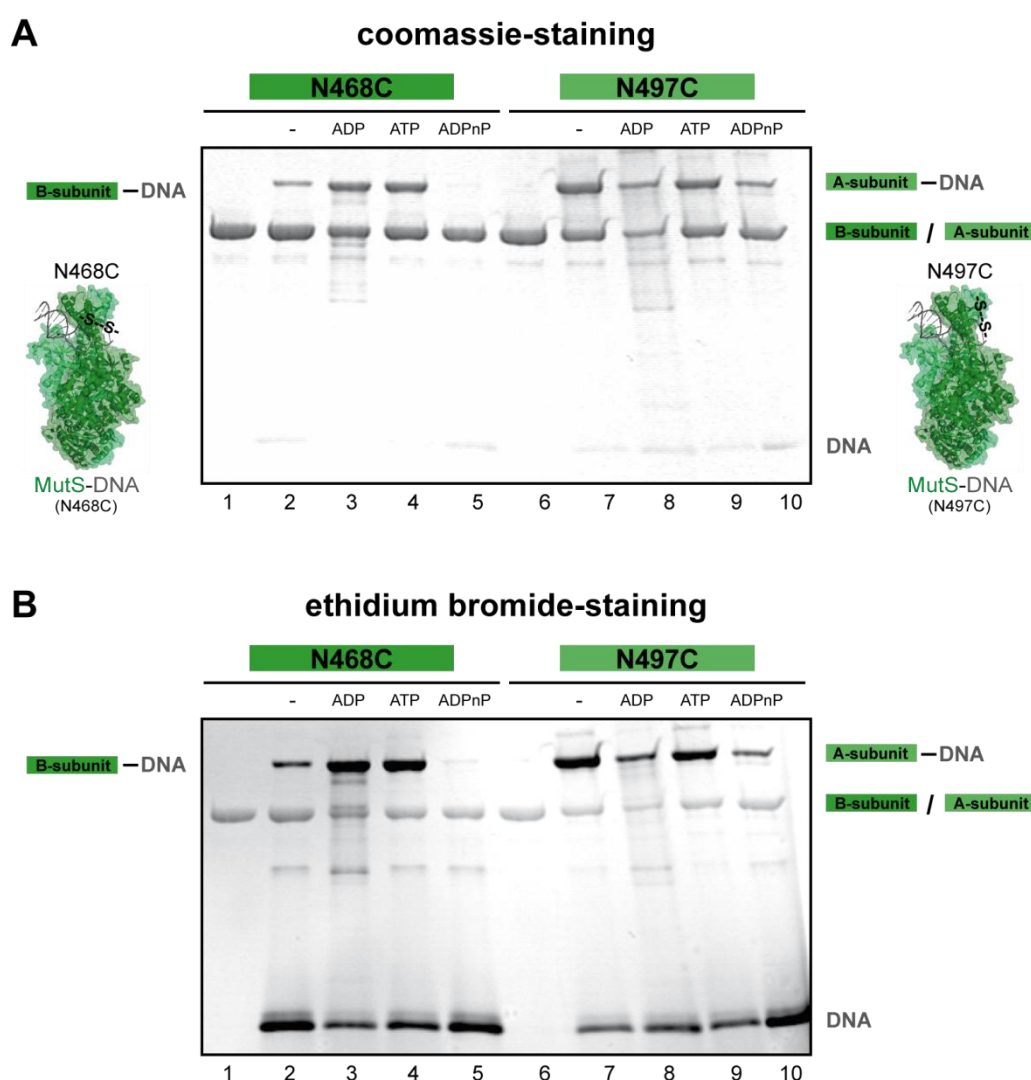


Figure 3-24: Nucleotide-dependent trapping of MutS-DNA complexes

A: Heteroduplex 30 bp DNA substrate (5 μ M) was incubated either with scMutS N486C or N497C (each 5 μ M monomer) in the absence or presence of the indicated nucleotide (1 mM) at 37 $^{\circ}$ C for 10 min. Crosslinking of MutS to DNA was visualized and monitored via denaturing SDS-PAGE in a 4 to 20 % gradient gel stained either with coomassie or ethidium bromide (B). In contrast to N468C, N497C is able to form the covalent coupled complex with DNA in the absence of any additional nucleotide (compare lane 2 and 7). However, both variants are efficiently crosslinked to the substrate in the presence of ADP (lane 3 and 8) or ATP (lane 4 and 9). As expected, almost no crosslink is observed for both variants after incubation with ADPnP (see text for details). **B:** Ethidium bromide stained gel of the same experiment as mentioned above. Covalent coupling of the substrate to one subunit of MutS was demonstrated by specific staining of DNA in the shifted MutS-DNA complex with ethidium bromide (see text for details).

However, high crosslinking yields (40-50 %) were achieved with both tested variants in the presence of ADP or ATP (Figure 3-24; lane 3, 4, 8 and 9). Reaching such high amounts of covalent coupled MutS-DNA complexes with ADP suggests specific trapping of MutS while sitting at the mismatch and during formation of the IRC (Figure 3-24; lane 3 and 8). Interestingly, crosslinking yields for each variant was also very high in the presence of ATP (Figure 3-24; lane 4 and 9), although MutS is proposed to form a *sliding clamp* which leaves the mismatch and prevents further DNA binding by closing the *clamp domain*. Consequently, crosslinking of MutS to the substrate was suggested to be less efficient under this condition. One plausible explanation for the achieved high yield of the desired complexes is given by the ATP-hydrolysis activity of MutS. Hydrolysis of ATP allows subsequent mismatch binding and crosslinking, thereby trapping the IRC because of at least one remaining ADP in the high affinity site. On the other hand, indeed it might be possible that crosslinking of MutS to DNA in the presence of ATP allowed trapping of MutS molecules prior to or during formation of the *sliding clamp*. With regard to the proposed mechanism of mismatch recognition and signalling by MutS, the achieved results with ATP suggest different species in solution that might undergo cyclic ATP-binding and hydrolysis as the consequence of permanent mismatch recognition without dissociation.

Beside this, only less crosslinked complex was observed after incubation with the non-hydrolyzable ATP-analogue ADPnP (Figure 3-24; lane 5 and 10). This was not surprising due to the fact that prevention of ATP-hydrolysis by this nucleotide avoids re-opening of the *sliding clamp* and subsequent DNA binding in contrast to the crosslink reaction when ATP was used (Figure 3-24; compare lane 4 and 5 or 9 and 10) (68). The small amounts of MutS-DNA complex achieved under this condition as shown for scMutS N497C might be the consequence of mismatch binding and crosslinking prior to *sliding clamp* formation induced by the nucleotide. The fact that trapping of the complex was avoided in the presence of ADPnP indicates DNA binding by MutS is required for efficient crosslinking. Finally, mass spectrometry performed by PD Dr. Günter Lochnit confirmed that indeed each single

cysteine variant of MutS is specifically crosslinked to the modified DNA substrate as expected (data not shown).

In conclusion, the used experimental setup allows efficient trapping of MutS-DNA complexes via thiol-specific crosslinking in the absence of any additional crosslinker, in which either the A or the B-subunit of the mismatch sensor appears to be specifically covalent coupled to the DNA substrate by a single disulfide bond. These MutS-DNA complexes might also exist in different conformations induced by the added nucleotide. Both scMutS variants were efficiently crosslinked in the presence of ADP which suggests specific trapping of the IRC as well as with ATP which indeed might permit trapping of MutS as the proposed *sliding clamp* under the used condition. It has to be mentioned, that the exact conformation of the achieved MutS-DNA complex could not be determined in this study and the question whether MutS indeed binds to the mismatch as proposed requires also further analysis. However, the achieved results with ADPnP in principle support the idea of DNA binding by the protein. Due to the fact that trapping of both scMutS variants was such efficient as demonstrated, it was attempted to purify the achieved complexes via size-exclusion chromatography (HPLC) after preparative crosslinking. MutS coupled to DNA is expected to elute earlier during gel-filtration because of bigger size and different shape compared to the protein alone and therefore in principle should allow separation from the uncrosslinked components. Moreover, the absence of any additional chemical crosslinker in the reaction, allows the direct purification via HPLC without previous removal of eventually disturbing reagents.

Size-exclusion chromatography (gel filtration) allowed successful purification of both crosslinked MutS-DNA complexes and is shown exemplary for the scMutS variant N497C (Figure 3-25). In contrast to MutS (~25 min) and DNA (~30 min) alone, the trapped complex elutes already after ~23 min due to the bigger mass and shape. Moreover, the corresponding elution profile showed a 260 to 280 ratio of 1.4 which was expected for a protein that binds to a nucleic acid in a 1:1 stoichiometry (Figure 3-25A).

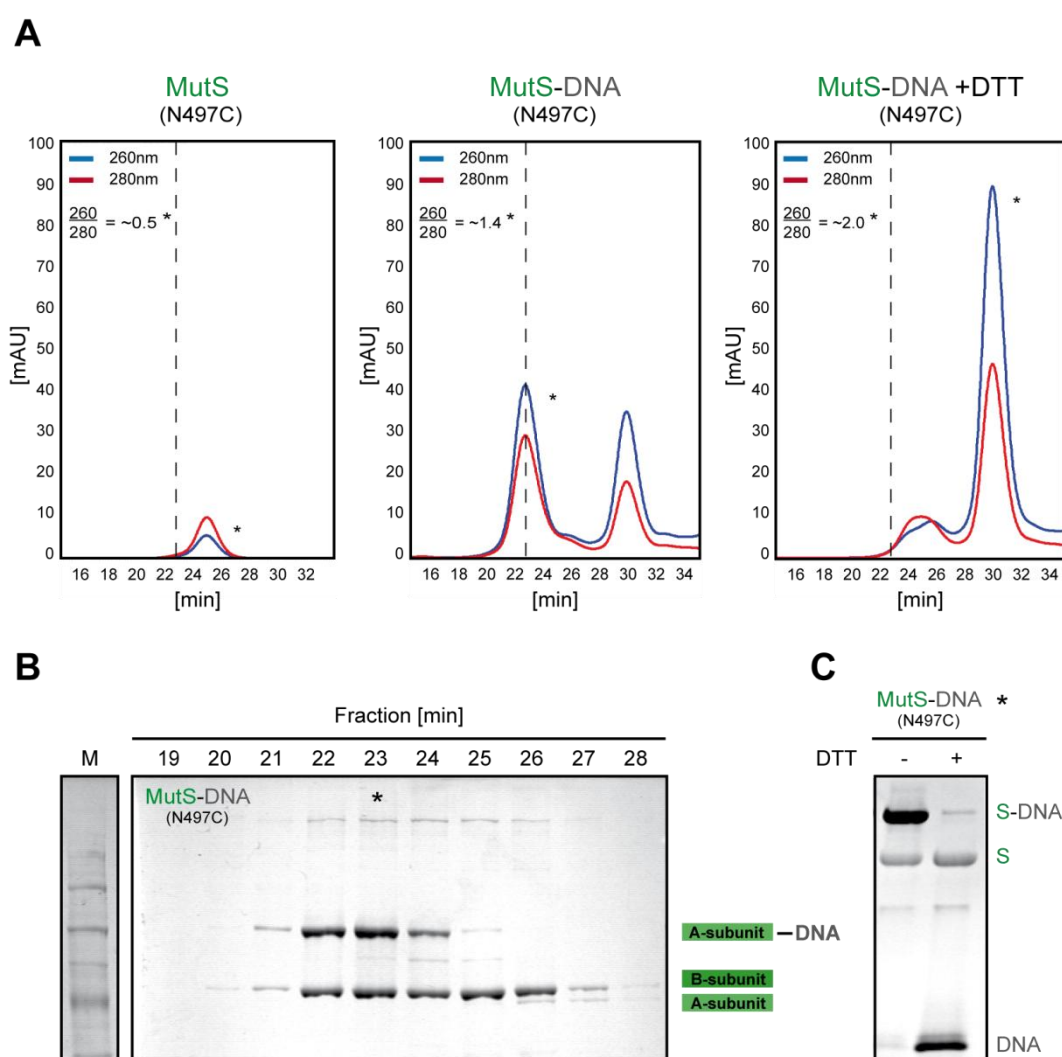


Figure 3-25: Purification of trapped MutS-DNA complexes via gel-filtration

A: Comparison of size-exclusion profiles for MutS (0.5 μ M), after incubation with the 30 bp heteroduplex substrate (0.5 μ M) in the presence of ATP (1 mM) as well as after treatment of the achieved MutS-DNA complex with DTT (N497C; from left to right) using a Superdex 200 10/300 HPLC gel-filtration column. The crosslinked complex elutes after ~23 min and therefore is well separated from uncrosslinked MutS (~25 min) and DNA (~30 min) via gel-filtration using a flow-rate of 500 μ l/min. In comparison to the expected 260/280 ratio for both MutS (~0.5) and DNA (~2.0) the observed ratio for the crosslinked complex with ~1.4 indicates purification of a MutS dimer covalent coupled to the substrate in a 1:1 stoichiometry. As expected, treatment with DTT reduces the disulfide bond demonstrated by disappearing of the complex and an increase in the signal for MutS and DNA. **B:** Analysis of collected fractions from minute 19 to 28 (each 500 μ l) via SDS-PAGE (6 %; coomassie staining). Fractions 22 and 23 contain the purified MutS-DNA complex, whereas the uncrosslinked protein is mainly present in fractions 24 to 26. **C:** Purified complex of scMutS N497C and DNA (fraction 23; *) in the absence and presence of DTT. Reduction of thiol-groups by DTT results in disappearing of the complex and appearing of free DNA as well as increasing of uncrosslinked MutS demonstrated by SDS-PAGE using a 4 to 20 % gradient gel (EtBr staining).

Finally, disappearing of the peak after treatment with DTT revealed that the molecule which elutes after ~23 min was indeed the desired trapped MutS-DNA complex (Figure 3-25A). Further analysis of collected fractions (min 19 to 28) via denaturing gel-electrophoresis as indicated demonstrated that the covalent coupled complex was efficiently separated from uncrosslinked MutS and DNA (Figure 3-25B).

In conclusion, the possibility to obtain trapped MutS-DNA complexes after preparative thiol-specific crosslinking and subsequent purification via size-exclusion chromatography allows further functional and structural studies in steps after mismatch recognition by MutS. So far it has to be determined whether MutS on a “leash” indeed binds to the mismatch and is still active (ATPase activity, DNA bending via FRET) after crosslinking. It should be possible to crosslink MutS to a longer DNA substrate containing an additional hemi-methylated GATC-site and to investigate whether recruitment of MutL and activation of downstream factors is still attainable (Mobile vs. Stationary MutS). Moreover, no co-crystal structure is available that shows MutS in the proposed *sliding clamp* conformation induced by ATP after mismatch recognition due to the dynamic of this complex. Consequently, trapped MutS on a “leash” is a promising starting point for crystallization trials in solving the structure of the puzzling MutS-DNA complex that is formed after conformational changes induced by ATP-binding.

4 Discussion

Maintaining of genome integrity and DNA stability denotes a fulltime challenge for each organism caused by permanent arising of damages and mismatches, possessing the capability to alter the encoded information, over thousands of times per day. As consequence of evolution, a brought repertoire of DNA repair systems exists, that guarantees integrity and stability of the genome in organisms belonging to all domains of life (11,12). However, the fact that several repair systems have overlapping substrate specificities obviously gives rise to the need to co-ordinate their activities in a well-nuanced relationship. The repair of T:G and U:G mismatches caused by spontaneous or induced deamination of cytosine and 5-methylcytosine as well as misincorporation during replication falls into this category (5,145). A failure of co-ordinated crosstalk during repair of these damages causes mutations leading to cancer in mammals or double-strand breaks triggering cell death (13). The results achieved in this study give insights in the mechanisms involved in the regulation of crosstalk in DNA mismatch repair.

Crosstalk in DNA mismatch repair

5-methylcytosine is used by many organisms ranging from bacteria to mammals as a physical or epigenetic tag that allows them to distinguish between DNA from different sources lacking this modification. A wide variety of biological phenomena including restriction-modification, gene silencing, epigenetic inheritance and stimulation of an immune response use C5-methylation of DNA (15-17). Consequently, several highly conserved repair systems have evolved to maintain these important sites within the genome. T:G mismatches induced by spontaneous deamination of 5-methylcytosines (5meC) or misincorporation during replication are target for MMR and VSPR in *E. coli*. In comparison to MMR, where cooperation of MutS, MutL and MutH is absolutely required mismatch recognition and strand

incision, Vsr includes both features in a single protein. Strains without Vsr are completely deficient in VSPR, and therefore show a high frequency of C to T mutations at 5-methylcytosines (117,121). The crosstalk between MMR and VSPR has been puzzling due to the fact that both competition and cooperation play a role during repair of a T:G mismatch after deamination of 5meC to T (5). Earlier *in vivo* studies show that overexpression of MutS reduces VSPR, indicating MutS and Vsr compete for mismatch binding and subsequent repair (127). On the other hand, VSPR is reduced, but not eliminated in cells, which are unable to produce MutS or MutL (162,163). Finally, overexpression Vsr inhibits MMR, an effect attenuated by co-overexpression of MutL or MutH but not MutS (129,130).

As shown in this work and by further studies *in vitro* using yeast-two hybrid analysis, analytical ultracentrifugation and chemical crosslinking (132,134,164), the physical and functional interaction of MutL with Vsr is responsible for the observations made *in vivo*. Vsr efficiently inhibits mismatch-provoked MutS and MutL-dependent activation of MutH (Figure 3-8). This finding supports a model of competition between the VSPR component and MutH for a common or overlapping binding site on MutL, explaining the inhibitory effect of Vsr on MMR *in vivo*, which is only reversed by overexpression of MutL or MutH (5,130,165). The interaction site for MutH and Vsr is located between the N- and C-terminal domains reminiscent to the position of the client binding site of Hsp90, which shares structural homology to MutL in the ATPase domain (160,166). However, the present study reveals that the physical interaction between MutL and Vsr is important but not sufficient for the observed enhancement of VSPR under physiological ionic conditions (150 mM KCl). Both MutL and MutS are necessary and sufficient for the stimulation of Vsr endonuclease activity and this functional interaction requires ATP-hydrolysis (Figure 3-9), similar to the mismatch-provoked activation of MutH (Figure 3-3) (167). Moreover, the MutS and MutL-dependent activation of Vsr is inhibited by MutH (134), which confirms the model of competition between both endonucleases for binding to MutL. Whereas the physical interaction between MutL and Vsr could be observed in the absence of ATP-hydrolysis and with the N-terminal domain of MutL (133), the functional interaction, resulting in activation of Vsr, requires

ATP-hydrolysis, as the ATPase deficient MutL E29A has almost completely lost its stimulatory ability (Figure 3-10). Similarly, this ATP-hydrolysis deficient variant of MutL is not able to support the mismatch-provoked activation of MutH at physiological ionic conditions (150 mM KCl) (data not shown). These results are at odds with experiments conducted at low ionic strength (20 mM NaCl), suggesting a role for ATP-hydrolysis by MutL only for steps after DNA incision by MutH and loading of UvrD helicase (168). However, the conclusions are fully consistent with data reporting the inability of MutS to further increase the MutH activation in the presence of MutL E29A at physiological ionic strength (169). Notably, at lower salt concentration (e.g. 50 mM KCl) MutL wild type and E29A are sufficient to activate MutH in a MutS and ATP-hydrolysis independent manner (data not shown) (169). In conclusion, the results achieved in this work clearly identify Vsr as new member in the permanent growing group of effector proteins stimulated or activated by the transient MutSL *damage sensor and signalling complex* (Figure 4-1).

The stimulatory effect of both MutS and MutL on VSPR is puzzling, especially since structural analysis of the MutS-DNA and Vsr-DNA complexes clearly reveal that MutS and Vsr cannot bind simultaneously to the same T:G mismatch (5). Finally, since mismatch binding by MutS and Vsr is mutually exclusive, only models involving a mobile rather a stationary MutS, which does not remain bound at the mismatch, are consistent with the observed MutS and MutL-dependent activation of Vsr (2,170). Similarly, MMR is also efficient even if mismatch and GATC-site are separated by only 4 bp, a distance which is too short to allow simultaneous binding of MutS at the mismatch and MutH at the GATC-site (Figure 3-8). At least two possible explanations exist, how MutS and MutL allow the access of Vsr to the T:G mismatch or MutH to the next GATC-site. One possibility is that MutS and MutL leave the mismatch before the arrival of the effector proteins, as proposed previously (5). The only way to explain the stimulatory effect is to postulate that the MutS–MutL complex induces conformational changes in the DNA, which allow Vsr easier to bind at its target site. However, the demonstrated functional interaction between MutS, MutL and Vsr reveals that this scenario is unlikely. More likely and consistent with the results achieved in this work, MutS and MutL act as damage sensors

recruiting any effector protein, such as MutH, UvrD or Vsr, to the corresponding site of action (Figure 4-1).

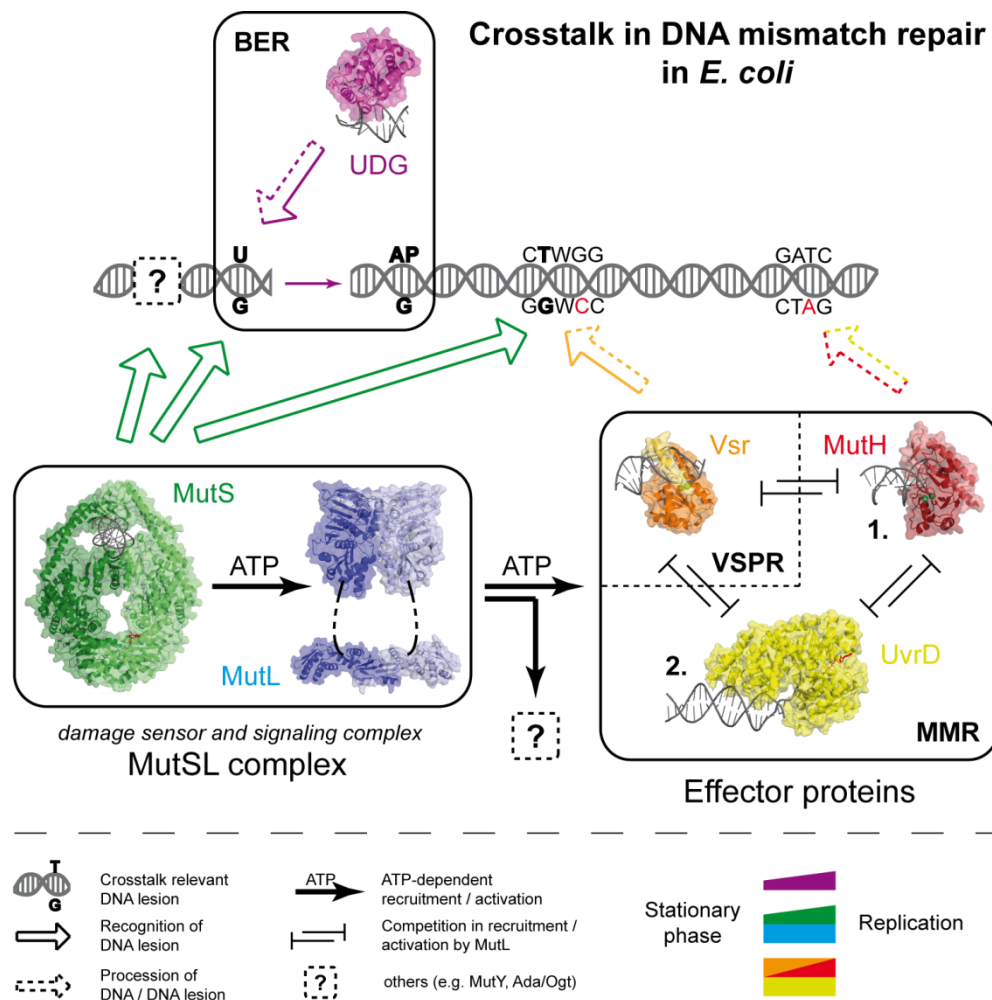


Figure 4-1: Modell of crosstalk in DNA mismatch repair in *E. coli*

The resulting ATP-dependent interactions between sensor(s) and effector(s) both displace the sensors and activate the effectors. This model is supported by recent *in vivo* studies showing that MutL recruits both Vsr and MutH endonucleases in response to several DNA damages recognized MutS (89). If the recruited protein is able to mediate repair, the MutS-MutL complex would dissociate. If the recruited protein is unable to mediate repair, the MutS-MutL complex would remain, allowing subsequent recruitment of another effector protein. Such a model would account for

the fact that MutS and MutL enhance Vsr activity, but are not required for VSPR. The inhibitory effect of Vsr on MMR explains why regulation of Vsr expression is necessary for proper MMR during replication. However, enhanced VSPR at a low Vsr concentration is very advantageous to assure fast and efficient repair of a T:G mismatch, which causes a C to T transition mutation if the correct G is excised by MMR (Figure 1-13). Additionally, the fact that MutH also inhibits VSPR explains the regulation of MutH expression during stationary phase. Beside this, it is possible that Vsr is kept low in growing cells not because the interference with MMR but it can stimulate T to C transition mutations at CTWGG-sites, as shown before (129). This problem seems to be solved by nature and evolution because these sites are significant under represented within the genome of *E. coli* (171).

Finally, in this work it is demonstrated that MutS is indeed capable to form the *initial recognition complex* (IRC) in the presence of the nicked VSPR intermediate ('T:G) (Figure 3-15) and therefore triggers initiation of MMR (data not shown). The possibility for MutS to initiate MMR at each step during ongoing VSPR increases the chance for arising of a lethal double-strand break when VSPR and MMR act simultaneously on both DNA strands which might explain why regulation of MutH expression is also required for stringent control. Moreover, binding of the 'T:G mismatch by MutS after initiation of VSPR is proposed to be prevented by a strong binding of Vsr to the processed repair intermediate (122). However, the evidence that MMR and VSPR in principle cooperate for efficient DNA repair is demonstrated by the fact that both repair pathways share components resulting in an enhanced VSPR pathway.

The question of when and how MutH or Vsr enter and leave the repair pathway needs to be addressed before the mechanistic details of competition and cooperation between various proteins interacting with MutL can be understood. Furthermore, the details in the hand off between MutH and UvrD for the required actions at a GATC-site during MMR are almost unknown. To this end, the *multiple loading* model is suitable to explain the well-coordinated initiation and completion of MMR *in vitro* and *in vivo* (Figure 4-2) (7). As proposed, MutS leaves the mismatch after recognition and therefore multiple MutS are able to form a *sliding clamp* on the same

substrate thereby recruiting MutL, which results in formation of numerous transient mobile *damage sensor and signalling complexes* (MutSL) that finally allow recruitment of any of the available effector proteins to its corresponding site as long as the damage is present. If the DNA contains a nick as starting point for strand excision either introduced by MutH or any other endonuclease, as demonstrated (Figure 3-5), only loading of UvrD by MutL permits subsequent steps in MMR. Beside this, DNA might be directly repaired by a DNA polymerase with nick-translation activity as shown for DNA polI when strand incision occurred upstream of a mismatch (Figure 3-6). Finally, excision as well as repair of the damage avoids further *sliding clamp* formation of MutS and activation of effector proteins by MutL. So far, the question whether the transient MutSL complex dissociates directly after successful activation of one effector protein or is able to recruit and stimulate several downstream repair factors in a role remains further determination. Moreover, it has not been shown that MutSLH forms indeed a transient quaternary complex on DNA during MMR. Although demonstrated that mismatch-provoked interaction of MutL with MutS occurs in the closed conformation of the N-terminal domain induced by ATP, it is not clear whether the dimeric form is also required for activation of an effector protein (172).

The observed similarities in stimulation of Vsr and MutH by MutSL offers new routes for future in-depth analysis of the activation of effector proteins in MMR and other pathways such as BER (MutY) or MTase repair (Ada/Ogt) in a comparative manner (135,173). Notably, UvrD, which is also recruited and stimulated by MutL (39), has been described for the first time as a member of the nucleotide-excision repair (NER) pathway involved in repair of damages caused by UV light (3). However, only one Vsr homolog from another organism has been analyzed but not in the context of MMR (174). Since homologs of the Vsr endonuclease are present in 198 bacterial species [REFSEQ 01-23-09 (175)] from across the bacterial kingdom in contrast to MutH homologs that are almost exclusively found in γ -proteobacteria (currently 115 bacterial species in REFSEQ), it is important to understand whether the observed physical and functional interaction between Vsr and MutL in *E. coli* is a general DNA repair pathway used also in other bacteria. The method for generation

of multipurpose DNA repair substrates and functional DNA repair assays involving the activation of MutH, UvrD and Vsr by MutSL as described in the present study might be exploited for the mechanistic analysis of DNA repair pathways in bacterial and eukaryotic systems.

In comparison to the demonstrated crosstalk between MMR and VSPR during repair of a T:G mismatch, U:G mismatches that arise as a result of either spontaneous or induced deamination of cytosines are target for MMR and BER (1,176). This seems to be problematic because uracil is not a regular component of DNA and if not repaired correctly, base pairing with A causes a C to T transition mutation (Figure 1-16) (141). Moreover, initiation of BER includes the catalytic release of uracil, thereby creating an AP-site (Figure 1-14). In contrast to conventional base-base mismatches, a special type of damage is formed by AP-sites. These sites represent non-instructive lesions that prevent DNA polymerases from properly selecting and fitting incoming dNTPs for a successful nucleotidyl transfer. Consequently, AP-sites force non-instructed base incorporation during DNA replication or will obstruct DNA synthesis by replicative DNA polymerases (177,178). AP-sites, like other replication-blocking DNA lesions, in principle trigger the engagement of specialized translesion synthesis (TLS) polymerases (179). Mutagenesis data suggest that these polymerases are recruited to incorporate preferentially A opposite AP-sites, a concept that has been described as the A-rule (6). Therefore, TLS polymerases allow DNA synthesis across lesions that are difficult to repair, thereby tolerating mismatches but avoiding replication fork collapse (180). However, the AP-site containing BER intermediate is also proposed to be recognized by MutS as an insertion or deletion loop (IDL) due to the remaining nucleotide and therefore sufficient to trigger initiation of MMR. Consequently, simultaneous initiation of BER and MMR, which might be directed to the correct G, dramatically increases the chance for arising of a non-instructed base incorporation or lethal double-strand break (Figure 1-16), which gives rise to the need to co-ordinate their activities in a well-nuanced relationship.

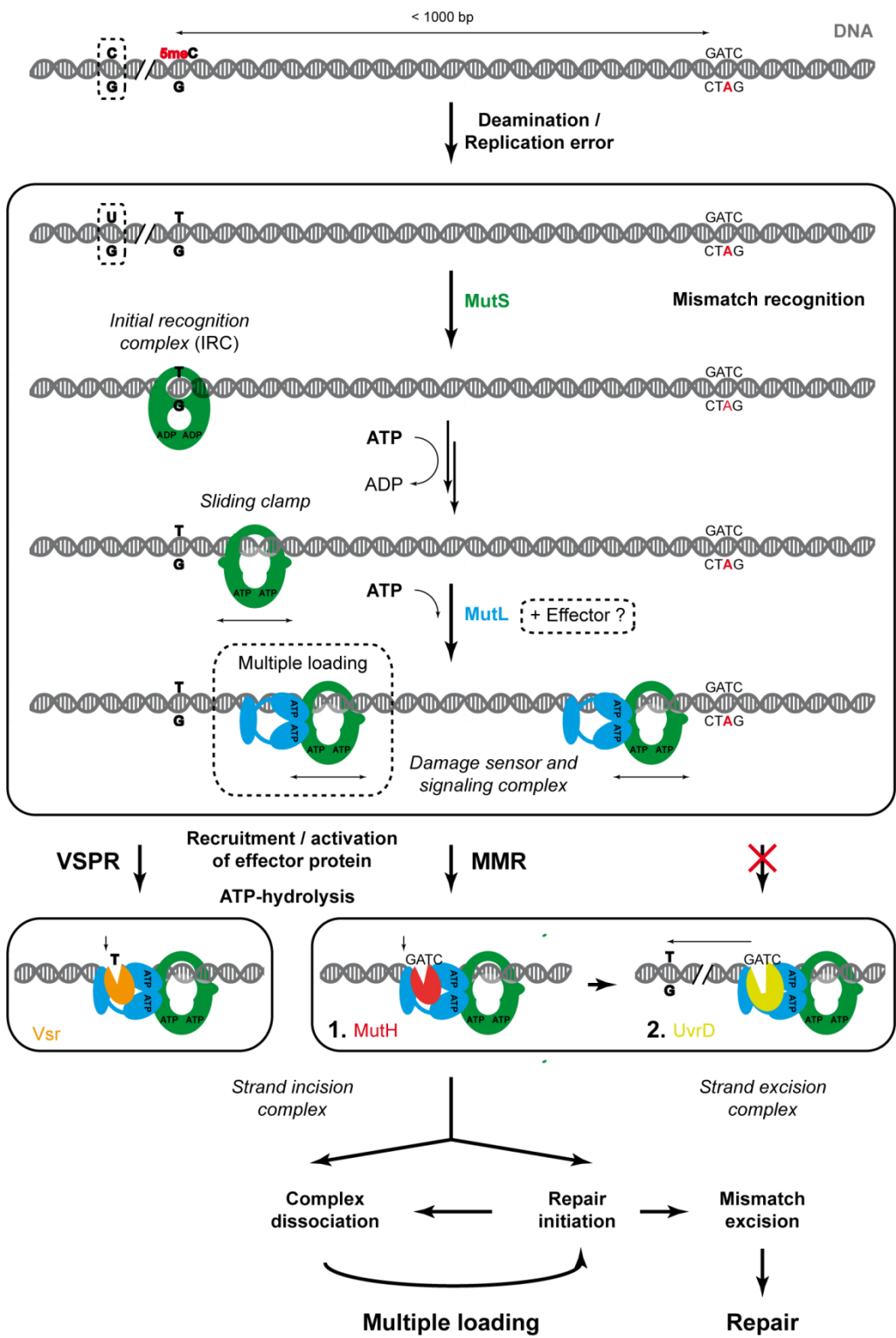


Figure 4-2: Model of damage sensor and signalling by MutSL
(See text for details)

Interestingly, these repair pathways also work together. UDG and MutS homologs are reported to cooperate for somatic hypermutation (SHM) in antigen-stimulated B-cells, where activation induced deaminase (AID) deaminates cytosines within the DNA thereby generating U:G mismatches in the immunoglobulin variable-gene region (145,147,181). The purpose is to induce a mutagenic process that results in affinity maturation of an antibody (182,183). These U:G mismatches are subject to repair, but the process obviously allows an increase in mutations and therefore is error prone. Cytosine deamination by AID also induces class-switch recombination (CSR) at the immunoglobulin locus that finally triggers initiation of recombination (184). Consequently, crosstalk between MMR and BER requires stringent control at the level of mismatch targeting and repair activation as well as by the involved components of both repair pathways (185).

As shown in this study, the presence of a single U:G mismatch within DNA very efficiently triggers initiation of both MMR and BER (Figure 3-17). Although a U:A base pair is processed by UDG (Figure 3-17) and induces small changes in the local flexibility of the, MutS tolerates this damage, as expected (Figure 3-17). Both U:A and T:A form a normal Watson-Crick base pair resulting in homoduplex DNA and therefore are not recognized by MutS as a mismatch. Only the U:G mismatch is sufficient to provoke activation of MutH by MutS and MutL and therefore in principle is suitable to induce recruitment and subsequent activation or stimulation of any present effector protein by the MutS-MutL complex. Indeed, Vsr endonuclease activity is also stimulated by MutS and MutL after replacement of the mismatched T within a Vsr recognition site (Dcm-site) by U (data not shown). However, BER is mainly responsible for efficient restoration of the original C:G base pair after spontaneous or induced deamination of cytosine (3).

To this end, the mechanisms assuring the preferential engagement of BER and preventing misengagement of MMR are unclear. One explanation for the preference might be the fact that UDG very fast catalyzes the release of uracil from DNA and allows initiation of BER prior to MMR (143,186). However, there is still no evidence for crosstalk that depends on a direct interaction between components of both repair pathways at the level of U:G mismatch targeting and downstream processes to assure

that unfavourable mutagenic interferences are avoided. In *E. coli*, MMR is mainly active during replication and both MutS and MutH are down regulated in stationary phase at least because of interference with VSPR (131). Moreover, strand incision as a result of unfavoured mismatch-provoked activation of MutH is prevented by the methylation status of the DNA during stationary phase (2). However, it has been shown in this and by other studies that other effector proteins are also recruited by the transient MutSL complex and therefore might provoke misengaged processing of DNA (89). The corresponding eukaryotic mismatch sensing complex (MutS α -MutL α) plays a crucial role in transduction of damage signalling to downstream factors that regulates important DNA metabolisms. In mammalian cells, glycosylases that compete with the MutS homolog for binding to T:G are almost eliminated during S-phase of the cell-cycle (187), but it was observed that especially UDG is present during S-phase and therefore competes with MutS for binding to U:G mismatches (J. Jiricny, personal communication). In general this seems to be advantageous for prevention of misengaged initiation of MMR. On the other hand it has been reported that homologs of UDG and MutS appear to work at different stages of the cell-cycle downstream of cytosine deamination to facilitate somatic hypermutation (SHM) and class-switch recombination (CSR) in immune cells (183). Finally, inhibition of UDG by the uracil glycosylase inhibitor (UGI) prevents initiation of BER, as expected (Figure 3-18), and might be used as a tool in crosstalk regulation.

The question whether misengagement of MMR still causes unfavourable mutagenic interferences after initiation of BER is important to understand requirement for crosstalk in DNA mismatch repair and therefore addressed in the present study. Discrimination between intact and damaged DNA denotes an important challenge for MutS as the first step in MMR. Specific binding of a mismatch induces conformational changes in MutS towards the *initial recognition complex* (IRC), which is indispensable for initiation of MMR (Figure 1-6) (72). In the present study, formation of the IRC was directly monitored by a well-established MutS binding and DNA bending assay (Michele Cristovao) based on fluorescent techniques (FRET) which allows determination of the mismatch binding orientation achieved by MutS, as shown here especially for a T:G and C:A mismatch within the

same sequence context (Figure 3-21). Crystal structures of MutS bound to either a T:G or C:A mismatch have been revealed that T and A, respectively, are specifically recognized by one subunit of the mismatch sensor resulting in a functionally hetero-dimeric MutS with different binding orientation (60). Additionally, activation of effector proteins by MutS and MutL after successful mismatch recognition was analyzed by appropriate *in vitro* DNA repair assays, as described.

As expected, both U:G and T:G mismatch within the same sequence context are bound by MutS in the same orientation, suggesting direct interactions of the mismatch binding subunit of MutS with U. Due to release of uracil by UDG and generation of an AP-site in the initial step of the BER pathway (Figure 1-14), the type of damage has changed dramatically. Although not the equal lesion, the remaining nucleotide opposite of the AP-site (AP:G) is proposed to be recognized by MutS as an insertion or deletion loop (IDL) such as an extra G and therefore suggested to have the capability to provoke initiation of MMR. Consequently, recognition of the remaining nucleotide as an IDL by MutS requires a change in the mismatch binding orientation of the protein due to the fact that the previously bound uracil is released by UDG. Although unexpected, the results achieved in this study clearly reveal that initiation of MMR is directly prevented after release of uracil by UDG (Figure 3-18) due to the fact that formation of the IRC is avoided in the presence of an AP-site Figure 3-20. Neither G nor A opposite an AP-site within the sequence context used here (5'-C(AP)WGG-3'/5'-G(G/A)WCC-3') are specifically recognized by MutS as a mismatch and bound in an orientation as shown for the corresponding IDL (Figure 3-22) which triggers initiation of MMR (data not shown).

It has to be mentioned that mismatch recognition by MutS to some extent is influenced by the sequence context in which the mismatch is included (188). Therefore, indeed it cannot be excluded that some AP-sites are recognized by MutS resulting in initiation of MMR. Beside this, these damages might induce a change in the pairing of neighbouring bases due to a possible interaction of the remaining nucleotide with a base next to the AP-site. The resulting mismatches might be targeted by MutS and therefore provoke initiation of MMR.

However, comparison of MutS binding and induced DNA bending in the presence of various crosstalk relevant lesions within the same sequence context as used in this study demonstrate that release of uracil converts a mismatch into a non-mismatch (homoduplex). A change in base pairing which generates mismatches that are recognized by MutS and trigger activation of downstream factors, was also not observed. Several conclusions can be drawn if MutS recognizes AP-sites within a different sequence context. Beside competition between MMR and BER for initiation of repair in the presence of a U:G mismatch, both pathways might also interfere at downstream steps as well as after processon of a U:A base pair to AP:A by UDG which finally would convert a non-mismatch into a mismatch. Moreover, initiation of MMR might be triggered after release of any damaged base targeted by one of the various glycosylases involved in the different BER pathways (3). Notably, experimental evidence suggest, that up to 10.000 abasic sites appear per cell and day (10). This denotes an enormous challenge for each organism if protection of AP-sites is required to avoid initiation of unfavoured repair pathways. On the other hand, activation of MMR by AP-sites as a consequence of ongoing BER to facilitate somatic hypermutation (SHM) and class-switch recombination (CSR) in immune cells might indeed be advantageous and therefore favoured. Exactly how AP-site protection is achieved remains unclear, although the engagement of UDG with a very slow dissociation rate after catalysis as shown for another glycosylase might provide an answer (187). Moreover, the cellular concentration of AP-lyases such as EndoIV is very high in *E. coli* and therefore might prevent misengaged initiation of MMR at AP-sites *in vivo* (J. Jiricny, personal communication). To this end, no biochemical data is available that directly demonstrates initiation of MMR at AP-sites and a possible change in the MutS binding orientation during mismatch recognition.

As mentioned, the processes of SHM and CSR prefer simultaneous actions by MMR and BER *in vivo*. In contrast to normal situations, active induced deamination by AID generates multiple U:G mismatches within the DNA that also trigger multiple initiation of both repair pathways. Although the presence of one U:G mismatch seems to be unproblematic, numerous mismatches together with single-nucleotide gaps that appear during BER indeed provoke processing of DNA

by the MMR system, as demonstrated recently (145). Formation of the *damage sensor and signalling complex* (MutSL) permits recruitment and activation of downstream repair factors using a generated single-nucleotide gap as entry point for strand excision and degradation to allow error-prone synthesis of DNA during SHM or arising of the desired double-strand break in CSR.

The fact that UDG catalytically converts a mismatch in to a lesion that is not recognized by MutS offers new possibilities to study the *multiple loading* model of DNA mismatch repair. This model is used to explain the hand off between MutH and UvrD for the required actions at a GATC-site during MMR (7,34). It is still unclear, whether a single MutSL complex is able to activate both or even more effector proteins in a role or multiple loading of repair factors is required to achieve well-coordinated and efficient repair. The capability to “switch-off” the U:G mismatch by UDG might be used to monitor the initial steps in MMR after formation of the MutSL complex thereby preventing multiple loading of MutS on DNA.

Trapping of transient MutS-DNA complexes

Although MMR is under investigations since 25 years, the mechanism how mismatch recognition is coupled to strand discrimination which can occur up to 1000 bp away from the lesion, is still puzzling (34). In principle two different models (stationary vs. mobile MutS) are used to explain how activation of effector proteins such as MutH and UvrD by MutL is achieved after successful mismatch recognition by MutS. In the first model, MutS is proposed to stay at the lesion and subsequent recruitment of MutL induces an ATP-dependent looping of the DNA to permit activation of downstream factors at the corresponding site of action (*Looping* model) (Figure 1-4). In the second model, MutS leaves the damage in form of a *sliding clamp* which is induced by ATP-binding after mismatch recognition. This conformational change allows free diffusion on DNA and recruitment of MutL thereby forming the transient mobile *damage sensor and signalling complex* (MutSL) which is proposed to carry repair factors to its corresponding target site (7). However, the demonstrated mismatch-provoked stimulation of Vsr by MutSL

supports the model in which MutS is rather mobile due to the fact that mismatch binding by Vsr and MutS simultaneously is mutual exclusive. Moreover, efficient activation of MutH even when the strand discrimination signal (hemi-methylated GATC-site) is only 4 bp away from the mismatch makes the scenario of a stationary MutS unlikely (Figure 3-8).

To this end, successful trapping of transient MutS-DNA complexes via site-directed crosslinking as shown in this study, offers new possibilities for functional and structural studies in the steps after mismatch recognition by MutS. The mismatch sensor on a “leash” serves as an optimal starting point to answer the question whether MutS indeed has to leave the damage in form of a *sliding clamp* to allow damage signalling and activation of downstream repair factors by MutL or can stay at the lesion for repair initiation via DNA looping (Figure 4-3). Moreover, a trapped MutS while sitting at the mismatch will prevent further recognition of this damage by a second protein, thereby offering a chance to analyze the *multiple loading* model of MMR in *E. coli* (7). The big advantage of thiol-specific crosslinking as used here is the possibility to cleave the created covalent disulfide bond by reducing agents such as DTT resulting in the release of MutS. Notably, the covalent coupled MutS-DNA complex was achieved in the absence of any additional crosslinker containing maleimide or methanthiosulfonate groups and it remains to determine whether trapping of these complexes is more or less efficient in the presence of crosslinker with varying length. Coupling of MutS to the DNA via a crosslinker increases the flexibility of the obtained complex and therefore might be required and advantageous for further functional and structural studies of the complex. So far, it cannot be excluded that the linker between MutS and the 3'-end of the DNA is too short to guarantee sufficient flexibility for required changes in the conformation of the protein after successful mismatch recognition. However, due to coupling of only one subunit of the homodimer, 50 % of crosslinked MutS which was almost reached in the presence of ADP/ATP is the highest yield that can be achieved in this type of experiment (Figure 3-24).

Although it was demonstrated by mass spectrometry (B. Spengler) that both single-cysteine variants of MutS (N468C and N497C) crosslink via the corresponding cysteine within the *clamp domain* to the modified DNA substrate as expected (data not shown), the question whether MutS in the trapped complex indeed binds to the mismatch as proposed, requires further verification. So far, the achieved results support the idea of DNA and mismatch binding by the protein after trapping. Crosslinking of MutS to DNA is nucleotide-dependent and favoured in the presence of a mismatch (Figure 3-24, S. Sekerina, personal communication) which is in agreement with the model of damage recognition by MutS (7). Furthermore, trapping of the complex was not possible when MutS was incubated with the non-hydrolyzable ATP-analogue ADPnP which induces the proposed conformational changes towards the *sliding clamp* thereby avoiding further mismatch and DNA binding (Figure 3-24). Although ATP also induces the *sliding clamp*, ATP-hydrolysis by MutS in the absence of a mismatch allows subsequent DNA binding and crosslinking to the substrate. Consequently, the possibility to obtain covalent coupled MutS-DNA complexes with ADP or ATP increases the chance for trapping MutS during formation of the *initial recognition complex* (IRC) or species of molecules which might indeed undergo the proposed conformational changes towards the *sliding clamp*. Finally, subsequent addition of ADPnP to the mismatch binding MutS on a “leash” might also induce the *sliding clamp* formation but prevented ATP-hydrolysis avoids completion of the ATPase-cycle and therefore freezes the mismatch sensor in this state. However, although trapping of these complexes was specific and very efficient under the used conditions, it has to be determined whether MutS is still active (ATPase activity) after crosslinking. FRET experiments similar to that used in this work for monitoring mismatch-provoked DNA bending by MutS might be suitable to demonstrate formation of the IRC by the trapped MutS-DNA complex.

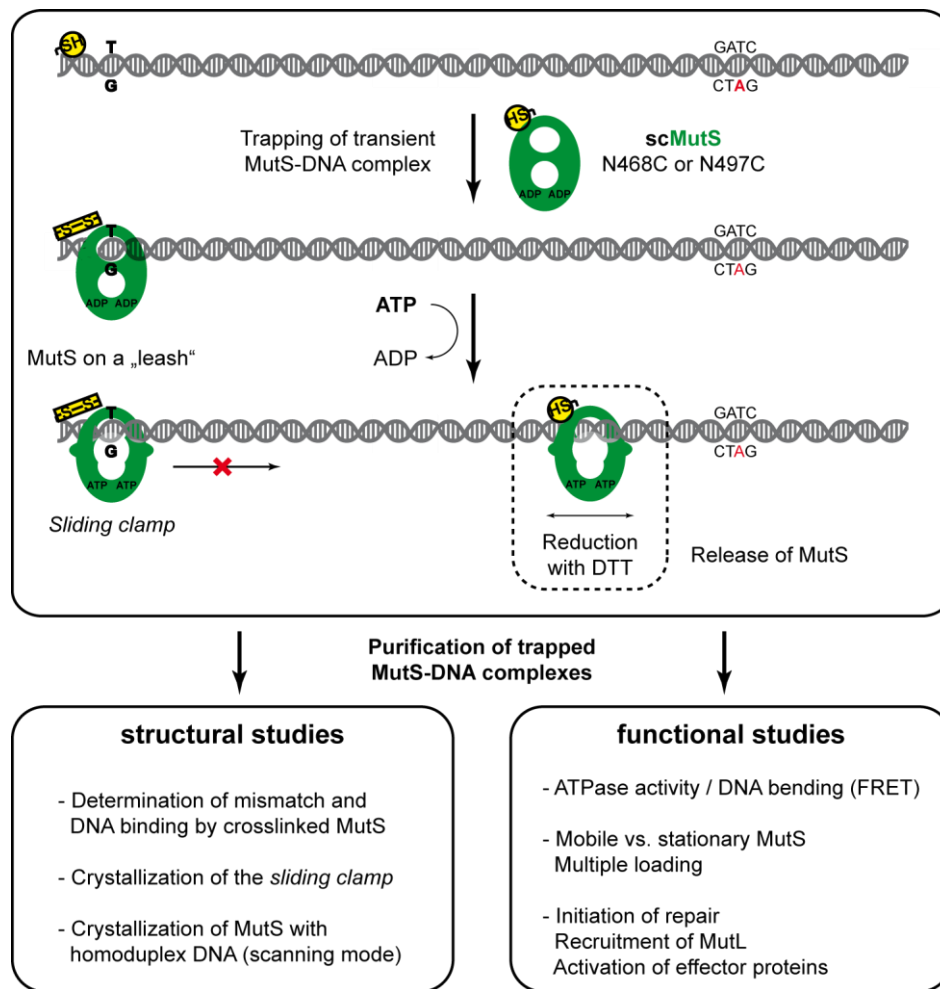


Figure 4-3: Overview of future studies in MMR using trapped MutS-DNA complexes

With regard to the orientation in which a T:G mismatch is recognized by the MutS homo-dimer in the presence of ADP (59) and the position of the cysteine within the *clamp domain* of the protein (Figure 3-23), the achieved results strongly suggest that scMutS N497C is covalent coupled with the mismatch binding (A) subunit whereas scMutS N468C crosslink with the unspecific bound (B) subunit to the DNA substrate. However, further analysis will be required to demonstrate clearly the trapping of both subunits separately in the resulting functionally hetero-dimeric MutS protein. Moreover, it is of interest to analyze whether crosslinking is affected in the presence of a C:A mismatch that is bound by MutS in a different orientation compared to T:G within the same sequence context (Figure 3-21). Due to the change in the mismatch binding orientation, coupling of DNA to the A-subunit is proposed

to be achieved when scMutS N468C instead of N497C is used. Finally, the capability to discriminate between the two functionally hetero-dimeric subunits of a homo-dimeric protein via specific crosslinking to the DNA substrate might be useful for studies in the MutS ATPase-cycle and the proposed asymmetric affinity for ADP and ATP (77). Beside the mentioned functional studies that can be performed, the trapped and purified MutS-DNA complex is the optimal starting point for crystallization trials to obtain the structure of MutS during formation of the *sliding clamp* or the structure of the mismatch sensor bound to homoduplex DNA (Scanning mode) after mismatch-independent crosslinking (Figure 4-3).

5 References

1. Jiricny, J. (2006) The multifaceted mismatch-repair system. *Nat Rev Mol Cell Biol*, **7**, 335-346.
2. Iyer, R.R., Pluciennik, A., Burdett, V. and Modrich, P.L. (2006) DNA mismatch repair: functions and mechanisms. *Chem Rev*, **106**, 302-323.
3. Robertson, A.B., Klungland, A., Rognes, T. and Leiros, I. (2009) DNA repair in mammalian cells: Base excision repair: the long and short of it. *Cell. Mol. Life Sci.*, **66**, 981-993.
4. Lieb, M. and Bhagwat, A.S. (1996) Very short patch repair: reducing the cost of cytosine methylation. *Mol. Microbiol.*, **20**, 467-473.
5. Bhagwat, A.S. and Lieb, M. (2002) Cooperation and competition in mismatch repair: very short-patch repair and methyl-directed mismatch repair in *Escherichia coli*. *Mol. Microbiol.*, **44**, 1421-1428.
6. Kunz, C., Saito, Y. and Schar, P. (2009) DNA Repair in mammalian cells: Mismatched repair: variations on a theme. *Cell. Mol. Life Sci.*, **66**, 1021-1038.
7. Acharya, S., Foster, P.L., Brooks, P. and Fishel, R. (2003) The coordinated functions of the *E. coli* MutS and MutL proteins in mismatch repair. *Mol. Cell*, **12**, 233-246.
8. Selmane, T., Schofield, M.J., Nayak, S., Du, C. and Hsieh, P. (2003) Formation of a DNA mismatch repair complex mediated by ATP. *J. Mol. Biol.*, **334**, 949-965.
9. Cristovao, M. (2009) Inauguraldissertation, Justus-Liebig-Universität, Giessen.
10. Lindahl, T. (1993) Instability and decay of the primary structure of DNA. *Nature*, **362**, 709-715.
11. Hoeijmakers, J.H. (2001) Genome maintenance mechanisms for preventing cancer. *Nature*, **411**, 366-374.
12. Friedberg, E.C., Walker, G. C. (2006) DNA Repair and Mutagenesis. *ASM Press*, **Second Edition**.
13. Friedberg, E.C., Aguilera, A., Gellert, M., Hanawalt, P.C., Hays, J.B., Lehmann, A.R., Lindahl, T., Lowndes, N., Sarasin, A. and Wood, R.D. (2006) DNA repair: from molecular mechanism to human disease. *DNA Repair (Amst)*, **5**, 986-996.
14. Ehrlich, M., Norris, K. F., Wang, R. Y., Kuo, K. C. and Gehrke, C. W. (1986) DNA cytosine methylation and heat-induced deamination. *Biosci. Rep.*, **6**, 387-393.
15. Wilson, G.G. and Murray, N.E. (1991) Restriction and modification systems. *Annu. Rev. Genet.*, **25**, 585-627.
16. Noyer-Weidner, M. and Trautner, T.A. (1993) In Jost, J. P. and Saluz, H. P. (eds.), *DNA methylation: Molecular Biology and Biological Significance*. Birkhauser Verlag, Basel, pp. 40-108.

17. Miranda, T.B.a.J., P.A. (2007) DNA methylation: the nuts and bolts of repression. *J. Cell. Physiol.*, **213**, 384-390.
18. Slupphaug, G., Kavli, B. and Krokan, H.E. (2003) The interacting pathways for prevention and repair of oxidative DNA damage. *Mutat. Res.*, **531**, 231-251.
19. York, S.J. and Modrich, P. (2006) Mismatch repair-dependent iterative excision at irreparable O6-methylguanine lesions in human nuclear extracts. *J. Biol. Chem.*, **281**, 22674-22683.
20. Modrich, P. and Lahue, R. (1996) Mismatch repair in replication fidelity, genetic recombination, and cancer biology. *Annu. Rev. Biochem.*, **65**, 101-133.
21. Kolodner, R.D. and Marsischky, G.T. (1999) Eukaryotic DNA mismatch repair. *Curr Opin Genet Dev*, **9**, 89-96.
22. Kolodner, R.D., Hall, N.R., Lipford, J., Kane, M.F., Rao, M.R., Morrison, P., Wirth, L., Finan, P.J., Burn, J., Chapman, P. *et al.* (1994) Human mismatch repair genes and their association with hereditary non-polyposis colon cancer. *Cold Spring Harb. Symp. Quant. Biol.*, **59**, 331-338.
23. Jiricny, J. and Nystrom-Lahti, M. (2000) Mismatch repair defects in cancer. *Curr Opin Genet Dev*, **10**, 157-161.
24. Harfe, B.D. and Jinks-Robertson, S. (2000) DNA mismatch repair and genetic instability. *Annu. Rev. Genet.*, **34**, 359-399.
25. Kunkel, T.A. and Erie, D.A. (2005) DNA Mismatch Repair. *Annu. Rev. Biochem.*, **74**, 681-710.
26. Jun, S.H., Kim, T.G. and Ban, C. (2006) DNA mismatch repair system. *Febs J*, **273**, 1609-1619.
27. Evans, E. and Alani, E. (2000) Roles for mismatch repair factors in regulating genetic recombination. *Mol. Cell. Biol.*, **20**, 7839-7844.
28. Aravind, L., Walker, D.R. and Koonin, E.V. (1999) Conserved domains in DNA repair proteins and evolution of repair systems. *Nucleic Acids Res.*, **27**, 1223-1242.
29. Su, S.S. and Modrich, P. (1986) Escherichia coli mutS-encoded protein binds to mismatched DNA base pairs. *Proc. Natl. Acad. Sci. U.S.A.*, **83**, 5057-5061.
30. Parker, B.O. and Marinus, M.G. (1992) Repair of DNA heteroduplexes containing small heterologous sequences in Escherichia coli. *Proc. Natl. Acad. Sci. U.S.A.*, **89**, 1730-1734.
31. Spampinato, C. and Modrich, P. (2000) The MutL ATPase Is Required for Mismatch Repair. *J. Biol. Chem.*, **275**, 9861-9869.
32. Ban, C. and Yang, W. (1998) Crystal structure and ATPase activity of MutL: implications for DNA repair and mutagenesis. *Cell*, **95**, 541-552.
33. Cooper, D.L., Lahue, R.S. and Modrich, P. (1993) Methyl-directed mismatch repair is bidirectional. *J. Biol. Chem.*, **268**, 11823-11829.
34. Kolodner, R.D., Mendillo, M.L. and Putnam, C.D. (2007) Coupling distant sites in DNA during DNA mismatch repair. *Proc. Natl. Acad. Sci. U.S.A.*, **104**, 12953-12954.

35. Selmane, T., Schofield, M.J., Nayak, S., Du, C.W. and Hsieh, P. (2003) Formation of a DNA mismatch repair complex mediated by ATP. *J. Mol. Biol.*, **334**, 949-965.
36. Modrich, P. (1987) DNA mismatch correction. *Annu. Rev. Biochem.*, **56**, 435-466.
37. Allen, D.J., Makhov, A., Grilley, M., Taylor, J., Thresher, R., Modrich, P. and Griffith, J.D. (1997) MutS mediates heteroduplex loop formation by a translocation mechanism. *EMBO J.*, **16**, 4467-4476.
38. Mechanic, L.E., Frankel, B.A. and Matson, S.W. (2000) Escherichia coli MutL loads DNA helicase II onto DNA. *J. Biol. Chem.*, **275**, 38337-38346.
39. Matson, S.W. and Robertson, A.B. (2006) The UvrD helicase and its modulation by the mismatch repair protein MutL. *Nucleic Acids Res.*, **34**, 4089-4097.
40. Viswanathan, M., Burdett, V., Baitinger, C., Modrich, P. and Lovett, S.T. (2001) Redundant exonuclease involvement in Escherichia coli methyl-directed mismatch repair. *J. Biol. Chem.*, **19**, 19.
41. Han, E.S., Cooper, D.L., Persky, N.S., Sutera, V.A., Jr., Whitaker, R.D., Montello, M.L. and Lovett, S.T. (2006) RecJ exonuclease: substrates, products and interaction with SSB. *Nucleic Acids Res.*, **34**, 1084-1091.
42. Lohman, T.M. and Ferrari, M.E. (1994) Escherichia coli single-stranded DNA-binding protein: multiple DNA-binding modes and cooperativities. *Annu. Rev. Biochem.*, **63**, 527-570.
43. Lobner-Olesen, A., Skovgaard, O. and Marinus, M.G. (2005) Dam methylation: coordinating cellular processes. *Curr Opin Microbiol*, **8**, 154-160.
44. Constantin, N., Dzantiev, L., Kadyrov, F.A. and Modrich, P. (2005) Human mismatch repair: reconstitution of a nick-directed bidirectional reaction. *J. Biol. Chem.*, **280**, 39752-39761.
45. Acharya, S., Wilson, T., Gradia, S., Kane, M.F., Guerrette, S., Marsischky, G.T., Kolodner, R. and Fishel, R. (1996) hMsh2 forms specific mispair-binding complexes with hMsh3 and hMsh6. *Proc. Natl. Acad. Sci. U.S.A.*, **93**, 13629-13634.
46. Umar, A., Risinger, J.I., Glaab, W.E., Tindall, K.R., Barrett, J.C. and Kunkel, T.A. (1998) Functional overlap in mismatch repair by human MSH3 and MSH6. *Genetics*, **148**, 1637-1646.
47. Macpherson, P., Humbert, O. and Karran, P. (1998) Frameshift mismatch recognition by the human MutS alpha complex. *Mutat. Res.*, **408**, 55-66.
48. Santucci-Darmanin, S. and Paquis-Flucklinger, V. (2003) [Homologs of MutS and MutL during mammalian meiosis]. *Med Sci (Paris)*, **19**, 85-91.
49. Svetlanov, A.a.C., P. E. (2004) mismatch repair proteins, meiosis and mice: understanding the complexities of mammalian meiosis. *Exp. Cell Res.*, **296**, 71-79.
50. Svetlanov, A., Baudat, F., Cohen, P.E. and de Massy, B. (2008) Distinct functions of MLH3 at recombination hot spots in the mouse. *Genetics*, **178**, 1937-1945.

-
51. Flores-Rozas, H. and Kolodner, R.D. (1998) The *Saccharomyces cerevisiae* MLH3 gene functions in MSH3-dependent suppression of frameshift mutations. *Proc. Natl. Acad. Sci. U.S.A.*, **95**, 12404-12409.
 52. Lipkin, S.M., Wang, V., Jacoby, R., Banerjee-Basu, S., Baxevanis, A.D., Lynch, H.T., Elliott, R.M. and Collins, F.S. (2000) MLH3: a DNA mismatch repair gene associated with mammalian microsatellite instability. *Nat. Genet.*, **24**, 27-35.
 53. Menecier, S., Coste, G., Servant, P., Bailone, A. and Sommer, S. (2004) Mismatch repair ensures fidelity of replication and recombination in the radioresistant organism *Deinococcus radiodurans*. *Mol Genet Genomics*, **272**, 460-469.
 54. Karran, P. and Bignami, M. (1994) DNA damage tolerance, mismatch repair and genome instability. *Bioessays*, **16**, 833-839.
 55. Eshleman, J.R. and Markowitz, S.D. (1996) Mismatch repair defects in human carcinogenesis. *Hum. Mol. Genet.*, **5**, 1489-1494.
 56. Chen, Y., Wang, J., Fraig, M.M., Metcalf, J., Turner, W.R., Bissada, N.K., Watson, D.K. and Schweinfest, C.W. (2001) Defects of DNA Mismatch Repair in Human Prostate Cancer. *Cancer Res.*, **61**, 4112-4121.
 57. Tessmer, I., Yang, Y., Zhai, J., Du, C., Hsieh, P., Hingorani, M.M. and Erie, D.A. (2008) Mechanism of MutS searching for DNA mismatches and signaling repair. *J. Biol. Chem.*
 58. Obmolova, G., Ban, C., Hsieh, P. and Yang, W. (2000) Crystal structures of mismatch repair protein MutS and its complex with a substrate DNA. *Nature*, **407**, 703-710.
 59. Lamers, M.H., Perrakis, A., Enzlin, J.H., Winterwerp, H.H., de Wind, N. and Sixma, T.K. (2000) The crystal structure of DNA mismatch repair protein MutS binding to a G x T mismatch. *Nature*, **407**, 711-717.
 60. Sixma, T.K. (2001) DNA mismatch repair: MutS structures bound to mismatches. *Curr. Opin. Struct. Biol.*, **11**, 47-52.
 61. Jiricny, J. (2000) Mismatch repair: the praying hands of fidelity. *Curr. Biol.*, **10**, R788-790.
 62. Alani, E., Lee, J.Y., Schofield, M.J., Kijas, A.W., Hsieh, P. and Yang, W. (2003) Crystal structure and biochemical analysis of the MutS.ADP.beryllium fluoride complex suggests a conserved mechanism for ATP interactions in mismatch repair. *J. Biol. Chem.*, **278**, 16088-16094.
 63. Gradia, S., Subramanian, D., Wilson, T., Acharya, S., Makhov, A., Griffith, J. and Fishel, R. (1999) hMSH2-hMSH6 forms a hydrolysis-independent sliding clamp on mismatched DNA. *Mol. Cell*, **3**, 255-261.
 64. Gorman, J., Chowdhury, A., Surtees, J.A., Shimada, J., Reichman, D.R., Alani, E. and Greene, E.C. (2007) Dynamic basis for one-dimensional DNA scanning by the mismatch repair complex Msh2-Msh6. *Mol. Cell*, **28**, 359-370.
 65. Yang, W. (2008) Structure and mechanism for DNA lesion recognition. *Cell Res*, **18**, 184-197.

-
66. Yamamoto, A., Schofield, M.J., Biswas, I. and Hsieh, P. (2000) Requirement for Phe36 for DNA binding and mismatch repair by Escherichia coli MutS protein. *Nucleic Acids Res.*, **28**, 3564-3569.
 67. Schofield, M.J., Brownnewell, F.E., Nayak, S., Du, C., Kool, E.T. and Hsieh, P. (2001) The Phe-X-Glu DNA binding motif of MutS. The role of hydrogen bonding in mismatch recognition. *J. Biol. Chem.*, **276**, 45505-45508.
 68. Lamers, M.H., Winterwerp, H.H. and Sixma, T.K. (2003) The alternating ATPase domains of MutS control DNA mismatch repair. *EMBO J.*, **22**, 746-756.
 69. Dufner, P., Marra, G., Raschle, M. and Jiricny, J. (2000) Mismatch recognition and DNA-dependent stimulation of the ATPase activity of hMutSalpha is abolished by a single mutation in the hMSH6 subunit. *J. Biol. Chem.*, **275**, 36550-36555.
 70. Holmes, S.F., Scarpinato, K.D., McCulloch, S.D., Schaaper, R.M. and Kunkel, T.A. (2007) Specialized mismatch repair function of Glu339 in the Phe-X-Glu motif of yeast Msh6. *DNA Repair (Amst)*, **6**, 293-303.
 71. Drotschmann, K., Yang, W., Brownnewell, F.E., Kool, E.T. and Kunkel, T.A. (2001) Asymmetric recognition of DNA local distortion. Structure-based functional studies of eukaryotic Msh2-Msh6. *J. Biol. Chem.*, **276**, 46225-46229.
 72. Wang, H., Yang, Y., Schofield, M.J., Du, C., Fridman, Y., Lee, S.D., Larson, E.D., Drummond, J.T., Alani, E., Hsieh, P. *et al.* (2003) DNA bending and unbending by MutS govern mismatch recognition and specificity. *Proc. Natl. Acad. Sci. U.S.A.*, **100**, 14822-14827.
 73. Yang, W., Junop, M.S., Ban, C., Obmolova, G. and Hsieh, P. (2000) DNA mismatch repair: from structure to mechanism. *Cold Spring Harb. Symp. Quant. Biol.*, **65**, 225-232.
 74. Natrajan, G., Lamers, M.H., Enzlin, J.H., Winterwerp, H.H., Perrakis, A. and Sixma, T.K. (2003) Structures of Escherichia coli DNA mismatch repair enzyme MutS in complex with different mismatches: a common recognition mode for diverse substrates. *Nucleic Acids Res.*, **31**, 4814-4821.
 75. Lebbink, J.H., Georgijevic, D., Natrajan, G., Fish, A., Winterwerp, H.H., Sixma, T.K. and de Wind, N. (2006) Dual role of MutS glutamate 38 in DNA mismatch discrimination and in the authorization of repair. *EMBO J.*, **25**, 409-419.
 76. Bjornson, K.P., Allen, D.J. and Modrich, P. (2000) Modulation of MutS ATP Hydrolysis by DNA Cofactors. *Biochemistry*, **39**, 3176-3183.
 77. Antony, E. and Hingorani, M.M. (2004) Asymmetric ATP binding and hydrolysis activity of the Thermus aquaticus MutS dimer is key to modulation of its interactions with mismatched DNA. *Biochemistry*, **43**, 13115-13128.
 78. Gradia, S., Acharya, S. and Fishel, R. (1997) The human mismatch recognition complex hMSH2-hMSH6 functions as a novel molecular switch. *Cell*, **91**, 995-1005.

-
79. Blackwell, L.J., Bjornson, K.P., Allen, D.J. and Modrich, P.L. (2001) Distinct MutS DNA-binding modes that are differentially modulated by ATP binding and hydrolysis. *J. Biol. Chem.*, **13**, 13.
80. Junop, M.S., Obmolova, G., Rausch, K., Hsieh, P. and Yang, W. (2001) Composite active site of an ABC ATPase: MutS uses ATP to verify mismatch recognition and authorize DNA repair. *Mol. Cell*, **7**, 1-12.
81. Antony, E. and Hingorani, M.M. (2003) Mismatch recognition-coupled stabilization of Msh2-Msh6 in an ATP-bound state at the initiation of DNA repair. *Biochemistry*, **42**, 7682-7693.
82. Iaccarino, I., Marra, G., Dufner, P. and Jiricny, J. (2000) Mutation in the magnesium binding site of hMSH6 disables the hMutSalphalpha sliding clamp from translocating along DNA. *J. Biol. Chem.*, **275**, 2080-2086.
83. Schofield, M.J., Nayak, S., Scott, T.H., Du, C. and Hsieh, P. (2001) Interaction of Escherichia coli MutS and MutL at a DNA mismatch. *J. Biol. Chem.*, **276**, 28291-28299.
84. Hays, J.B., Hoffman, P.D. and Wang, H. (2005) Discrimination and versatility in mismatch repair. *DNA Repair (Amst)*, **4**, 1463-1474.
85. Drotschmann, K., Yang, W. and Kunkel, T.A. (2002) Evidence for sequential action of two ATPase active sites in yeast Msh2-Msh6. *Dna Repair*, **1**, 743-753.
86. Grilley, M., Welsh, K.M., Su, S.S. and Modrich, P. (1989) Isolation and characterization of the Escherichia coli mutL gene product. *J. Biol. Chem.*, **264**, 1000-1004.
87. Drotschmann, K., Aronshtam, A., Fritz, H.J. and Marinus, M.G. (1998) The Escherichia coli MutL protein stimulates binding of Vsr and MutS to heteroduplex DNA. *Nucleic Acids Res.*, **26**, 948-953.
88. Hall, M.C. and Matson, S.W. (1999) The Escherichia coli MutL protein physically interacts with MutH and stimulates the MutH-associated endonuclease activity. *J. Biol. Chem.*, **274**, 1306-1312.
89. Polosina, Y.Y., Mui, J., Pitsikas, P. and Cupples, C.G. (2009) The Escherichia coli mismatch repair protein MutL recruits the Vsr and MutH endonucleases in response to DNA damage *J. Bacteriol.*, **in press**.
90. Guarne, A., Ramon-Maiques, S., Wolff, E.M., Ghirlando, R., Hu, X., Miller, J.H. and Yang, W. (2004) Structure of the MutL C-terminal domain: a model of intact MutL and its roles in mismatch repair. *EMBO J.*, **23**, 4134-4145.
91. Guarne, A., Junop, M.S. and Yang, W. (2001) Structure and function of the N-terminal 40 kDa fragment of human PMS2: a monomeric GHL ATPase. *EMBO J.*, **20**, 5521-5531.
92. Bergerat, A., de Massy, B., Gadelle, D., Varoutas, P.C., Nicolas, A. and Forterre, P. (1997) An atypical topoisomerase II from Archaea with implications for meiotic recombination [see comments]. *Nature*, **386**, 414-417.
93. Dutta, R. and Inouye, M. (2000) GHKL, an emergent ATPase/kinase superfamily. *Trends Biochem. Sci.*, **25**, 24-28.

-
94. Iyer, L.M., Abhiman, S. and Aravind, L. (2008) MutL homologs in restriction-modification systems and the origin of eukaryotic MORC ATPases. *Biol Direct*, **3**, 8.
 95. Ban, C., Junop, M. and Yang, W. (1999) Transformation of MutL by ATP binding and hydrolysis: a switch in DNA mismatch repair. *Cell*, **97**, 85-97.
 96. Giron-Monzon, L., Manelyte, L., Ahrends, R., Kirsch, D., Spengler, B. and Friedhoff, P. (2004) Mapping protein-protein interactions between MutL and MutH by cross-linking. *J. Biol. Chem.*, **279**, 49338-49345.
 97. Schofield, M.J. and Hsieh, P. (2003) DNA mismatch repair: molecular mechanisms and biological function. *Annu. Rev. Microbiol.*, **57**, 579-608.
 98. Jacquelin, D.K., Filiberti, A., Argarana, C.E. and Barra, J.L. (2005) The *Pseudomonas aeruginosa* MutL protein functions in *Escherichia coli*. *Biochem. J.*, **388**, 879-887.
 99. Yang, W. (2000) Structure and function of mismatch repair proteins. *Mutat. Res.*, **460**, 245-256.
 100. Kadyrov, F.A., Dzantiev, L., Constantin, N. and Modrich, P. (2006) Endonucleolytic function of MutL α in human mismatch repair. *Cell*, **126**, 297-308.
 101. Joseph, N., Sawarkar, R. and Rao, D.N. (2004) DNA mismatch correction in *Haemophilus influenzae*: characterization of MutL, MutH and their interaction. *DNA Repair (Amst)*, **3**, 1561-1577.
 102. Au, K.G., Welsh, K. and Modrich, P. (1992) Initiation of methyl-directed mismatch repair. *J. Biol. Chem.*, **267**, 12142-12148.
 103. Lee, J.Y., Chang, J., Joseph, N., Ghirlando, R., Rao, D.N. and Yang, W. (2005) MutH complexed with hemi- and unmethylated DNAs: Coupling base recognition and DNA cleavage. *Mol. Cell*, **20**, 155-166.
 104. Ban, C. and Yang, W. (1998) Structural basis for MutH activation in *E. coli* mismatch repair and relationship of MutH to restriction endonucleases. *EMBO J.*, **17**, 1526-1534.
 105. Friedhoff, P., Thomas, E. and Pingoud, A. (2003) Tyr212: a key residue involved in strand discrimination by the DNA mismatch repair endonuclease MutH. *J. Mol. Biol.*, **325**, 285-297.
 106. Loh, T., Murphy, K.C. and Marinus, M.G. (2001) Mutational analysis of the MutH protein from *Escherichia coli*. *J. Biol. Chem.*, **276**, 12113-12119.
 107. Soultanas, P. and Wigley, D.B. (2000) DNA helicases: 'inching forward'. *Curr. Opin. Struct. Biol.*, **10**, 124-128.
 108. Kuhn, B., Abdel-Monem, M. and Hoffmann-Berling, H. (1979) DNA helicases. *Cold Spring Harb. Symp. Quant. Biol.*, **43 Pt 1**, 63-67.
 109. Tomko, E.J., Fischer, C.J., Niedziela-Majka, A. and Lohman, T.M. (2007) A nonuniform stepping mechanism for *E. coli* UvrD monomer translocation along single-stranded DNA. *Mol. Cell*, **26**, 335-347.
 110. Lee, J.Y. and Yang, W. (2006) UvrD helicase unwinds DNA one base pair at a time by a two-part power stroke. *Cell*, **127**, 1349-1360.
 111. Dao, V. and Modrich, P. (1998) Mismatch-, MutS-, MutL-, and Helicase II-dependent unwinding from the single-strand break of an incised heteroduplex. *J. Biol. Chem.*, **273**, 9202-9207.

-
112. Sancar, A. (1999) Excision repair invades the territory of mismatch repair. *Nat. Genet.*, **21**, 247-249.
 113. Mechanic, L.E., Hall, M.C. and Matson, S.W. (1999) Escherichia coli DNA helicase II is active as a monomer. *J. Biol. Chem.*, **274**, 12488-12498.
 114. Ali, J.A. and Lohman, T.M. (1997) Kinetic measurement of the step size of DNA unwinding by Escherichia coli UvrD helicase [published erratum appears in Science 1997 Apr 4;276(5309):21]. *Science*, **275**, 377-380.
 115. Hall, M.C., Jordan, J.R. and Matson, S.W. (1998) Evidence for a physical interaction between the Escherichia coli methyl- directed mismatch repair proteins MutL and UvrD. *EMBO J.*, **17**, 1535-1541.
 116. Genschel, J. and Modrich, P. (2006) Analysis of the excision step in human DNA mismatch repair. *Methods Enzymol.*, **408**, 273-284.
 117. Lieb, M. (1991) Spontaneous mutation at a 5-methylcytosine hotspot is prevented by very short patch (VSP) mismatch repair. *Genetics*, **128**, 23-27.
 118. Sohail, A., Lieb, M., Dar, M. and Bhagwat, A.S. (1990) A gene required for very short patch repair in Escherichia coli is adjacent to the DNA cytosine methylase gene. *J. Bacteriol.*, **172**, 4214-4221.
 119. Hennecke, F., Kolmar, H., Brundl, K. and Fritz, H.J. (1991) The vsr gene product of E. coli K-12 is a strand- and sequence-specific DNA mismatch endonuclease. *Nature*, **353**, 776-778.
 120. Dzidic, S. and Radman, M. (1989) Genetic requirements for hyper-recombination by very short patch mismatch repair: involvement of Escherichia coli DNA polymerase I. *Mol. Gen. Genet.*, **217**, 254-256.
 121. Petropoulos, L., Vidmar, J.J., Passi, E. and Cupples, C.G. (1994) A simple assay for monitoring the mutagenic effects of 5-methylcytosine deamination in Escherichia coli. *Mut. Res.*, **304**, 181-185.
 122. Tsutakawa, S.E., Jingami, H. and Morikawa, K. (1999) Recognition of a TG mismatch: the crystal structure of very short patch repair endonuclease in complex with a DNA duplex. *Cell*, **99**, 615-623.
 123. Gonzalez-Nicieza, R., Turner, D.P. and Connolly, B.A. (2001) DNA binding and cleavage selectivity of the Escherichia coli DNA G:T- mismatch endonuclease (vsr protein). *J. Mol. Biol.*, **310**, 501-508.
 124. Bhagwat, A.S. and Connolly, B. (2006) In Siede, W., Kow, Y. W. and Doetsch, P. W. (eds.), *DNA damage recognition*. Marcel Dekker Inc, New York, pp. 476-492.
 125. Bell, D.C. and Cupples, C.G. (2001) Very-Short-Patch Repair in Escherichia coli Requires the dam Adenine Methylase. *J. Bacteriol.*, **183**, 3631-3635.
 126. Jones, M., Wagner, R. and Radman, M. (1987) Mismatch repair and recombination in E. coli. *Cell*, **50**, 621-626.
 127. Zell, R. and Fritz, H.J. (1987) DNA mismatch-repair in Escherichia coli counteracting the hydrolytic deamination of 5-methyl-cytosine residues. *EMBO J.*, **6**, 1809-1815.
 128. Lieb, M., Rehmat, S. and Bhagwat, A.S. (2001) Interaction of MutS and Vsr: Some Dominant-Negative mutS Mutations That Disable Methyladenine-Directed Mismatch Repair Are Active in Very-Short- Patch Repair. *J. Bacteriol.*, **183**, 6487-6490.

-
129. Doiron, K.M., Viau, S., Koutroumanis, M. and Cupples, C.G. (1996) Overexpression of *vsr* in *Escherichia coli* is mutagenic. *J. Bacteriol.*, **178**, 4294-4296.
130. Macintyre, G., Doiron, K.M. and Cupples, C.G. (1997) The Vsr endonuclease of *Escherichia coli*: an efficient DNA repair enzyme and a potent mutagen. *J. Bacteriol.*, **179**, 6048-6052.
131. Feng, G., Tsui, H.C. and Winkler, M.E. (1996) Depletion of the cellular amounts of the MutS and MutH methyl-directed mismatch repair proteins in stationary-phase *Escherichia coli* K-12 cells. *J. Bacteriol.*, **178**, 2388-2396.
132. Monastiriakos, S.K., Doiron, K.M., Siponen, M.I. and Cupples, C.G. (2004) Functional interactions between the MutL and Vsr proteins of *Escherichia coli* are dependent on the N-terminus of Vsr. *DNA Repair (Amst)*, **3**, 639-647.
133. Mansour, C.A., Doiron, K.M. and Cupples, C.G. (2001) Characterization of functional interactions among the *Escherichia coli* mismatch repair proteins using a bacterial two-hybrid assay. *Mutat. Res.*, **485**, 331-338.
134. Heinze, R.J., Giron-Monzon, L., Solovyova, A., Elliot, S.L., Geisler, S., Cupples, C.G., Connolly, B.A. and Friedhoff, P. (2009) Physical and functional interactions between *Escherichia coli* MutL and the Vsr repair endonuclease. *Nucleic Acids Res.*
135. Rye, P.T., Delaney, J.C., Netirojjanakul, C., Sun, D.X., Liu, J.Z. and Essigmann, J.M. (2008) Mismatch repair proteins collaborate with methyltransferases in the repair of O(6)-methylguanine. *DNA Repair (Amst)*, **7**, 170-176.
136. Tsutakawa, S.E. and Morikawa, K. (2001) The structural basis of damaged DNA recognition and endonucleolytic cleavage for very short patch repair endonuclease. *Nucleic Acids Res.*, **29**, 3775-3783.
137. Turner, D.P. and Connolly, B.A. (2000) Interaction of the *E. coli* DNA G:T-mismatch endonuclease (*vsr* protein) with oligonucleotides containing its target sequence. *J. Mol. Biol.*, **304**, 765-778.
138. Visnes, T., Døseth, B., Pettersen, H.S., Hagen, L., Sousa, M.M., Akbari, M., Otterlei, M., Kavli, B., Slupphaug, G. and Krokan, H.E. (2009) Uracil in DNA and its processing by different DNA glycosylases. *Philos. Trans. R. Soc. Lond. B Biol. Sci.*, **364**, 563-568.
139. Kubota, Y., Nash, R.A., Klungland, A., Schar, P., Barnes, D.E. and Lindahl, T. (1996) Reconstitution of DNA base excision-repair with purified human proteins: interaction between DNA polymerase beta and the XRCC1 protein. *EMBO J.*, **15**, 6662-6670.
140. Lindahl, T. and Nyberg, B. (1974) Heat-induced deamination of cytosine residues in deoxyribonucleic acid. *Biochemistry*, **13**, 3405-3410.
141. Duncan, B.K. and Weiss, B. (1982) Specific mutator effects of *ung* (uracil-DNA glycosylase) mutations in *Escherichia coli*. *J. Bacteriol.*, **151**, 750-755.
142. Slupphaug, G., Mol, C.D., Kavli, B., Arvai, A.S., Krokan, H.E. and Tainer, J.A. (1996) A nucleotide-flipping mechanism from the structure of human uracil-DNA glycosylase bound to DNA [see comments]. *Nature*, **384**, 87-92.

-
143. Visnes, T., Akbari, M., Hagen, L., Slupphaug, G. and Krokan, H.E. (2008) The rate of base excision repair of uracil is controlled by the initiating glycosylase. *DNA Repair (Amst)*, **7**, 1869-1881.
 144. Jaruga, P. and Dizdaroglu, M. (1996) Repair of products of oxidative DNA base damage in human cells. *Nucleic Acids Res.*, **24**, 1389-1394.
 145. Schanz, S., Castor, D., Fischer, F. and Jiricny, J. (2009) Interference of mismatch and base excision repair during the processing of adjacent U/G mispairs may play a key role in somatic hypermutation. *Proc. Natl. Acad. Sci. U.S.A.*
 146. Larson, E.D., Bednarski, D.W. and Maizels, N. (2008) High-fidelity correction of genomic uracil by human mismatch repair activities. *BMC Mol Biol*, **9**, 94.
 147. Steele, E.J. (2009) Mechanism of somatic hypermutation: critical analysis of strand biased mutation signatures at A:T and G:C base pairs. *Mol. Immunol.*, **46**, 305-320.
 148. Lakowicz, J.R. (2006) Principles of fluorescence spectroscopy. *New York Springer*.
 149. Hillisch, A., Lorenz, M. and Diekmann, S. (2001) Recent advances in FRET: distance determination in protein-DNA complexes. *Curr. Opin. Struct. Biol.*, **11**, 201-207.
 150. Sapsford, K.E., Berti, L. and Medintz, L. E. (2006) Materials for fluorescence resonance energy transfer analysis: beyond traditional donor -acceptor combinations. *Angew Chem Int Ed Engl*, **45**, p. 4562-4589.
 151. Clegg, R.M., Murchie, A.I., Zechel, A., Carlberg, C., Diekmann, S. and Lilley, D.M. (1992) Fluorescence resonance energy transfer analysis of the structure of the four-way DNA junction. *Biochemistry*, **31**, 4846-4856.
 152. Banerjee, A., Santos, W.L. and Verdine, G.L. (2006) Structure of a DNA glycosylase searching for lesions. *Science*, **311**, 1153-1157.
 153. Corn, J.E. and Berger, J.M. (2007) FASTDXL: a generalized screen to trap disulfide-stabilized complexes for use in structural studies. *Structure*, **15**, 773-780.
 154. Ausubel, F.M., Brent, R., Kingston, R. E., Moore, D. D., Smith, J. A., and Seidman, J. G. . (1992-2005) *Current Protocols in Molecular Biology* John Wiley & Sons, New York
 155. Kirsch, R.D. and Joly, E. (1998) An improved PCR-mutagenesis strategy for two-site mutagenesis or sequence swapping between related genes. *Nucleic Acids Res.*, **26**, 1848-1850.
 156. Wang, H. and Hays, J.B. (2001) Simple and rapid preparation of gapped plasmid DNA for incorporation of oligomers containing specific DNA lesions. *Mol Biotechnol*, **19**, 133-140.
 157. Runyon, G.T., Bear, D.G. and Lohman, T.M. (1990) Escherichia coli helicase II (UvrD) protein initiates DNA unwinding at nicks and blunt ends. *Proc. Natl. Acad. Sci. U.S.A.*, **87**, 6383-6387.
 158. Yang, Y., Sass, L.E., Du, C., Hsieh, P. and Erie, D.A. (2005) Determination of protein-DNA binding constants and specificities from statistical analyses

- of single molecules: MutS-DNA interactions. *Nucleic Acids Res.*, **33**, 4322-4334.
159. Miller, S., Edwards, M.D., Ozdemir, C. and Booth, I.R. (2003) The closed structure of the MscS mechanosensitive channel - Cross-linking of single cysteine mutants. *J. Biol. Chem.*, **278**, 32246-32250.
160. Ahrends, R., Kosinski, J., Kirsch, D., Manelyte, L., Giron-Monzon, L., Hummerich, L., Schulz, O., Spengler, B. and Friedhoff, P. (2006) Identifying an interaction site between MutH and the C-terminal domain of MutL by crosslinking, affinity purification, chemical coding and mass spectrometry. *Nucleic Acids Res.*, **34**, 3169-3180.
161. Geyer, H., Geyer, R. and Pingoud, V. (2004) A novel strategy for the identification of protein-DNA contacts by photocrosslinking and mass spectrometry. *Nucleic Acids Res.*, **32**, e132.
162. Lieb, M. (1987) Bacterial genes mutL, mutS, and dcm participate in repair of mismatches at 5-methylcytosine sites. *J. Bacteriol.*, **169**, 5241-5246.
163. Jones, M., Wagner, R., and Radman, M. . (1987) Mismatch repair of deaminated 5-methyl-cytosine. *J. Mol. Biol.*, **193**, 155-159.
164. Mansour, C.A., Doiron, K.M.J. and Cupples, C.G. (2001) Characterization of functional interactions among the Escherichia coli mismatch repair proteins using a bacterial two-hybrid assay. *Mut. Res.*, **485**, 331-338.
165. Giron-Monzon, L. (2006), Justus-Liebig-Universität, Giessen.
166. Pearl, L.H.a.P., C. . (2006) Structure and mechanism of the Hsp90 molecular chaperone machinery. *Annu. Rev. Biochem.*, **75**, 271-294.
167. Lahue, R.S., Su, S.S. and Modrich, P. (1987) Requirement for d(GATC) sequences in Escherichia coli mutHLS mismatch correction. *Proc. Natl. Acad. Sci. U.S.A.*, **84**, 1482-1486.
168. Robertson, A.B., Pattishall, S.R., Gibbons, E.A. and Matson, S.W. (2006) MutL-catalyzed ATP hydrolysis is required at a post-UvrD loading step in methyl-directed mismatch repair. *J. Biol. Chem.*, **281**, 19949-19959.
169. Junop, M.S., Yang, W., Funchain, P., Clendenin, W. and Miller, J.H. (2003) In vitro and in vivo studies of MutS, MutL and MutH mutants: correlation of mismatch repair and DNA recombination. *DNA Repair (Amst)*, **2**, 387-405.
170. Li, G.M. (2008) Mechanisms and functions of DNA mismatch repair. *Cell Res*, **18**, 85-98.
171. Bhagwat, A.S. and McClelland, M. (1992) DNA mismatch correction by Very Short Patch repair may have altered the abundance of oligonucleotides in the E. coli genome. *Nucleic Acids Res.*, **20**, 1663-1668.
172. Winkler, I. (2009), Justus-Liebig Universität, Giessen.
173. Bai, H. and Lu, A.L. (2007) Physical and functional interactions between Escherichia coli MutY glycosylase and mismatch repair protein MutS. *J. Bacteriol.*, **189**, 902-910.
174. Laging, M. (2000) Dissertation, Georg-August-Universität zu Göttingen, Göttingen.
175. Pruitt, K.D., Tatusova, T. and Maglott, D. R. (2007) NCBI reference sequences (RefSeq): a curated non-redundant sequence database of genomes, transcripts and proteins. *Nucl. Acids Res.*, **35**, D61-D65.

-
176. Krokan, H.E., Drablos, F. and Slupphaug, G. (2002) Uracil in DNA--occurrence, consequences and repair. *Oncogene*, **21**, 8935-8948.
 177. Tornaletti, S., Maeda, L. S. and Hanawalt, P. C. (2006) Transcription arrest at an abasic in the transcribed strand of template DNA. *Chem. Res. Toxicol.*, **19**, 1215-1220.
 178. Wang, Y., Sheppard, T. L., Tornaletti, S., Maeda, L. S. and Hanawalt (2006) Transcriptional inhibition by an oxidized abasic site in DNA. *Chem. Res. Toxicol.*, **19**, 234-241.
 179. McCulloch, S.D., Kokoska, R.J., Garg, P., Burgers, P.M. and Kunkel, T.A. (2009) The efficiency and fidelity of 8-oxo-guanine bypass by DNA polymerases delta and eta. *Nucleic Acids Res.*, **37**, 2830-2840.
 180. Cox, M.M., Goodman, M. F., Kreuzer, K. N., Sherratt, D. J., Sandler, S. J., Marians, K. J. (2000) The importance of repairing stalled replication forks. *Nature*, **404**, 37-41.
 181. Reynaud, C.A., Delbos, F., Faili, A., Gueranger, Q., Aoufouchi, S. and Weill, J.C. (2009) Competitive repair pathways in immunoglobulin gene hypermutation. *Philos. Trans. R. Soc. Lond. B Biol. Sci.*, **364**, 613-619.
 182. Vallur, A.C., Yabuki, M., Larson, E. D., Maizels, N. (2007) AID in antibody perfection. *Cell. Mol. Life Sci.*, **64**.
 183. Di Noia, J.M., Neuberger, M. S. (2007) Molecular mechanisms of antibody somatic hypermutation. *Annu. Rev. Biochem.*, **76**, 1-22.
 184. Stavnezer, J., Guikema, J.E. and Schrader, C.E. (2008) Mechanism and regulation of class switch recombination. *Annu. Rev. Immunol.*, **26**, 261-292.
 185. Liu, M., Duke, J.L., Richter, D.J., Vinuesa, C.G., Goodnow, C.C., Kleinstein, S.H. and Schatz, D.G. (2008) Two levels of protection for the B cell genome during somatic hypermutation. *Nature*, **451**, 841-845.
 186. Kavli, B., Otterlei, M., Slupphaug, G. and Krokan, H. E. (2007) Uracil in DNA - general mutagen, but normal intermediate in acquired immunity. *DNA Repair (Amst)*, **6**, 505-516.
 187. Cortazar, D., Kunz, C., Saito, Y., Steinacher, R. and Schar, P. (2007) The enigmatic thymine DNA glycosylase. *DNA Repair (Amst)*, **6**, 489-504.
 188. Mazurek, A., Johnson, C.N., Germann, M.W. and Fishel, R. (2009) Sequence context effect for hMSH2-hMSH6 mismatch-dependent activation. *Proc. Natl. Acad. Sci. U.S.A.*